

Minor Bodies in the Planetary System

Hermann Boehnhardt

MPI for Solar System Research

Katlenburg-Lindau

Some Basics

| | |
|-------------------|--|
| Ecliptic | plane of the Earth orbit around the sun projected into the solar system and sky |
| Astronomical Unit | mean distance Earth – Sun (149.6×10^6 km) |
| Inclination | angle of orbital plane to Ecliptic |
| Obliquity | angle of rotation axis and orbital plane |
| Elongation | angle between Sun and planet as seen from observer (Earth), greatest elongation (inner planets only) |
| Opposition | planet and Sun are seen with elongations close to 180 deg (outer planets only) |
| Conjunction | planet and Sun are seen with elongation close to 0 deg (upper/lower conjunction) |

The Planetary System - Overview

- Ingredients:

- Sun: central star
- Planets: Mercury, Venus, Earth, Mars, Jupiter, Saturn, Uranus, Neptune
- Moons and rings: 6 planets with moons and moonlets, 4 planets with rings or ringlets
- *Minor bodies: Dwarf planets, Asteroids, Transneptunian Objects, Comets,*
- The rest: *meteorites, dust,* solar wind

Benchmarks

- **Dimensions:** solar system extension $\sim 100000\text{AU}$
planetary system extension $\sim 0.4\text{-}32/50/1000/100000\text{AU}$
- **Geometry:** flat disk close to Ecliptic and equator of the Sun ($<50\text{AU}$)
- **Masses:** $1+0.0015$ solar masses (mostly concentrated in the Sun)
- **Angular momentum:** mostly in planets (due to large distances)
- **Barycenter:** close to photosphere of the Sun
reflex motion of the Sun indicates presence of planet(s)
→ detection of Jupiter around the Sun through radial velocity shift of photospheric lines of the Sun
amplitude $\delta v = 2\pi R_0 / U_{\text{Jup}}$
 $R_0 =$ Sun radius (700000km)
 $U_{\text{Jup}} =$ orbit period of Jupiter (11.8y)

→ $\delta v \sim 10 \text{ m/s}$ (over 11.8y)
measurement accuracy \sim few m/s (HD spectrographs)
problem is orbital period

Basic Physics

- Planck's law

$$B(\lambda) = (2hc^2/\lambda^5) / [\exp(hc/(2\pi\lambda kT)) - 1]$$

- Wien's law

$$\lambda_{\max} T = 2880 [\mu\text{mK}]$$

- Energy balance

$$F_0/r^2 \pi R^2 (1-A) = \sigma T^4 4\pi R^2$$

- Surface temperature (atmosphereless)

$$T = (1-A)^{1/4} 273 r^{1/2} \text{ (fast rotator)}$$

$$T = (1-A)^{1/4} 324 r^{1/2} \text{ (slow rotator)}$$

➔ snowline ($T < 273\text{K}$): somewhere in asteroid belt

λ = wavelength

Λ_{\max} = wavelength of radiation maximum

T = temperature

h, c, σ, k = Planck const, speed of light, Stefan const, Boltzmann const,

A = surface albedo

R = body radius

F_0 = solar flux at 1 AU

r = distance from the Sun

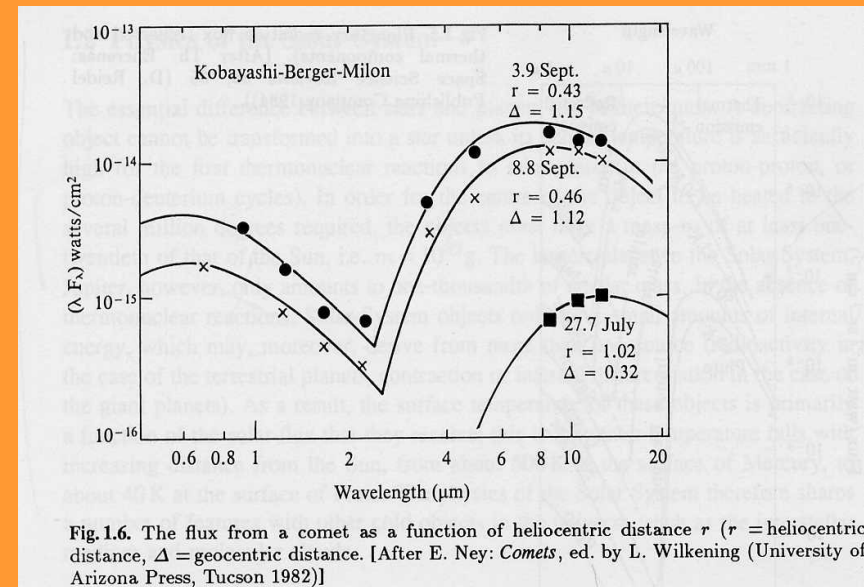
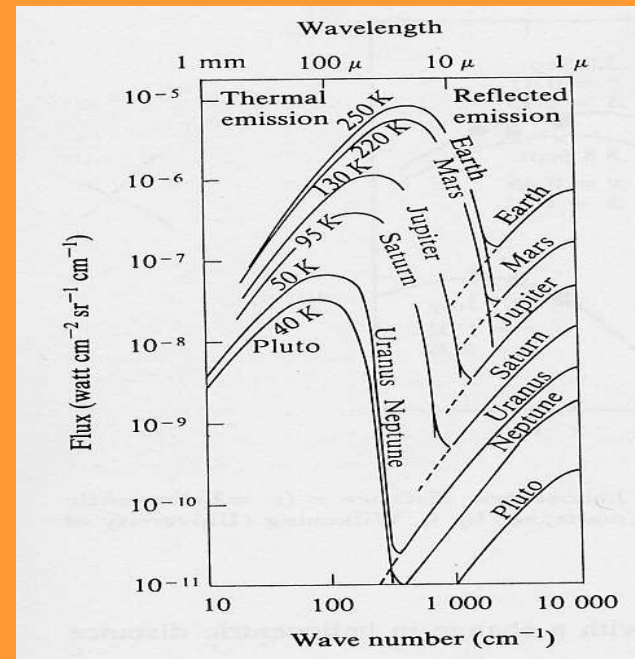


Fig. 1.6. The flux from a comet as a function of heliocentric distance r (r = heliocentric distance, Δ = geocentric distance). [After E. Ney: *Comets*, ed. by L. Wilkening (University of Arizona Press, Tucson 1982)]

Bodies with and without atmosphere

- **Criterion for possible stable atmosphere:**

(1) $E_{\text{kin}}(\text{gas}) < E_{\text{pot}}(\text{gas})$

$$v^2 < v_{\text{escape}}^2 = 2 \gamma m / R$$

(2) Mean velocity of gas

$$\underline{v}^2 = 2 G T / \mu$$

$$\rightarrow (m \mu) / (R T) < G / \gamma$$

Sequence of stability of atmosphere: Jupiter – Saturn, Neptune, Uranus, Earth, Venus, Mars, Pluto, Triton, Titan → other bodies without atmosphere

γ = gravity constant

m, R = body mass, radius

G = gas constant

T = gas temperature

μ = mean molecular weight

Orbits

- **Ellipse**, parabola, hyperbola
- Newtonian 2-body solution \sim good approximation

- Orbit plane defined by
 - I = inclination (to Ecliptic/equator)
 - Ω = argument of ascending node

- Dynamics defined by

$$r = a (1 - e^2) / (1 + e \cos v) \quad (\text{Ellipse})$$

r = length of radius vector

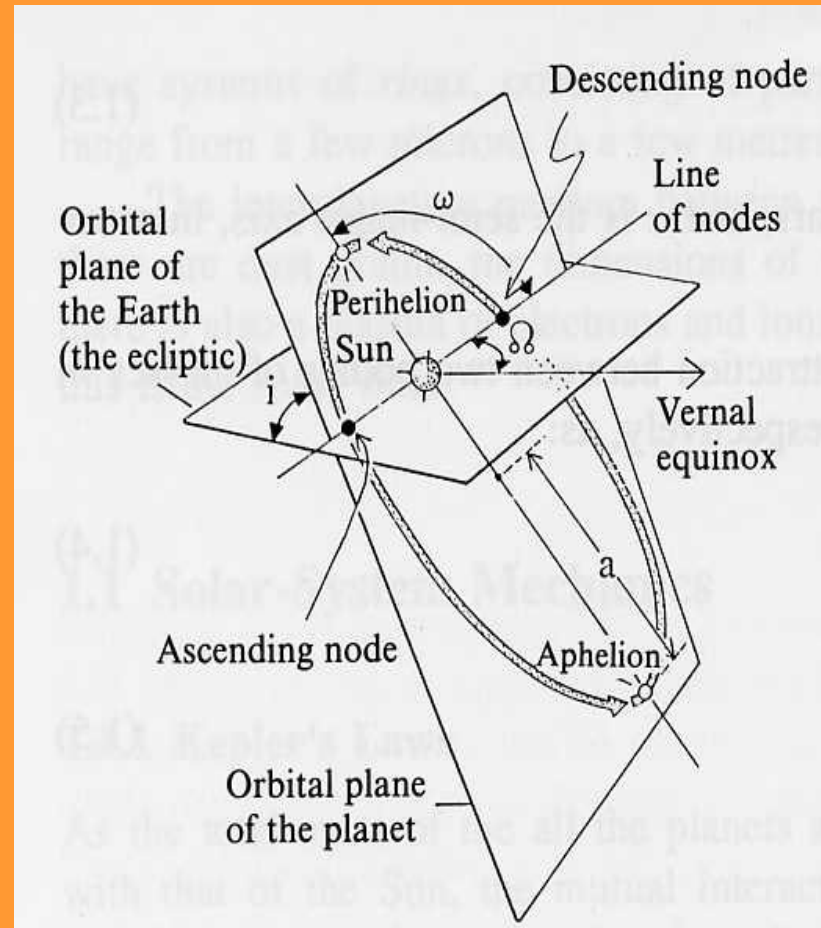
a = semi-major axis

e = eccentricity

v = true anomaly (angle between perihelion and actual orbit position as seen from central body)

Location of orbit in plane defined by

ω = argument of perihelion (angle between Ω



- time dependance $r = r(t)$

$$\cos v = (\cos E - e) / (1 - e \cos E)$$

$$E = M - e \sin E$$

$$M = n (t - T_p)$$

E = excentric anomaly
 M = mean anomaly
 T_p = time of perihelion
 n = mean motion rate

- Kepler's law 1+2+3
 - Orbit = ellipse with the Sun in one focus
 - $r^2 dv/dt = G$
 $G^2 = a(1-e^2) / [\gamma (M_0+m)]$
 - $P^2/a^3 = \gamma (M_0+m)/4\pi^2$
 P = orbital period
 M_0 = solar mass
 m = planet's mass
 γ = gravity constant

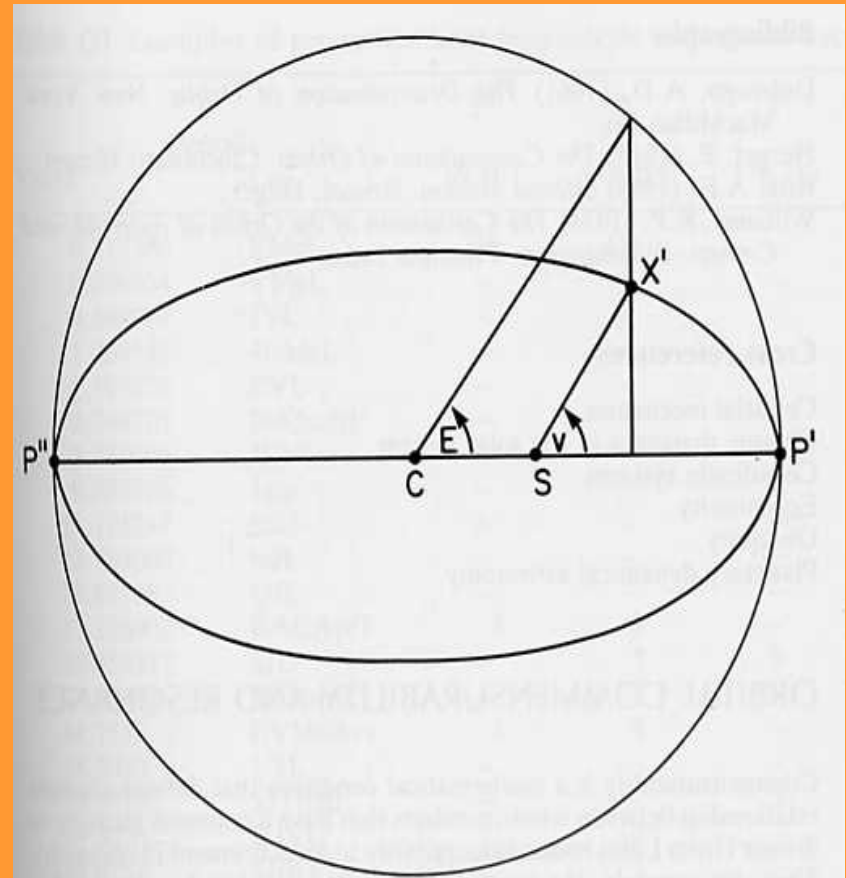


Figure O7 The true orbit seen face-on. The Sun S is at a focus. P' and P'' are the perihelion and aphelion points. The ratio CS/CP' is the eccentricity e. The perihelion distance SP' is $q = a(1 - e)$. The aphelion distance SP'' is $Q = a(1 + e)$. The circumscribing circle is the auxiliary circle. When the true planet is at X', its true anomaly is v and its eccentric anomaly is E .

Overview Tables of the Planets

TABLE I
Planetary Orbits^a

| Planet | Semimajor axis (AU) | Eccentricity | Inclination (°) | Period (years) |
|---------|---------------------|--------------|-----------------|----------------|
| Mercury | 0.38710 | 0.205631 | 7.0048 | 0.2408 |
| Venus | 0.72333 | 0.006773 | 3.3947 | 0.6152 |
| Earth | 1.00000 | 0.016710 | 0.0000 | 1.0000 |
| Mars | 1.52366 | 0.093412 | 1.8506 | 1.8807 |
| Jupiter | 5.20336 | 0.048393 | 1.3053 | 11.856 |
| Saturn | 9.53707 | 0.054151 | 2.4845 | 29.424 |
| Uranus | 19.1913 | 0.047168 | 0.7699 | 83.747 |
| Neptune | 30.0690 | 0.008586 | 1.7692 | 163.723 |
| Pluto | 39.4817 | 0.248808 | 17.1417 | 248.02 |

^a J2000, Epoch: January 1, 2000

← dwarf planet

TABLE III
Physical Parameters for the Sun and Planets

| Name | Mass (kg) | Equatorial radius (km) | Density (g cm ⁻³) | Rotation period | Obliquity (°) | Escape velocity (km sec ⁻¹) |
|---------|------------------------|------------------------|-------------------------------|-----------------|-------------------|---|
| Sun | 1.989×10^{30} | 696,000 | 1.41 | 24.65–34 days | 7.25 ^a | 617.7 |
| Mercury | 3.302×10^{23} | 2,439 | 5.43 | 58.646 days | 0 | 4.43 |
| Venus | 4.868×10^{24} | 6,051 | 5.20 | 243.018 days | 177.33 | 10.36 |
| Earth | 5.974×10^{24} | 6,378 | 5.52 | 23.934 hr | 23.45 | 11.19 |
| Mars | 6.418×10^{23} | 3,396 | 3.93 | 24.623 hr | 25.19 | 5.03 |
| Jupiter | 1.899×10^{27} | 71,492 | 1.33 | 9.925 hr | 3.08 | 59.54 |
| Saturn | 5.685×10^{26} | 60,268 | 0.69 | 10.656 hr | 26.73 | 35.49 |
| Uranus | 8.683×10^{25} | 25,559 | 1.32 | 17.24 hr | 97.92 | 21.33 |
| Neptune | 1.024×10^{26} | 24,764 | 1.64 | 16.11 hr | 28.80 | 23.61 |
| Pluto | 1.32×10^{22} | 1,170 | 2.1 | 6.387 days | 119.6 | 1.25 |

^a Solar obliquity relative to the ecliptic.

← dwarf planet

Asteroids

- **Summary**

- Asteroids = remnants from formation disk between Mars and Jupiter
- irregular shape except large ones
- Did not make it to form a planet (Jupiter influence)
- Continuous loss of asteroids from belt
- Kirkwood gaps = gravitational scattering by Jupiter
- Hirayama families = collision groups
- Taxonomy classes = differentiated bodies
- Solar distance distribution of taxonomic classes with signature from formation period

Orbits

- Asteroid belt:

- largest concentration between Mars and Jupiter
- much lower at other (larger&smaller) distances
- within asteroid belts gaps with low number density

→ Kirkwood gaps

- Gaps are located at integer-ratio resonances between asteroid and Jupiter revolution periods

Resonance effects: Jupiter increases eccentricity of asteroids when in resonance orbit, short life time of objects in resonance orbits

→ asteroid becomes planet crossing and is at high risk to collide with terrestrial planets

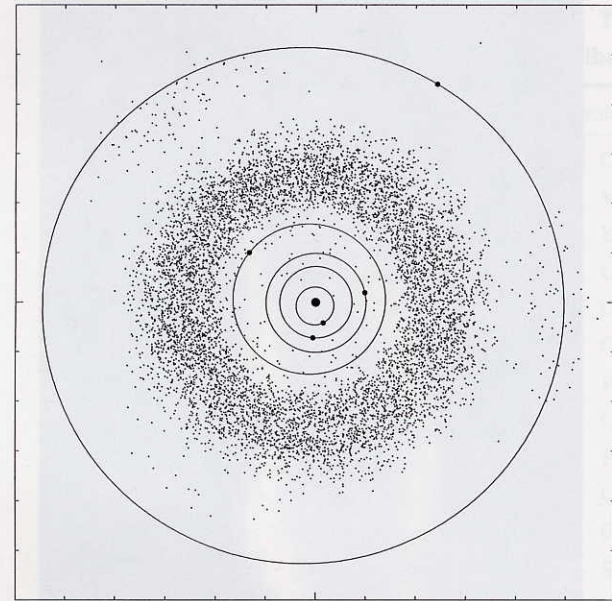
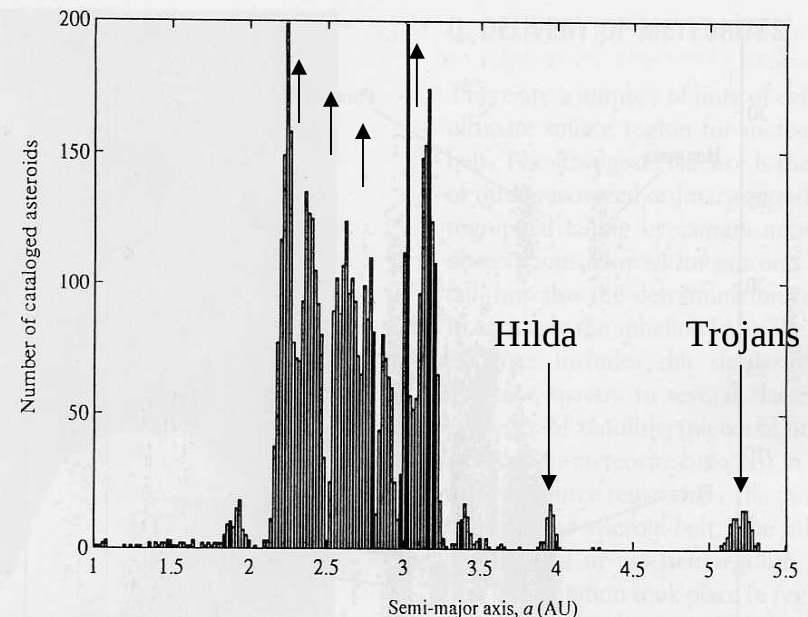


FIGURE 3 Positions projected onto the ecliptic plane for October 4, 2000 of the planets Mercury through Jupiter and 7722 numbered asteroids with accurately known orbits. (Copyright 1998 Institute for Remote Exploration.)



- Exception 1: Hilda group is in 3:2 resonance with Jupiter
dynamically this resonance has a long lifetime, i.e. asteroids will be collected here
- Exception 2: Trojans are in 1:1 orbit with Jupiter and remain associated with the two stable Lagrangian points ($\sim 60^\circ$ ahead or behind Jupiter)
→ solar system application of restricted three-body problem
equal side triangle Sun-Jupiter-Trojan is a dynamically stable configuration

Trojans at other planets: Earth, Mars & Neptune have Trojan-type asteroids

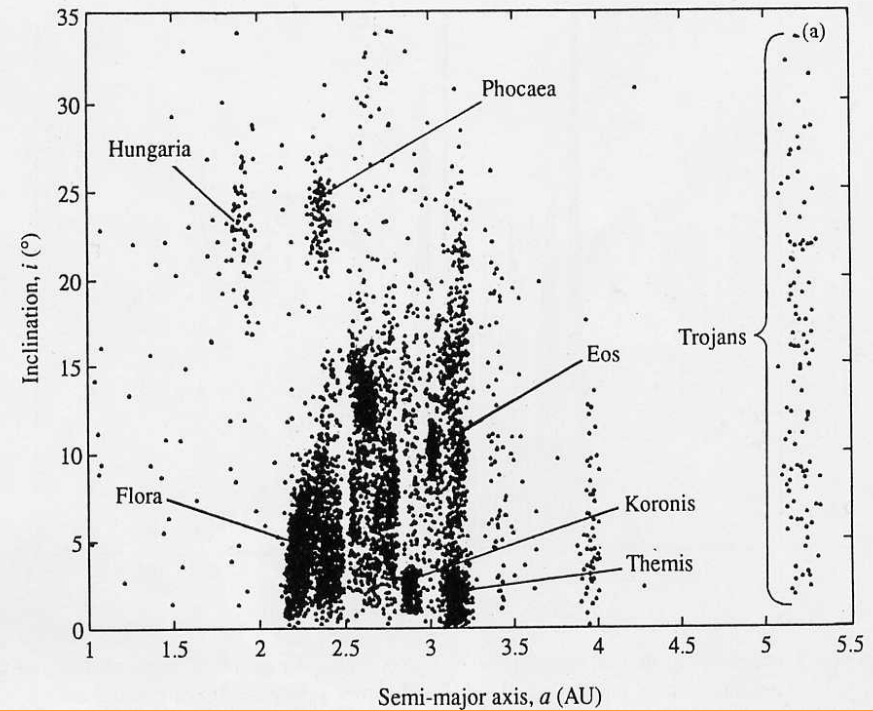
- Planet crossers:
 - Amor group = Mars crossers
 - Apollo group = Earth crossers with $a > 1$ AU
 - Aten group = Earth crossers with $a < 1$ AU

Planet crossers do not have very long lifetime due to the high probability to become

- either scattered by planet in very different orbit or
- to collide with the planet

- **Collision families:**

- Clustering of asteroid orbits with certain orbital parameters (a,i) or (a,e) groups
→ Hirayama families
- Collision families
- Family members may have different taxonomic properties since they can originate from different part of possibly differentiated bodies by the collision event (for instance from the crust - S-type, from the core - M type)



- **Double asteroids:**

- Double asteroids exist (first discovery: Ida+Dactyl discovered by GALILEO probe during flyby)
- Formation through impact (?) through rotational break-up (small ones only)

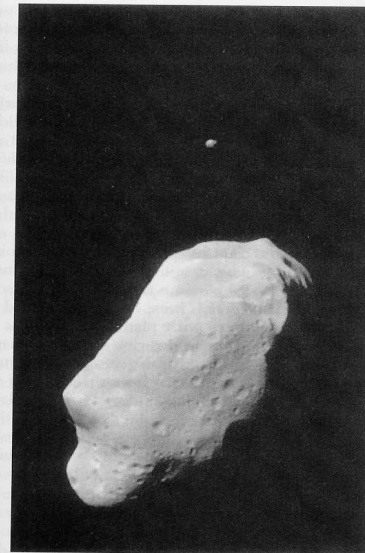
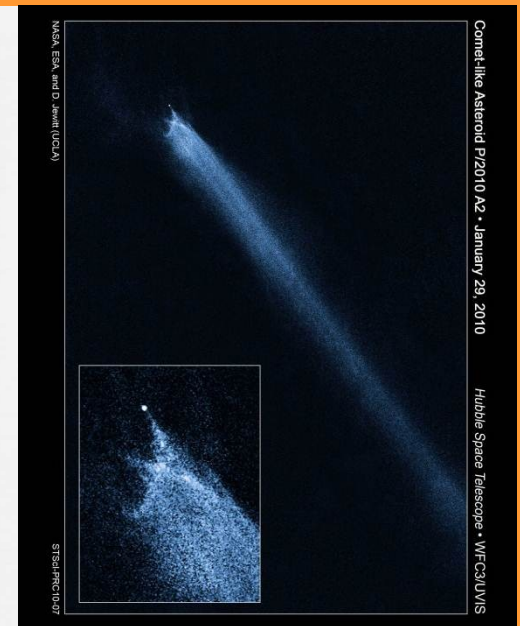


FIGURE 6 243 Ida and its satellite, Dactyl. (Courtesy of NASA/JPL-Caltech.)

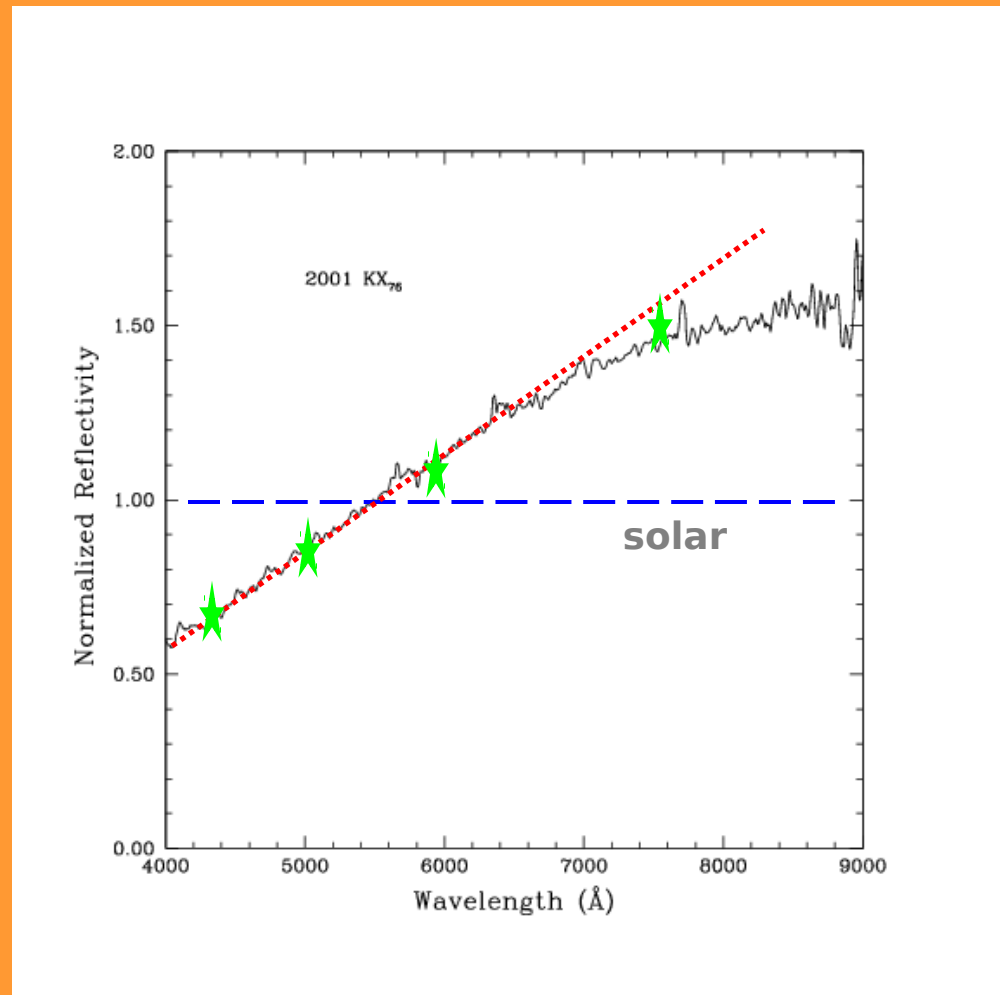


Reflectance spectroscopy

Recipe:

- take object spectrum
- take solar analogue spectrum
- divide the two spectra
- intrinsic spectrum of the object
- solar = flat without slope
- gradient = diverse object
- continuum
- absorption/emission = object specific materials

(works also for photometry)



Composition/Taxonomy

- Classification scheme based on telescopic (reflectance spectroscopy and/or photometry) and (few) flyby observations, first in-situ/lab analysis available (Hayabusa sample small)
- Main taxonomic classes (more classes exist, see table):
 - Indications/examples for differentiation of the internal structure of asteroids exists, however also for non-differentiation
Note: similarities between asteroid and meteorite spectra are used for classification and identification of surface materials
 - A, S, V, R types: pyroxene and olivine absorptions
→ silicate/basaltic bodies, heated material from early period of the Sun could come from mantle of a differentiated body
 - E, M, T types: metal-rich absorptions
→ from inner metal core or mantle of differentiated body (wet – hydrated, dry -anhydrous)
 - C, D, G, P types: carbon+organics, low albedo objects, mostly featureless
→ primitive material in two forms:
(wet – dry)
- Taxonomic class distribution in belt:
 - Non-uniform
 - Primitive classes in outer part
 - Silicate – metal-rich classes in center and inner belt

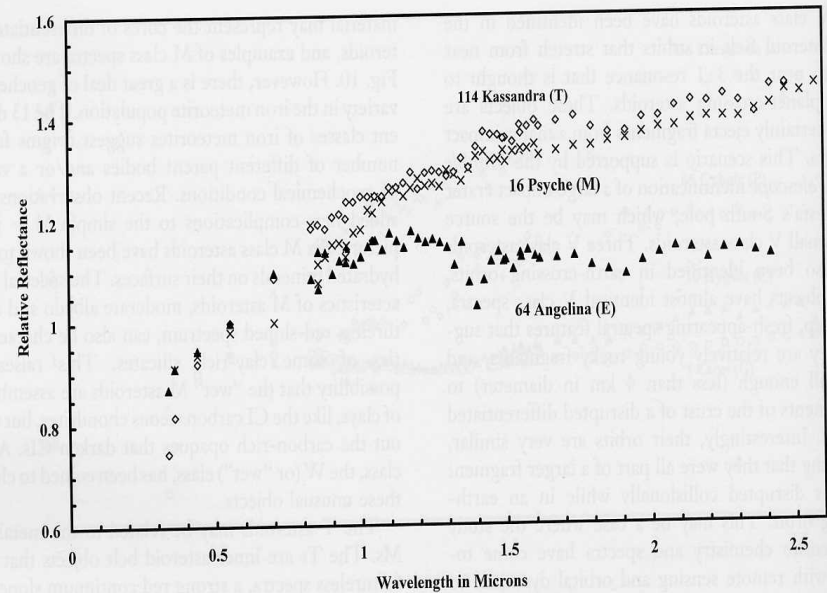
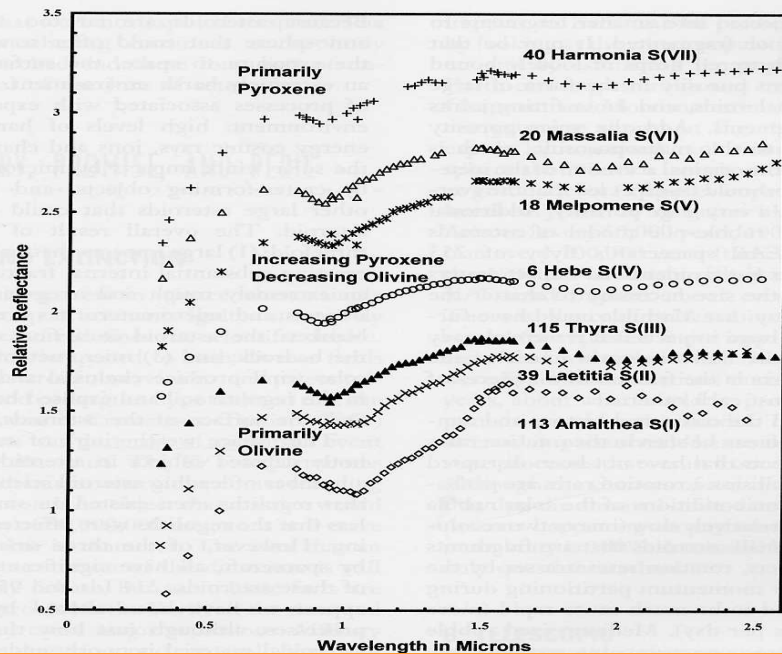
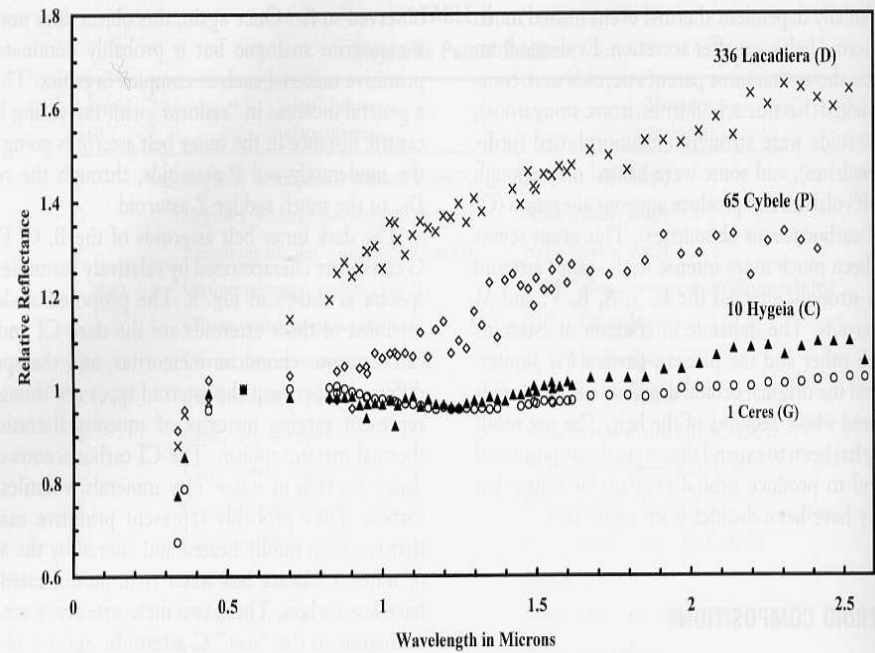
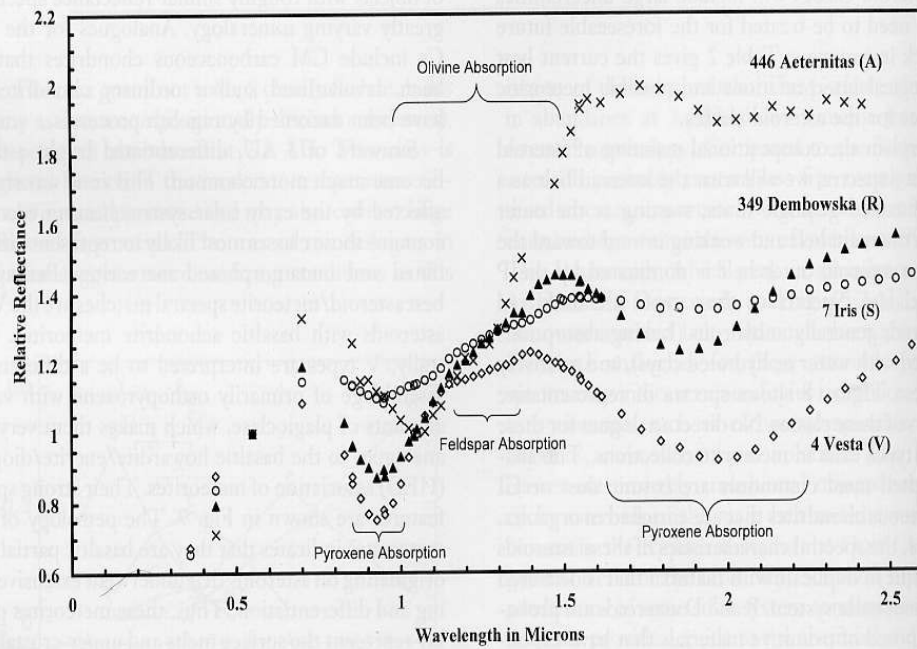


FIGURE 10 Red-sloped M, T, and E classes. These asteroids lack strong absorptions, but have large differences in albedo.

TABLE II
Meteorite Parent Bodies

| Asteroid class | Inferred major surface minerals | Meteorite analogues |
|----------------|--|--|
| Z | Organics + anhydrous silicates? (+ice??) | None (cosmic dust?) |
| D | Organics + anhydrous silicates? (+ice??) | None (cosmic dust?) |
| P | Anhydrous silicates + organics? (+ice??) | None (cosmic dust?) |
| C (dry) | Olivine, pyroxene, carbon (+ice??) | "CM3" chondrites, gas-rich/blk chondrites? |
| K | Olivine, orthopyroxene, opaques | CV3, CO3 chondrites |
| Q | Olivine, pyroxene, metal | H, L, LL chondrites |
| C (wet) | Clays, carbon, organics | CI1, CM2 chondrites |
| B | Clays, carbon, organics | None (highly altered CI1, CM2??) |
| G | Clays, carbon, organics | None (highly altered CI1, CM2??) |
| F | Clays, opaques, organics | None (altered CI1, CM2??) |
| W | Clays, salts???? | None (opaque-poor CI1, CM2??) |
| V | Pyroxene, feldspar | Basaltic achondrites |
| R | Olivine, pyroxene | None (olivine-rich achondrites?) |
| A | Olivine | Brachinites, pallasites |
| M | Metal, enstatite | Irons (+EH, EL chondrites?) |
| T | Troilite? | Troilite-rich irons (Mundrabilla?) |
| E | Mg-pyroxene | Enstatite achondrites |
| S | Olivine, pyroxene, metal | Stony irons, IAB irons, lodranites, windonites, siderophyres, ureilites, H, L, LL chondrites |

- **Taxonomic class distribution in belt:**
 - Non-uniform
 - Primitive classes in the outer part of the belt
 - Silicate – metal-rich classes in center and inner belt
 - Scenario: differentiation of object interior possible in inner belt due to heating by the early Sun (T-Tauri phase), some larger asteroids in central zone of the belt may have developed molten interiors due to gravitational/radioactive heating

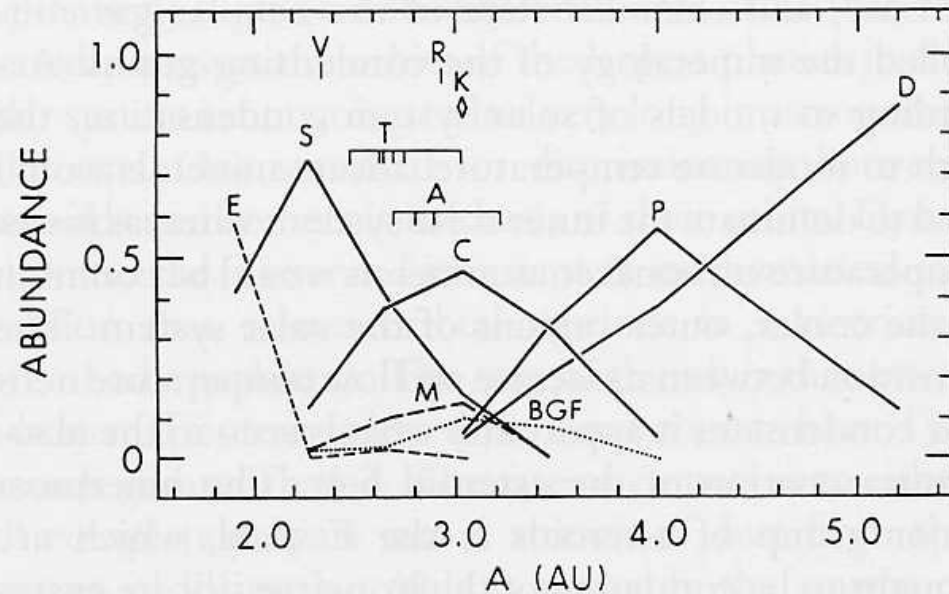


FIGURE 7 Distribution of taxonomic classes from Bell *et al.* (1989). (Courtesy of University of Arizona Press.)

Collision Effects

- Impact craters: exists in flyby images
 - Regolith surface
 - impact events seen in asteroid belt
- Simulation conclusions:
 - Only large objects survive mostly ,unaffected‘ from bombardment
 - Smaller objects (radius < 300km) experienced intense collisional evolution
 - Disruption
 - Re-accretion due to self gravity
 - loose rubble piles
 - high porosity and low density
 - Higher rotation rates from impact events
 - Very small bodies (< 1km) suffer from rotational break-up due to YORP effect

Asteroids&other bodies

Meteorite link:

- Orbit similarity
meteorites originate – in parts – from asteroids
- Spectrum similarity
→ indirect evidences, but with very useful conclusions

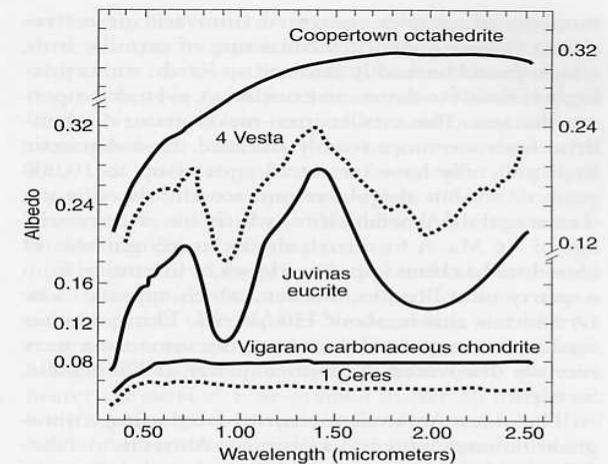


FIGURE 16 Spectral reflectances of the Cooperstown IIIIE coarse octahedrite, Juvinas eucrite and V-class asteroid 4 Vesta, and Vigarano C3V chondrite and G-class asteroid 1 Ceres. The albedo scale for all but Cooperstown is on the left; that for Cooperstown is on the right. Solid lines delineate meteorite spectra and dashed lines define asteroid spectra. (Courtesy of Dr. Lucy-Ann McFadden, University of Maryland.)

- Comet link:

- Orbit similarity

- Tisserand constant of orbit as invariance parameter

- $$a_j/a + 2 (a/a_j (1-e^2))^{1/2} \cos i = C$$

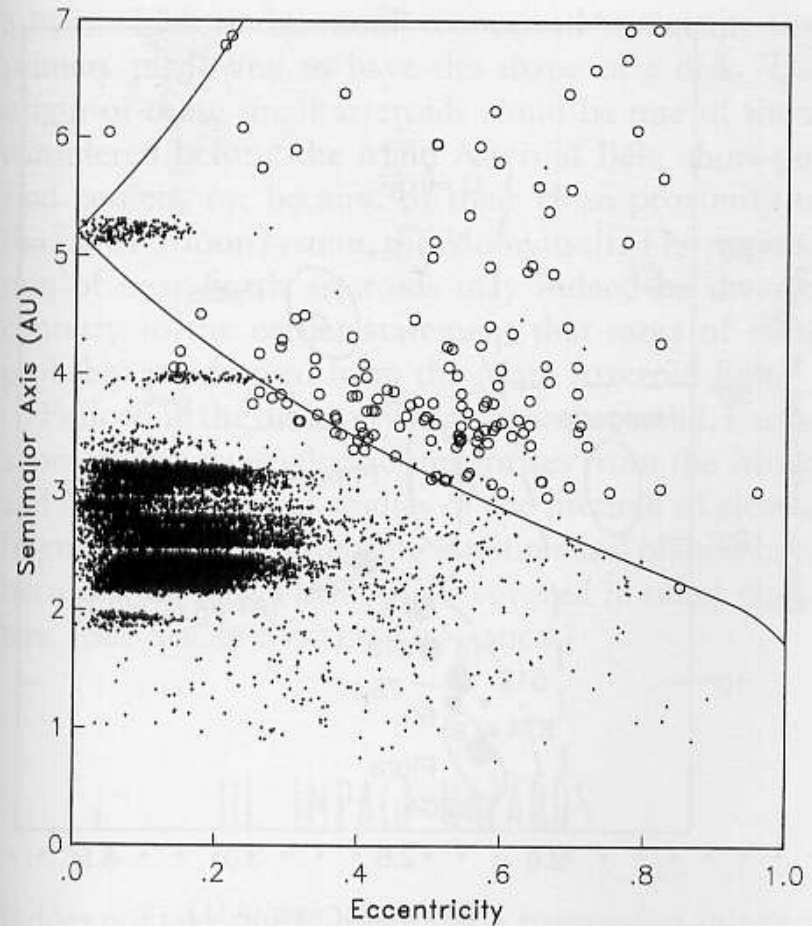
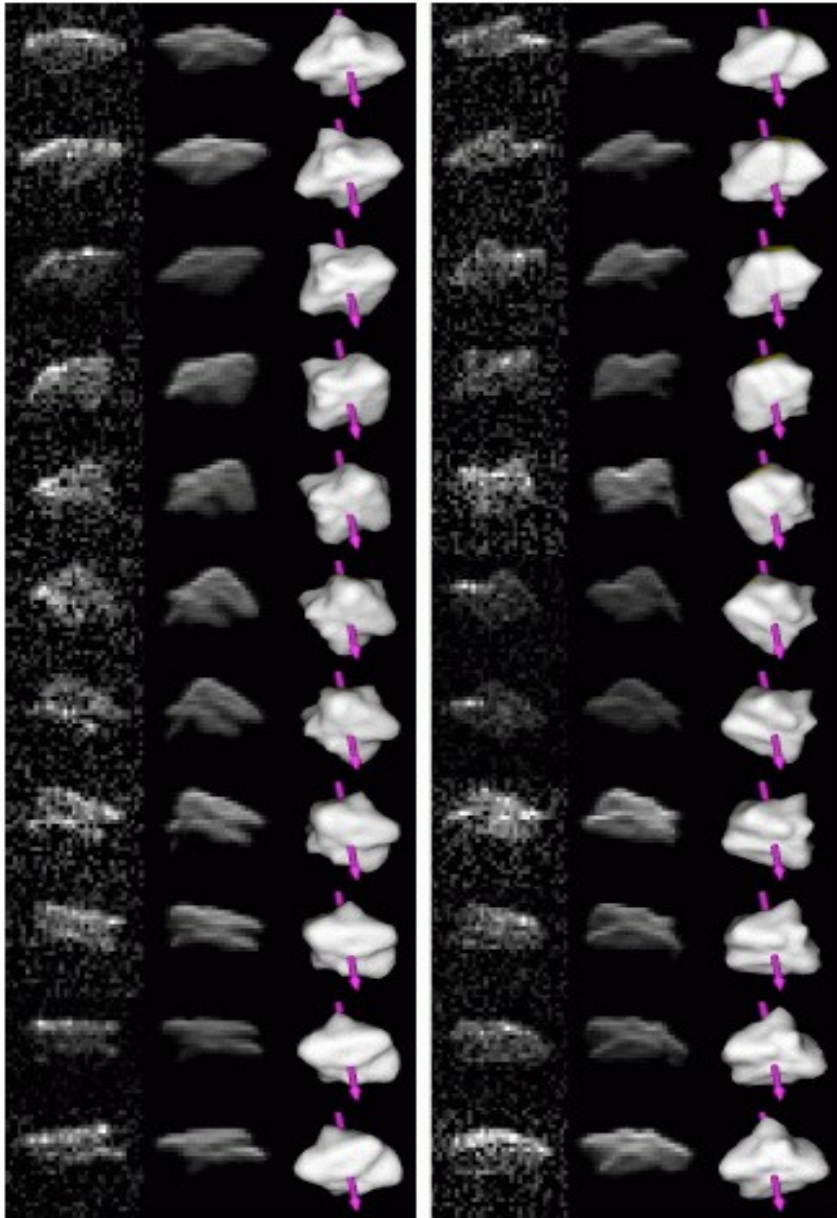


FIGURE 6 Graph of the Tisserand invariant. The solid line represents the Tisserand invariant with a value of 3. (Graph provided by Jeff Bytof, Jet Propulsion Laboratory, Pasadena, Calif.)

Radar image of 2000 PH5



Sizes, Shapes, Rotation

- Sizes:
 - 1000km \rightarrow m \rightarrow mm etc.
 - Only a few ones $>$ 500km diameter
 - Size distribution N versus mass m:
 $N(m) \sim m^{-3}$
 \rightarrow indicative for collision dominated size distribution
- Shapes:
 - Irregular except largest ones
(spacecraft + radar + lightcurves)
 - Triaxial ellipsoids
- Rotation:
 - Fast rotators more frequent
(irregular periodic lightcurves)
 \rightarrow in agreement with collision scenario, but strong bias from observations (long periods need longer observing time)



Mathilde

Gaspra

Ida

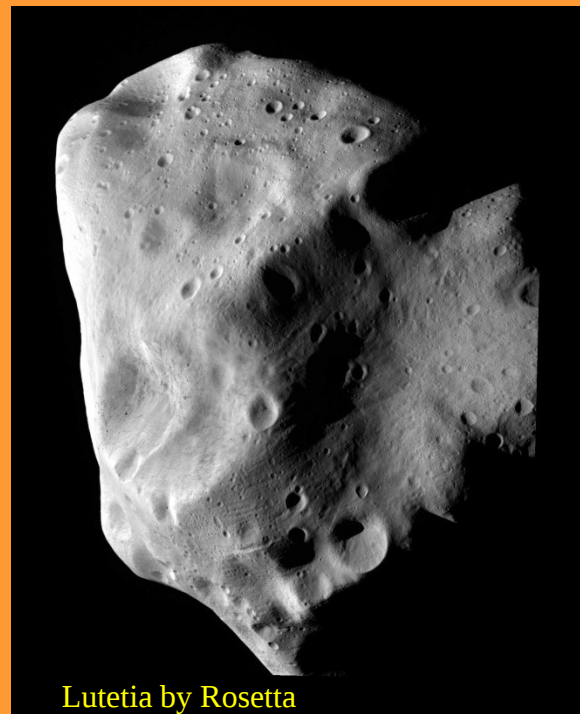


Eros by Shoemaker

December 3 2000 23:08:30 21° 146°



1999 SF56 by Hayabusa



Lutetia by Rosetta

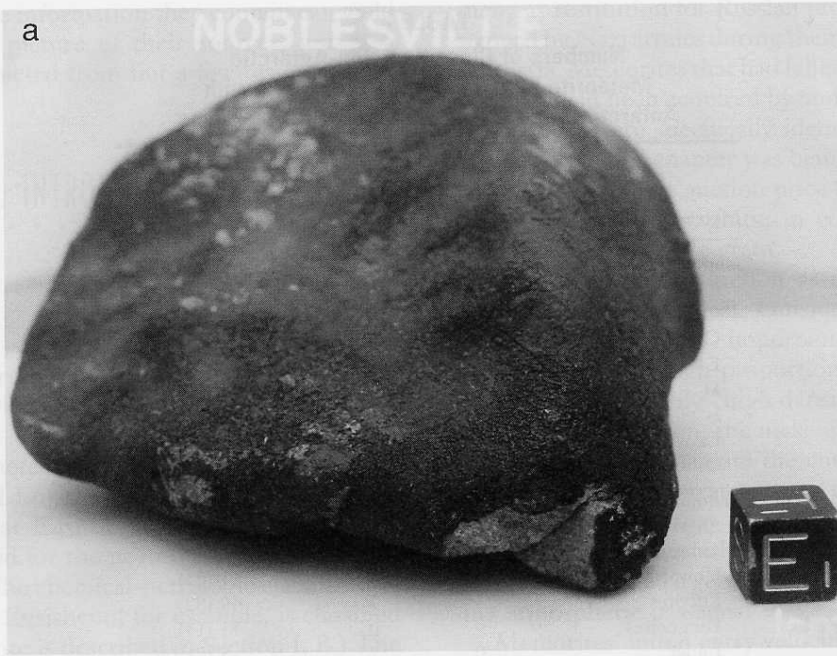


Steins by Rosetta

Meteorites

- **Summary**

- Differentiated (associated with asteroids) and undifferentiated (primitive) meteorites
- Chondrites: ,uniform‘ age $4.6 \cdot 10^9$ y = age of the solar system
- Solar composition (except volatile elements)
- Organics found (L aminoacids)
- Some isotopic peculiarities indicate non-uniform mixture of solar nebula



Meteorite with crust

Only the upper few cms are heated during entry in the atmosphere, the interior remains at deeply frozen temperature

Mars meteorite (SNC)

With signature of atmospheric ablations

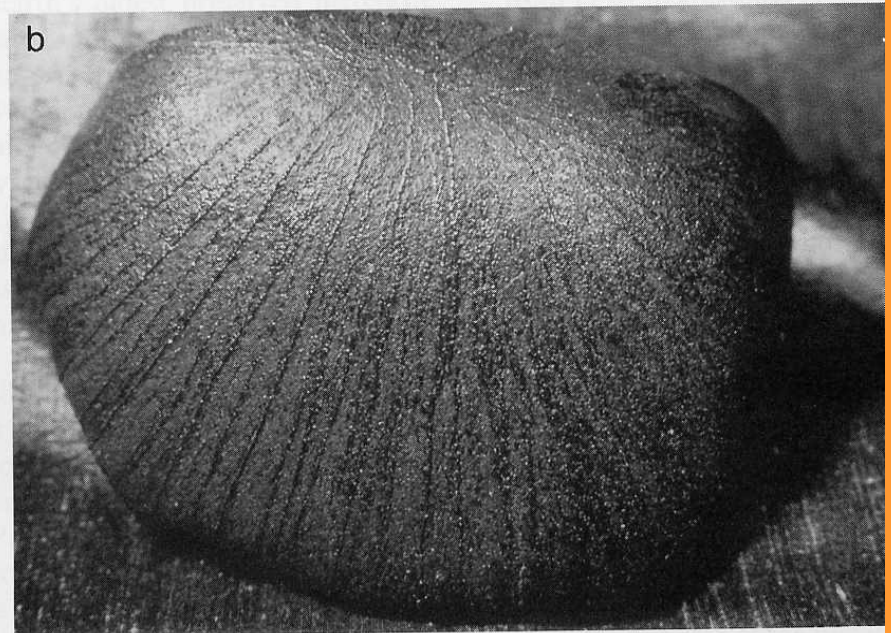




FIGURE 5 (continued)

Meteorites in the sky
and hitting a car

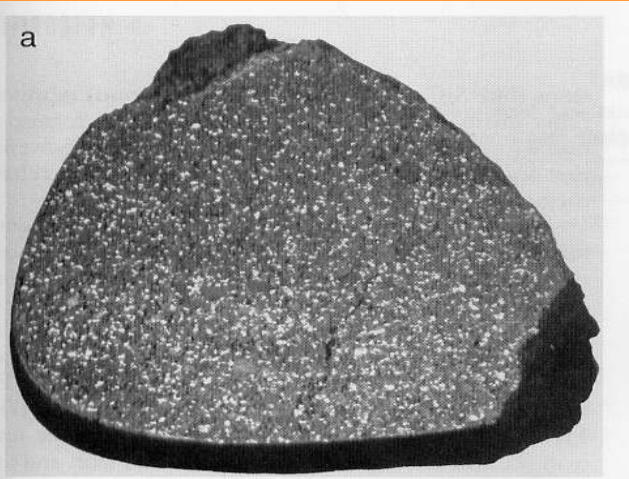
Allende meteorite



Large meteoroids: Above, a fireball (shown by arrow) of an 80 m object with estimated mass of 1 Mtonne, that apparently skipped out of the atmosphere, observed on August 10, 1972 moving left to right over Grand Teton National Park. (Photo courtesy of Dennis Milton) Below, the 1-km diameter Meteor Crater in Arizona formed by the explosive impact of the Canyon Diablo IA octahedrite meteoroid about 50 ka ago. (Photo courtesy of Allan E. Morton)

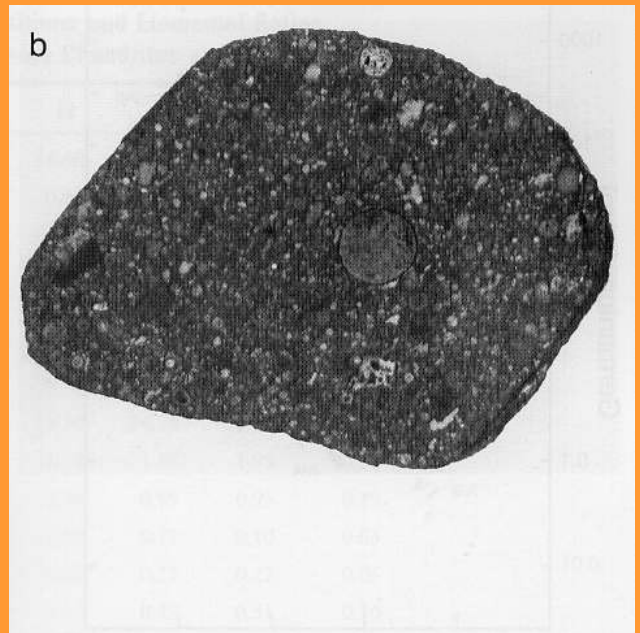


Meteorite - Types

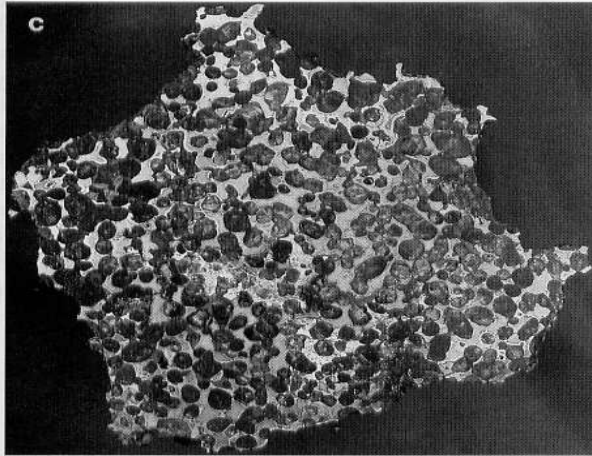


Chondrites
(spherical
chondrules are
present)

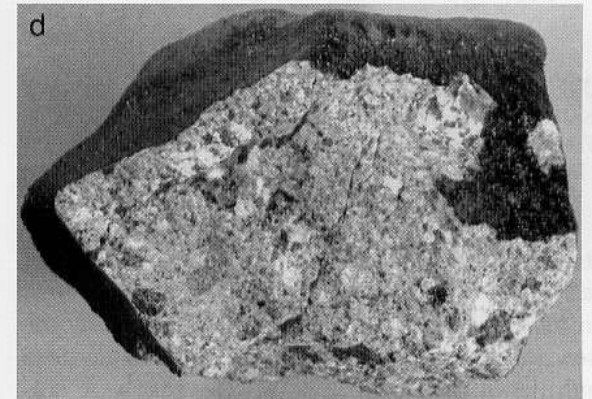
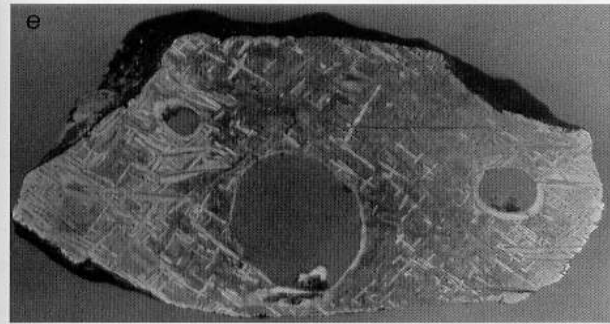
undifferentiated



Achondrites
differentiated



Nickel-Iron
differentiated

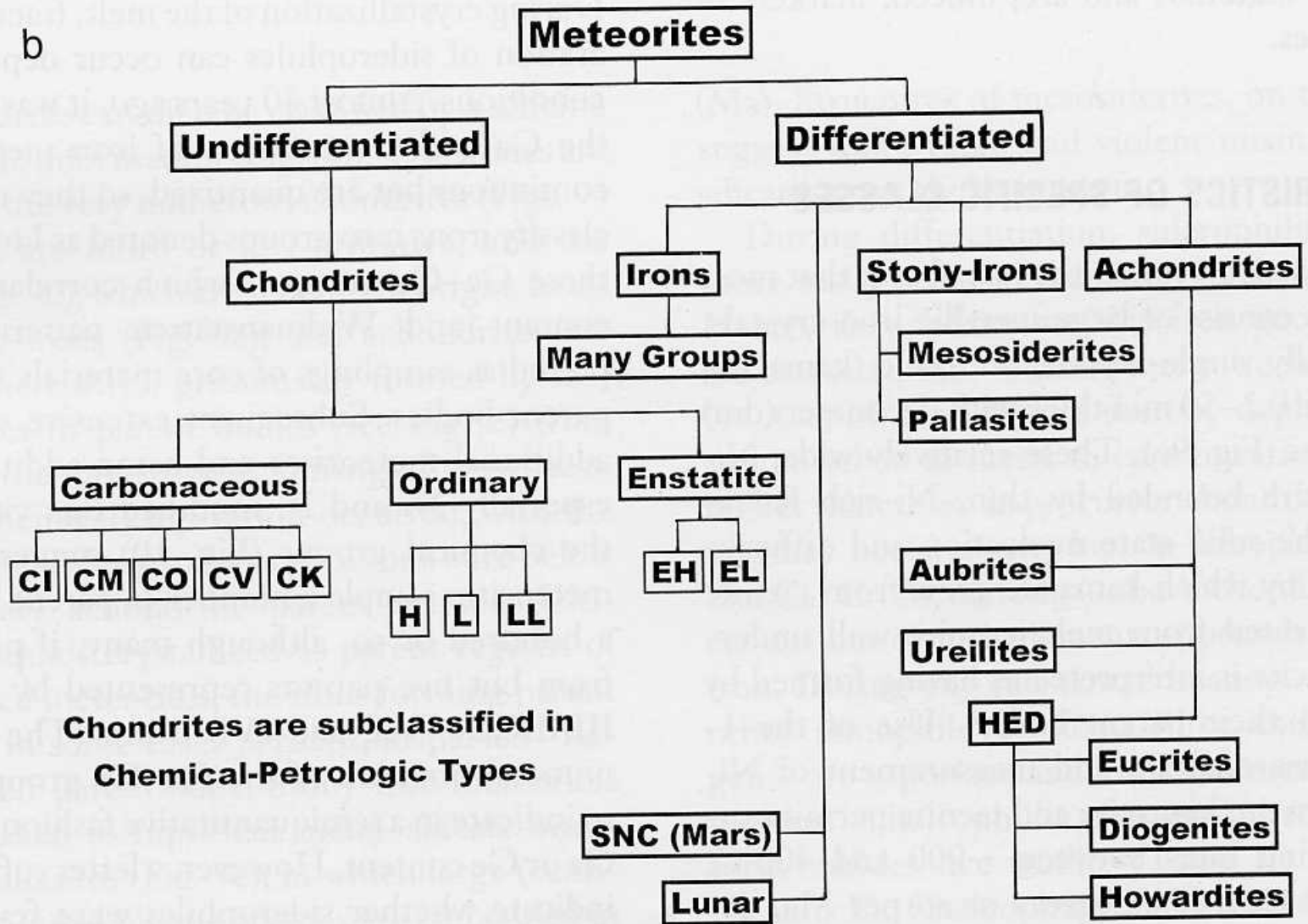


Tectides
terrestrial molten impact ejecta
not considered

Classification

- **Differentiated meteorites:** contain processed material, i.e. were part of a larger differentiated body and became meteorite as a collision product
 - Iron (4 %), Stony-Iron (1%), Achondrites (9%)
 - molten core, mantle-crust, crust of asteroids
 - differentiated meteorites have a clear link to asteroids
 - Widmanstätten pattern in iron meteorites: Ni content determines crystallisation
 - zones have different Ni content and crystallised at different times
- **Undifferentiated meteorites:** most original, unprocessed material from Solar System formation or before, chondrite types classified by iron content
 - normal Chondrites (81 %), carbonaceous Chondrites (5 %)
 - chondrule: spherical inclusion of silicate (olivine etc.) in surrounding matrix, created by melting and rapid cooling (re-crystallisation at ~1600K) process at zero gravity
 - either during early phase of the Sun or existent already before formation of the solar system (interstellar grains)
 - matrix material is produced by gentle aggregation of molecules at surface in space (surface reactions in cold environment under high energy radiation
 - formation of complex - also organic - molecules)

b



**Chondrites are subclassified in
Chemical-Petrologic Types**

a

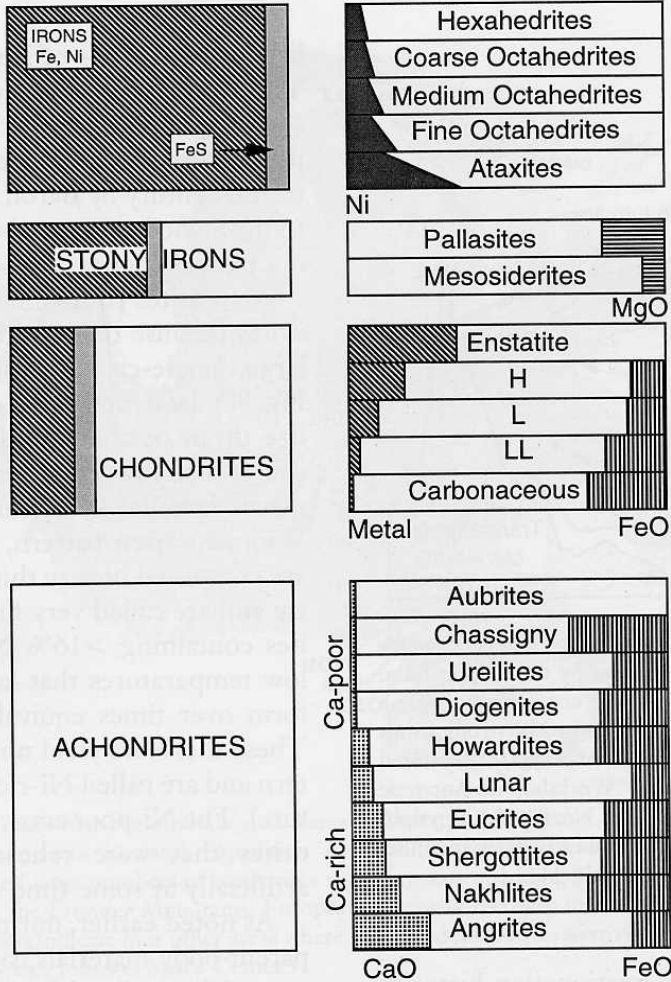


TABLE III
Average Chemical Compositions and Elemental Ratios of Carbonaceous and Ordinary Chondrites and Eucrites

| Species ^a | C1 | C2M | C3V | H | L | LL | EUC |
|--------------------------------|-------|-------|-------|-------|-------|-------|--------|
| SiO ₂ | 22.69 | 28.97 | 34.00 | 36.60 | 39.72 | 40.60 | 48.56 |
| TiO ₂ | 0.07 | 0.13 | 0.16 | 0.12 | 0.12 | 0.13 | 0.74 |
| Al ₂ O ₃ | 1.70 | 2.17 | 3.22 | 2.14 | 2.25 | 2.24 | 12.45 |
| Cr ₂ O ₃ | 0.32 | 0.43 | 0.50 | 0.52 | 0.53 | 0.54 | 0.36 |
| Fe ₂ O ₃ | 13.55 | | | | | | |
| FeO | 4.63 | 22.14 | 26.83 | 10.30 | 14.46 | 17.39 | 19.07 |
| MnO | 0.21 | 0.25 | 0.19 | 0.31 | 0.34 | 0.35 | 0.45 |
| MgO | 15.87 | 19.88 | 24.58 | 23.26 | 24.73 | 25.22 | 7.12 |
| CaO | 1.36 | 1.89 | 2.62 | 1.74 | 1.85 | 1.92 | 10.33 |
| Na ₂ O | 0.76 | 0.43 | 0.49 | 0.86 | 0.95 | 0.95 | 0.29 |
| K ₂ O | 0.06 | 0.06 | 0.05 | 0.09 | 0.11 | 0.10 | 0.03 |
| P ₂ O ₅ | 0.22 | 0.24 | 0.25 | 0.27 | 0.22 | 0.22 | 0.05 |
| H ₂ O ⁺ | 10.80 | 8.73 | 0.15 | 0.32 | 0.37 | 0.51 | 0.30 |
| H ₂ O ⁻ | 6.10 | 1.67 | 0.10 | 0.12 | 0.09 | 0.20 | 0.08 |
| Fe ⁰ | | 0.14 | 0.16 | 15.98 | 7.03 | 2.44 | 0.13 |
| Ni | | | 0.29 | 1.74 | 1.24 | 1.07 | 0.01 |
| Co | | | 0.01 | 0.08 | 0.06 | 0.05 | 0.00 |
| FeS | 9.08 | 5.76 | 4.05 | 5.43 | 5.76 | 5.79 | 0.14 |
| C | 2.80 | 1.82 | 0.43 | 0.11 | 0.12 | 0.22 | 0.00 |
| S (elem) | 0.10 | | | | | | |
| NiO | 1.33 | 1.71 | | | | | |
| CoO | 0.08 | 0.08 | | | | | |
| NiS | | | 1.72 | | | | |
| CoS | | | 0.08 | | | | |
| SO ₃ | 5.63 | 1.59 | | | | | |
| CO ₂ | 1.50 | 0.78 | | | | | |
| Total | 98.86 | 99.82 | 99.84 | 99.99 | 99.99 | 99.92 | 100.07 |
| ΣFe | 18.85 | 21.64 | 23.60 | 27.45 | 21.93 | 19.63 | 15.04 |
| Ca/Al | 1.08 | 1.18 | 1.10 | 1.11 | 1.12 | 1.16 | 1.12 |
| Mg/Si | 0.90 | 0.89 | 0.93 | 0.82 | 0.80 | 0.80 | 0.19 |
| Al/Si | 0.085 | 0.085 | 0.107 | 0.066 | 0.064 | 0.062 | 0.290 |
| Ca/Si | 0.092 | 0.100 | 0.118 | 0.073 | 0.071 | 0.072 | 0.325 |
| Ti/Si | 0.004 | 0.006 | 0.006 | 0.004 | 0.004 | 0.004 | 0.0019 |
| ΣFe/Si | 1.78 | 1.60 | 1.48 | 1.60 | 1.18 | 1.03 | 0.66 |
| ΣFe/Ni | 18.12 | 16.15 | 16.85 | 15.84 | 17.73 | 18.64 | |
| Fe ⁰ /Ni | | | 9.21 | 5.67 | 2.29 | | |
| Fe ⁰ /ΣFe | | | 0.58 | 0.32 | 0.12 | | |

^a ΣFe includes all iron in the meteorite whether existing in metal (Fe⁰), FeS, iron silicates as Fe²⁺ (FeO), or Fe³⁺ (Fe₂O₃). The symbol H₂O⁻ indicates loosely bound (adsorbed?) water removable by heating up to 110°C; H₂O⁺ indicates chemically bound water that can be lost only above this temperature. (Data courteously provided by Dr. E. Jarosewich, Smithsonian Institution.)

Note: almost all meteorites contain iron

First check: magnetism of probe

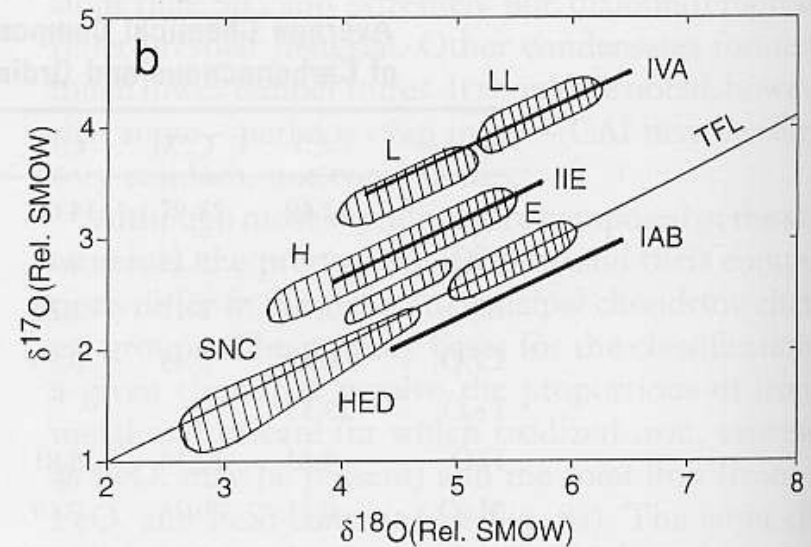
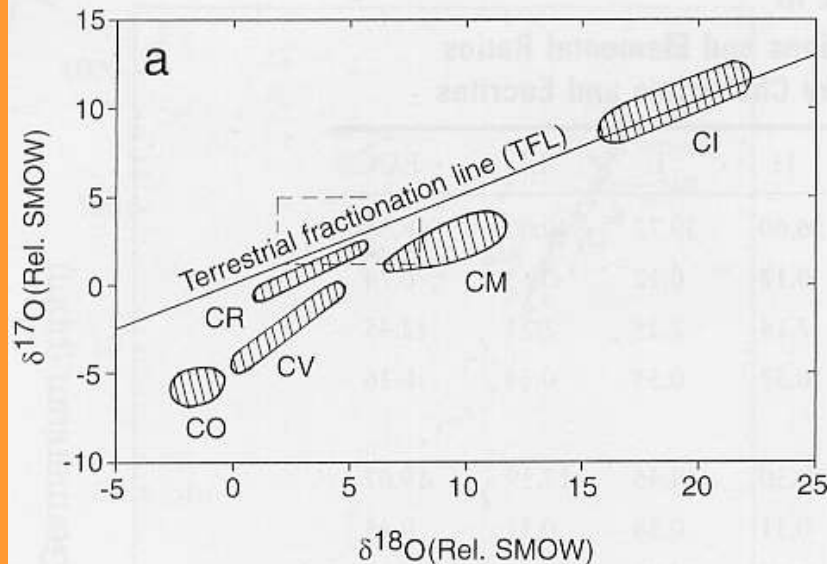
Verification: spallation isotope

Composition of chondrites is dominated by SiO₂, Fe₂O₃ and MgO

Oxygen Isotopics & Solar Chemistry

- Oxygen Isotopics

- Concept: mass-dependent process involving O will create $^{17}\text{O}/^{18}\text{O}$ content with ratio $\frac{1}{2}$ (mass-fractionation: slow process with minor but measurable effects)
- Earth, moon, many chondrites and some achondrites on $\frac{1}{2}$ fractionation line
- Some other chondrites deviate
 - ➔ solar system was created from a non-heterogeneous (O) isotopic mixture (most likely of pre-solar origin)



- Isotopic composition CI to solar photosphere:
 - Overall isotopic composition of CI chondrites is basically identical to solar photosphere (with some exceptions: gaseous and light elements, small deviations for mass-fractionation)

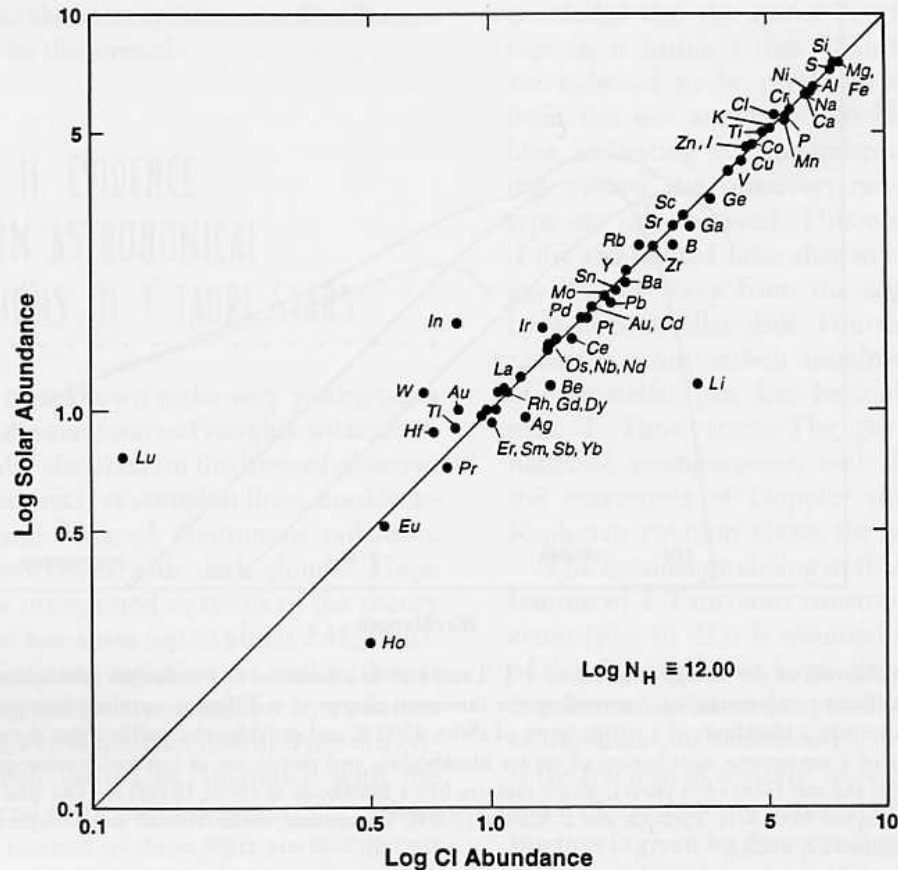


FIGURE 7 Elemental abundances in the solar photosphere are shown on a log–log plot versus those abundances measured in the CI carbonaceous chondrites. The abundances are normalized to 10^{12} hydrogen atoms: $\log N_{\text{H}} = 12.00$. The remarkable 1:1 correspondence displayed for all but the most volatile elements is strong evidence for the creation of the CI meteorites out of unfractionated solar material, as well as for the essential homogeneity of the solar nebula. (Even some of the deviations are well understood. For instance, lithium in the Sun is low relative to CI abundances because lithium has been destroyed by nuclear reactions in the Sun.)

Organics & Hydration

- Organics (carbonaceous chondrites):

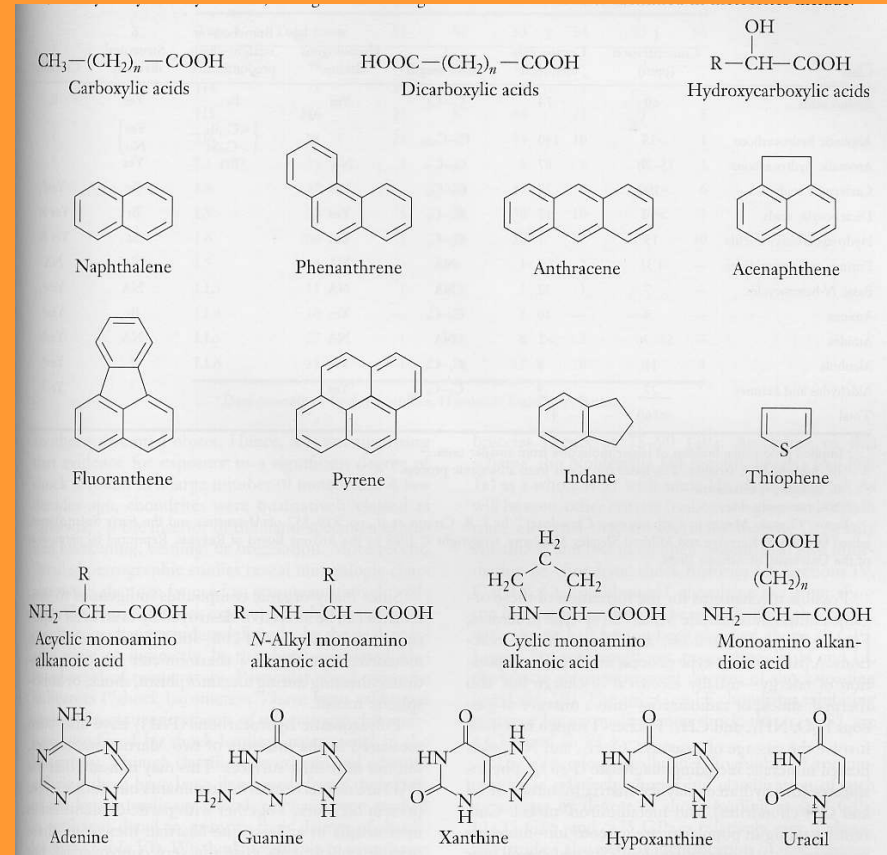
- More than 400 organics compounds identified in meteorites
- All of non-biogenic, preterrestrial origin, but some with pre-biotic relevance

(aminoacids of Murchinson & Orgueil L>D chirality)

- many organics never hotter than 200-300K otherwise it would not exist in carbonaceous chondrites

- Hydration Effects:

- Many chondrites contain signatures from hydration (chemistry modification due to presence of water – also in liquid form, inclusion of water molecules in mineral lattice)



→ Obs. indications for water ice in the asteroid belt: water ice absorption in Themis, main belt comets

Chronology with Meteorites

- Pre-requisite: state/phase transition locks isotopic ratio in meteorite
radioactive and stable nuclides are measurable

- Number of daughter nuclides D_t at time t

$$D_t = D_0 + M_0 - M_t = D_0 + M_t (e^{\lambda t} - 1) \quad (1)$$

D_0, M_0 = daughter (unknown), mother (measured) nuclides at 'locking' time

D_t, M_t = daughter, mother nuclides measured in lab

λ = decay time of isotope

Trick: find/measure stable isotope D_x : $d D_x / dt = 0$

$$(D / D_x)_t = (D / D_x)_0 + (M / D_x)_t (e^{\lambda t} - 1)$$

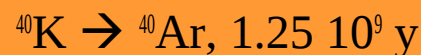
Linear relation: $y = I + x * m \rightarrow$ determine m , i.e. age t of the probe

$$t = 1 / \lambda \ln (1 + ((D / D_x)_t - (D / D_x)_0) / (M / D_x)_t)$$

Formation age = time of crystallisation

Radiation age = duration of high energy irradiation in space

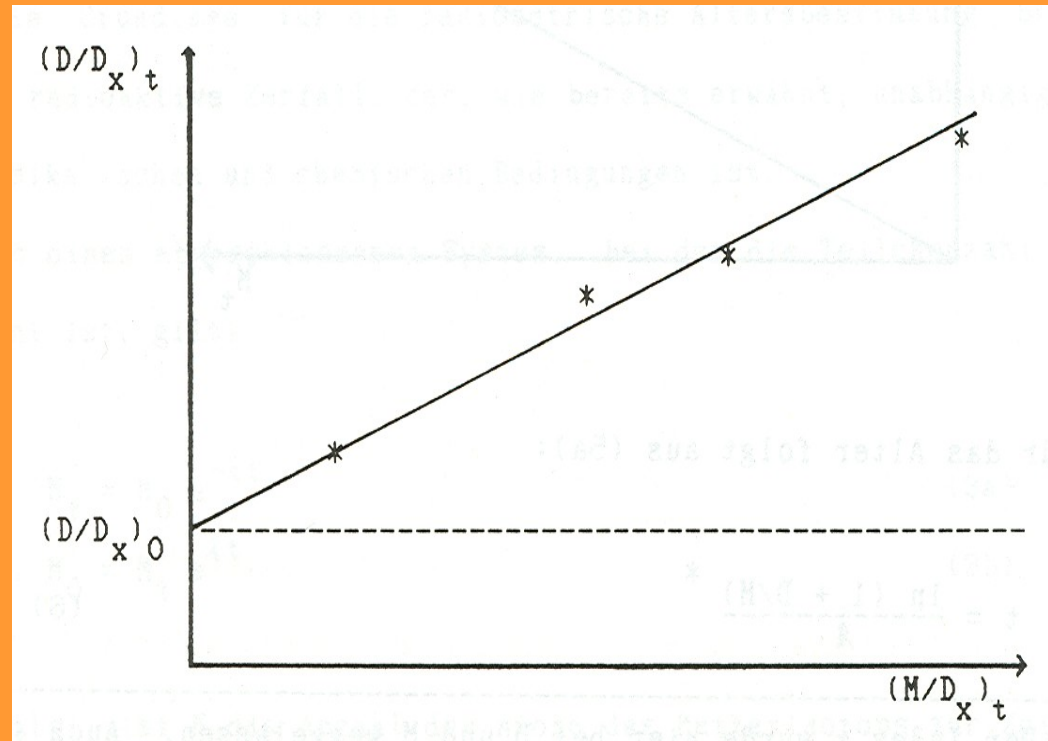
Nuclides used:



Age determination of meteorites

Recipe:

- measure radioactive isotopes “mother” & “daughter”
- plot linear relation
- determine slope $m = \exp(\lambda t) - 1$
- determine $y_0 = (D / D_x)_0$
- calculate age



Solidification age of chondrites

- $4.56 \cdot 10^9$ y $\pm 10^7$ y (H-types)
- ingredients of solar system agglomerated quasi-simultaneously during a short time
- many L-types heated within last 10^9 y (shock-heating)

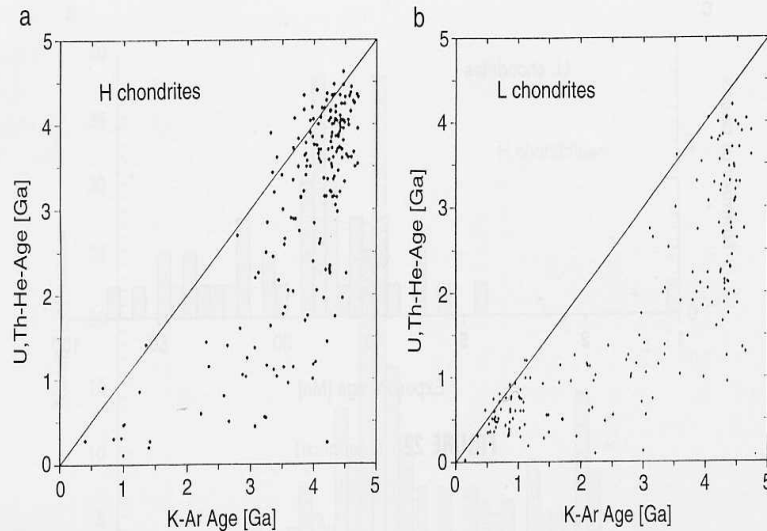


FIGURE 24 Gas retention ages of H and L chondrites. Data obtained from the U, Th-He and K-Ar methods are plotted against each other. The 45° line represents concordant ages. The very different trends indicate that the thermal histories of the two types of ordinary chondrites differ. The concordant long ages of H chondrites suggest that, in general, their parent body or bodies have remained thermally unaltered since they formed 4–4.5 Ga ago. The concordant short ages of L chondrites suggest that they were shock-heated in a major collision(s) 0.1–1.0 Ga ago. Nearly all discordant meteorites lie below the concordance lines because radiogenic ^4He is lost far more readily than is radiogenic ^{40}Ar .

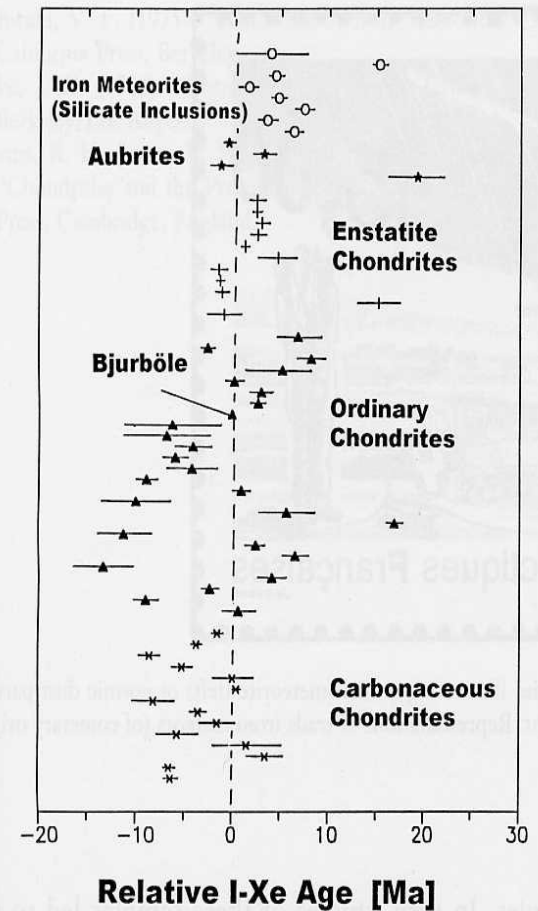


FIGURE 26 ^{129}I – ^{129}Xe formation ages for various sorts of chondrites, aubrites, and silicate portions of iron meteorites, relative to that of Bjurböle (older ages to the left and more recent ones to the right).

Cosmic ray exposure age

Meteorite being exposed to cosmic rays in space

→ ~100 million years (chondrites)

→ before they were included in larger body

→ iron meteorites last longer (IIIAB types may be produced by single massive impact event)

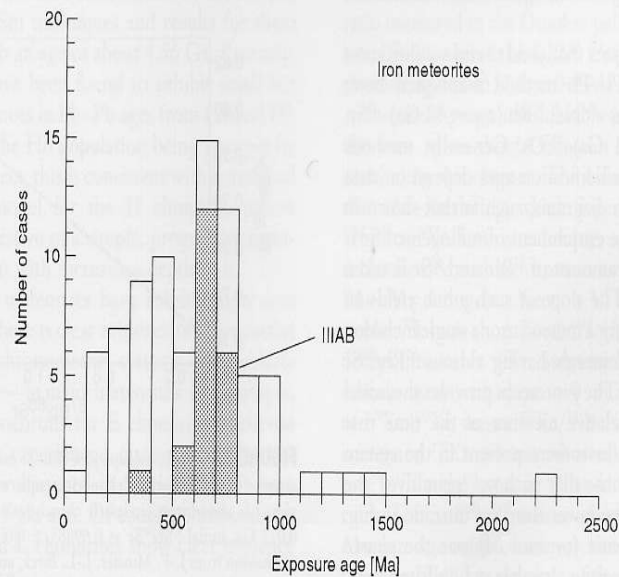


FIGURE 23 Cosmic ray exposure ages determined by the ^{40}K - ^{41}K method for iron meteorites. The group IIIAB irons, nearly all of which were apparently produced by a single, massive collision of their parent body 650 ± 60 Ma ago, are depicted in the shaded region.

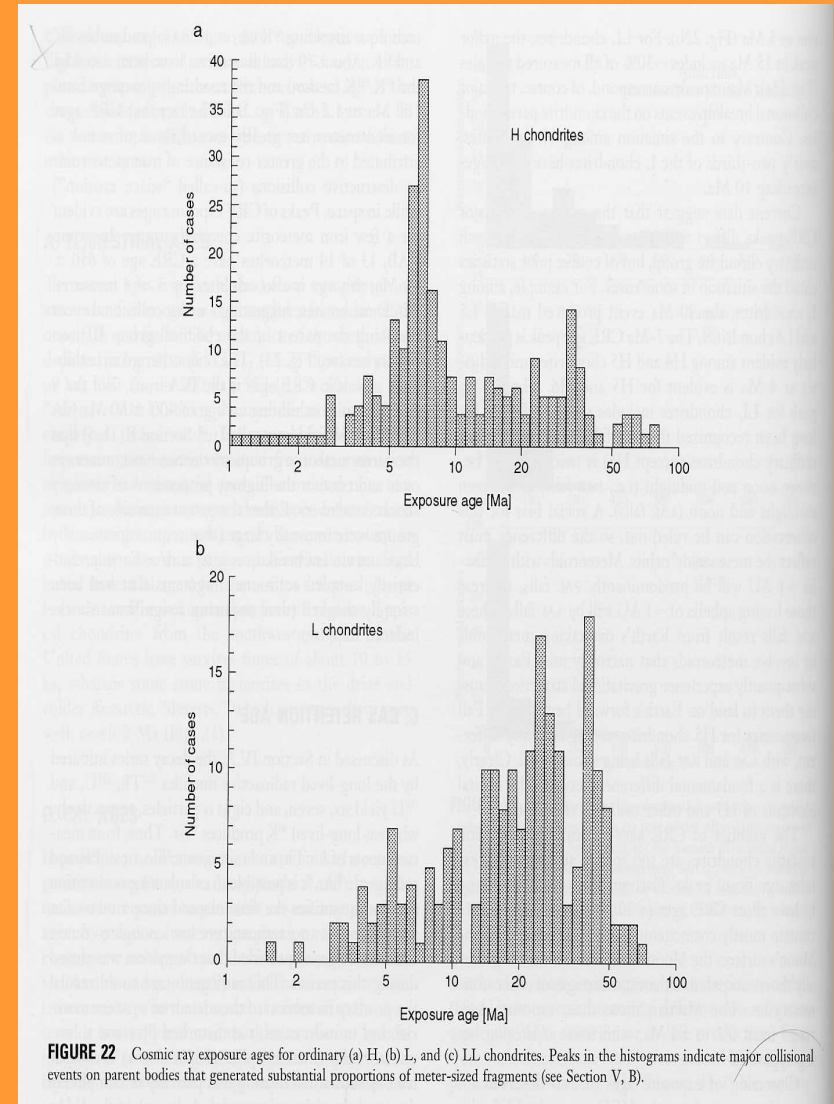


FIGURE 22 Cosmic ray exposure ages for ordinary (a) H, (b) L, and (c) LL chondrites. Peaks in the histograms indicate major collisional events on parent bodies that generated substantial proportions of meter-sized fragments (see Section V, B).

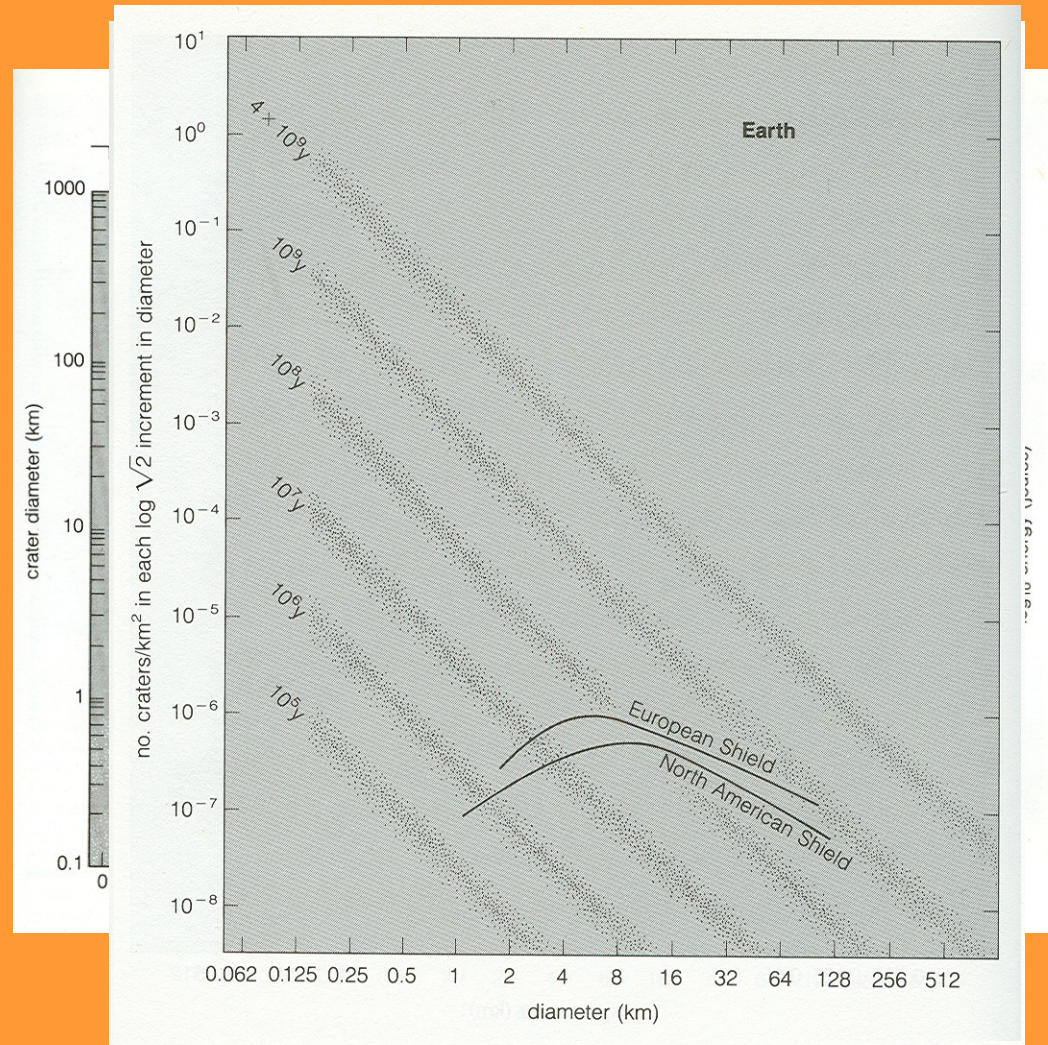
Dating of surface ages

Recipe:

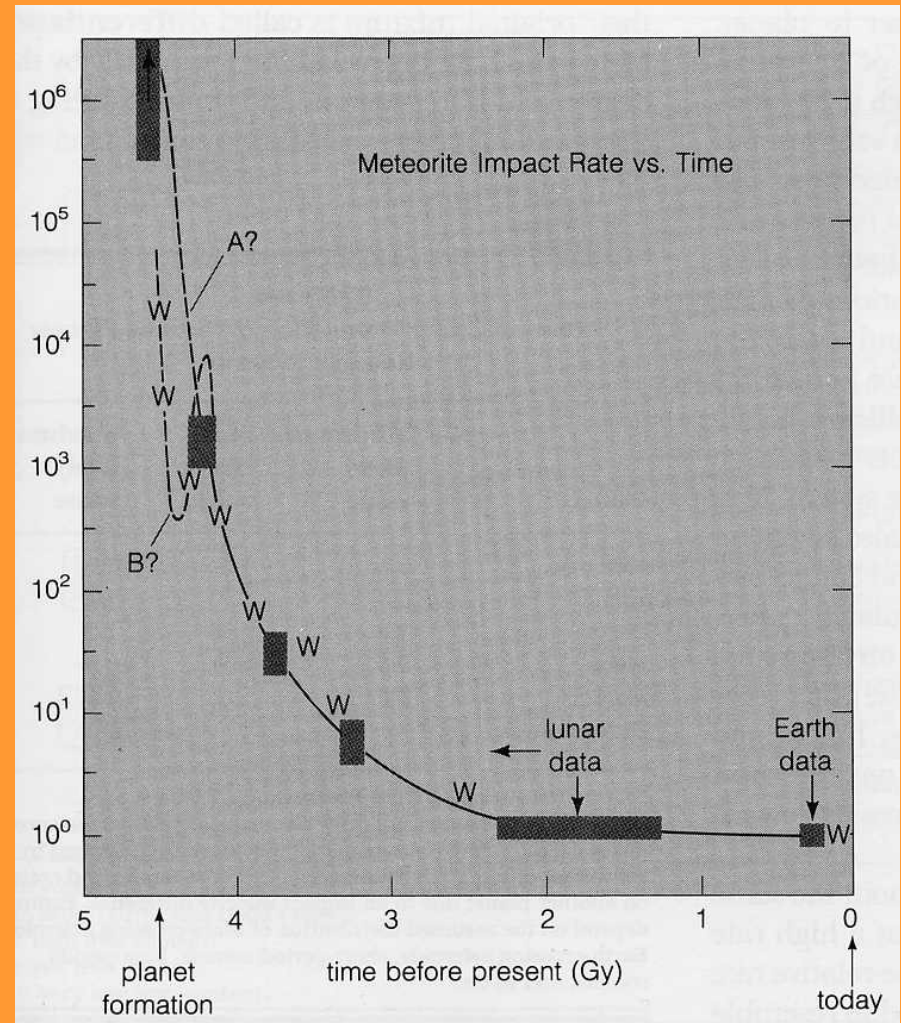
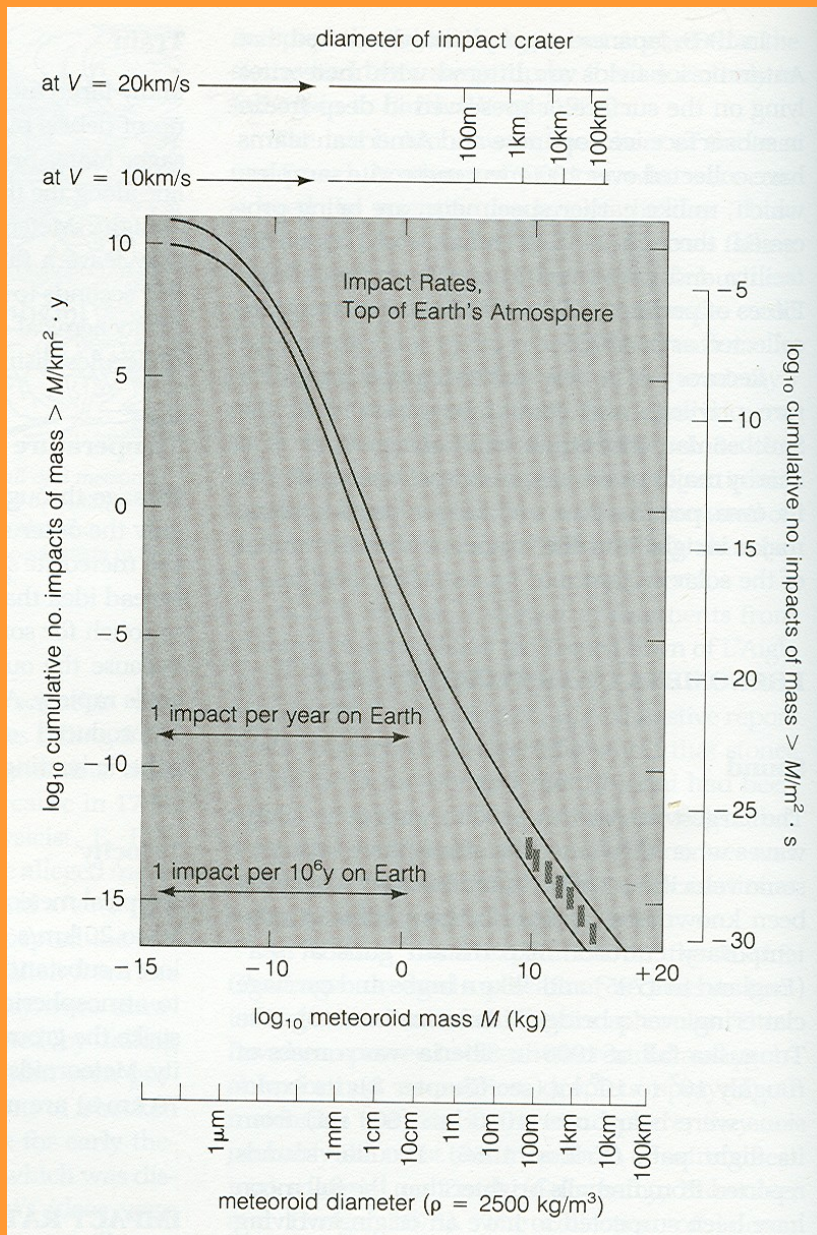
- count surface density of craters
- plot surface density versus diameter of craters
- compare with isochrone lines
- calibration of isochrone lines mostly from sample analysis of Apollo moon missions

Moon: old surface modeled by early and late heavy bombardment

Earth: young surface due to tectonics, erosion, life



Cratering and planetary system formation



Comets

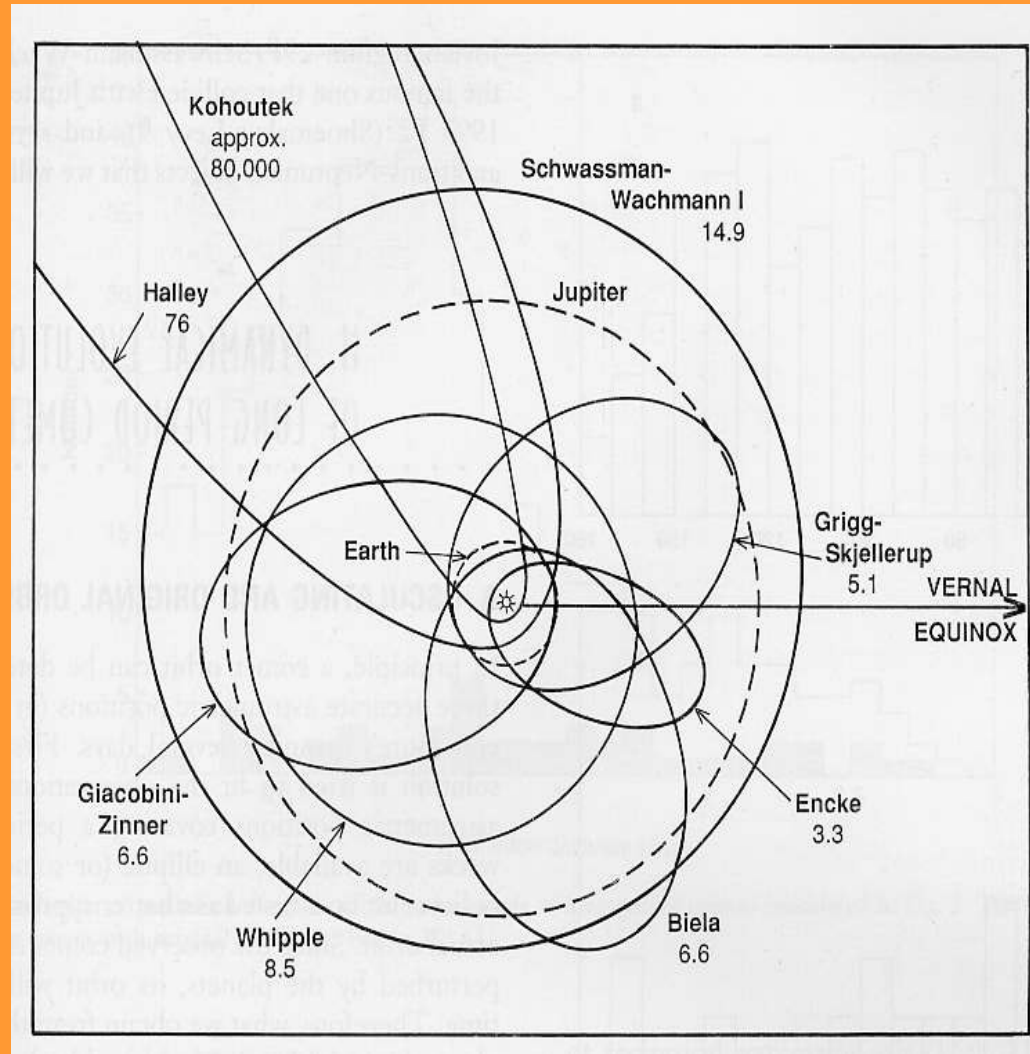
- **Summary**
 - Elliptical-hyperbolic orbits
 - Two reservoirs: short period comets & Oort cloud comets
 - Dirty snowball nucleus, km size
 - Main composition: water and silicates, some organics
 - Solar composition, possibly primordial (frozen)



Comet Hale-Bopp with dust and ion tail

Orbits

- Forms: ellipse+hyperbola
(parabola easy fit of the other two)
 - ➔ no extreme hyperbola found
($e \gg 1$; max. 1.005)
 - ➔ all observed comets belong to the solar system, hyperbolas caused by non-gravitational forces (reaction forces due to outgassing when active close to the Sun)
- Dynamical classes:
 - Short-period comets ($P < 200$ y)
Ecliptic oriented
captured and dominated by Jupiter gravity (Jupiter family comets)
,old' comets (evolved)



- Long-period comets ($P > 200$ y)
- isotropic distribution, highly eccentric
- distribution of inverse semi-major axis peaks for large distances from the Sun
- Oort cloud of comets (10^{12})
- less evolved objects (new comets)
- perturbations by stars & molecular clouds of our galaxy cause Oort comet to enter into the planetary system

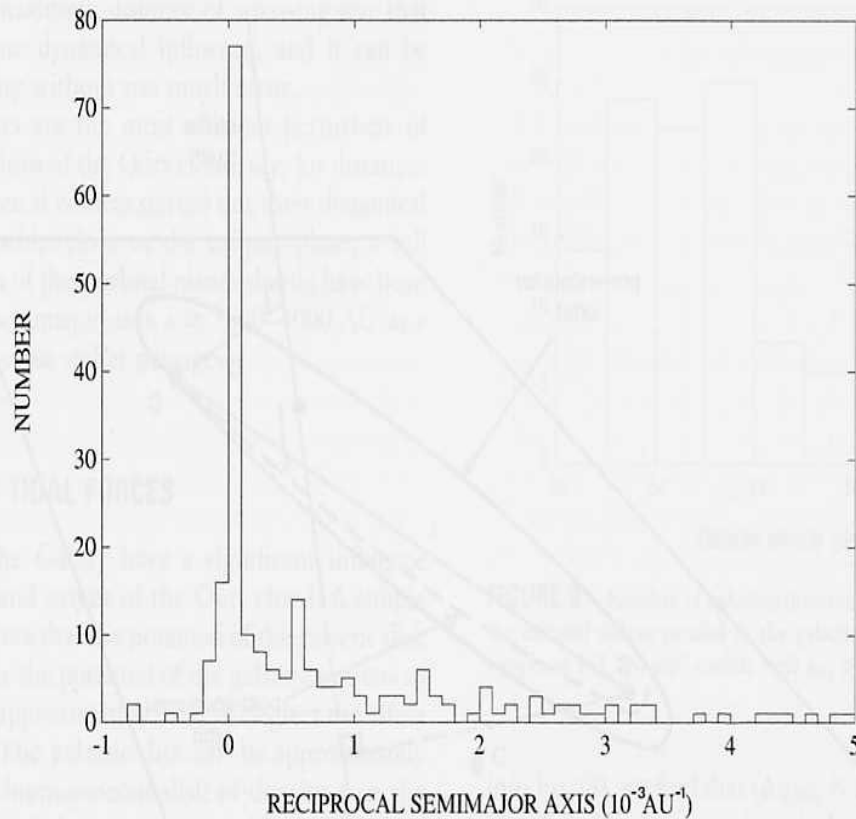


FIGURE 6 Distribution of the original inverse semimajor axes of observed long-period comets with $(1/a)_{\text{orig}} < 5 \times 10^{-3} \text{ AU}^{-1}$.

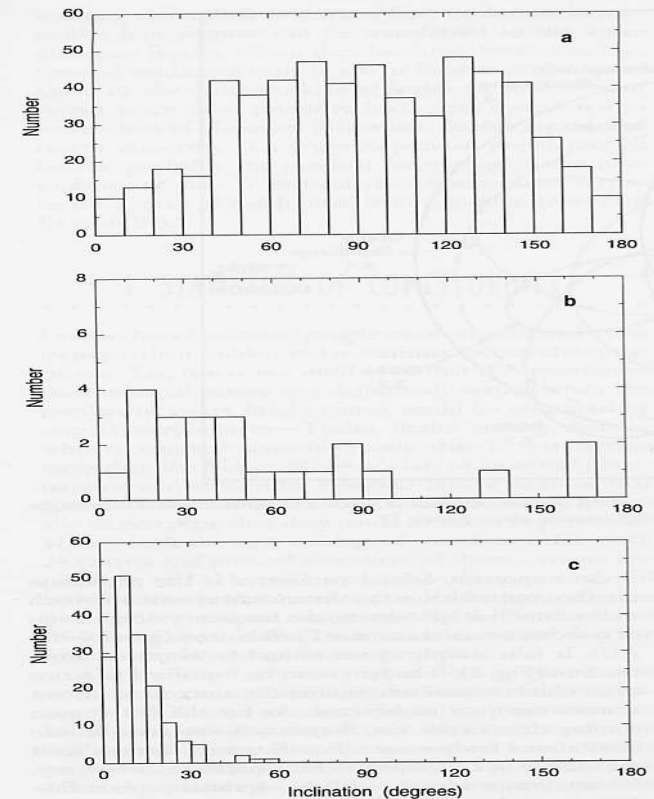


FIGURE 2 Inclination distributions of (a) long-period comets discovered after 1758 (the Kreutz family of sungrazing comets has been considered as a single comet, as well as C/1988F1 and C/1988J1, which move in similar orbits), (b) intermediate-period comets with $20 < P < 200$ yr, and (c) short-period comets with $P \leq 20$ yr.

Nature

- Nucleus: dirty snowball that becomes active when getting close (<5 AU) to the Sun
 - Sizes: a few 100 m – some 10 km
(Wirtanen 600m) (Hale-Bopp 30km)
 - Shape: irregular with surface structures
 - Albedo: 1-5 %, darkest solar system objects
 - Rotation: a few hours (if measured)
- Density: 0.1 – 1 g/cm³ (uncertain)
- very weak structure (10⁴ dyn/cm²)
- Different models for nuclei exist
 - Rubble pile (c)
 - Agglomerate with crust (d)

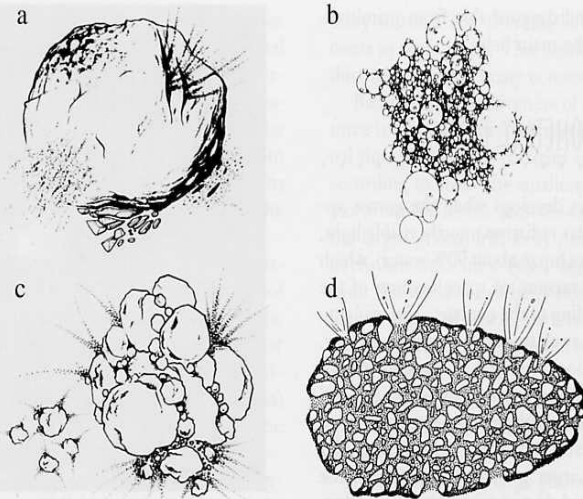


FIGURE 3 Four artist's concepts of suggested models for the structure of cometary nuclei: (a) the icy conglomerate model, (b) the fluffy aggregate model, (c) the primordial rubble pile, and (d) the icy-glue model. Evidence has continued to mount that the fluffy aggregate and the primordial rubble pile are the most likely representations of nucleus structure. All but model (d) were suggested prior to the Halley spacecraft encounters in 1986.



FIGURE 2 A composite image of the nucleus of Comet P/Halley as photographed by the camera onboard the *Giotto* spacecraft on March 14, 1986. The Sun is located toward the left, 29° above the horizontal. Note the elongated and irregular shape of the nucleus, which has dimensions of 16 × 8 × 7 km. The heterogeneity of the irregular surface is well illustrated; several surface features can be seen, including active regions and hills. The smallest features that can be resolved are about 100 m across. (Courtesy of H. U. Keller, Max-Planck-Institut für Aeronomie.)

How do they look like?

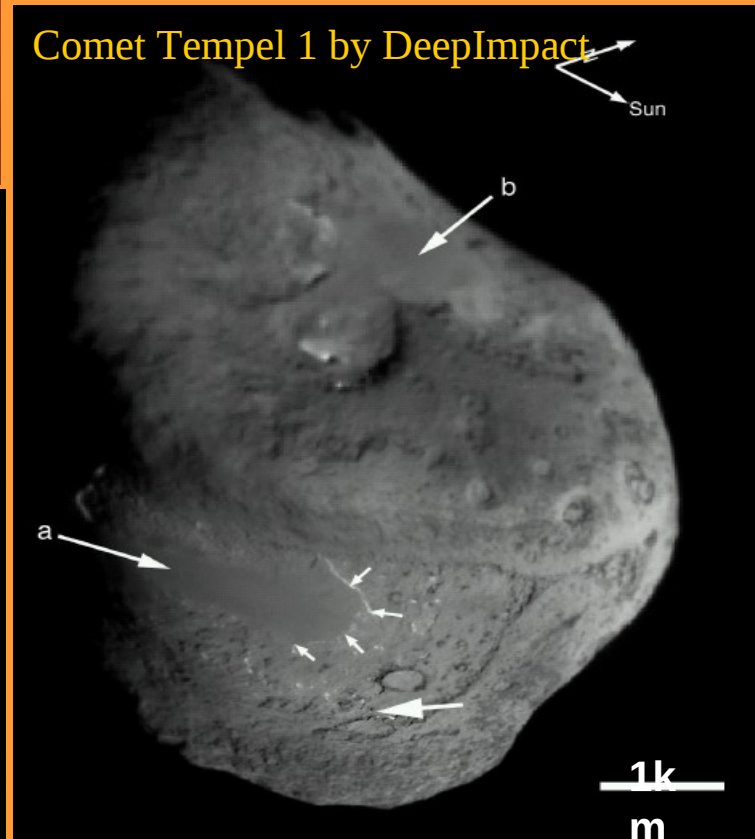
Comet Halley by GIOTTO



Comet Borrelly by DEEPSPACE 1



Comet Tempel 1 by DeepImpact



Comet Wild2 by STARDUST

Coma: activity develops when nucleus is heated close to the Sun (on sunward side)

- Extension: $5 \cdot 10^4 - 3 \cdot 10^6$ km
- Frozen ice sublimates to gas
 - H_2O : ~80% ice
 - $CO+CO_2+H_2CO$: 4+3+2 (distant activity to several 10 AU)
 - Lots of organics identified
- Embedded dust is accelerated by gas
 - Mass ratio gas:dust 0.1-10
 - Silicate (fosterite), CHON, metallic
 - crystalline (hot) & amorphous (cold) silicates → protosolar nebula got mixed up before comet formation
- Total production rates (gas, dust)
 - $10^{23}-10^{32}$ molecules/s (several 100 tons/s max)
 - mass loss ~ 10000 revolutions life time in inner solar system
 - continuous supply of comet required
- Crust formation: dust remains or falls back to surface
- Activity frequently localized

Activity comes from upper few cm-m of the nucleus, nucleus core remains at low temperature 40-80K)

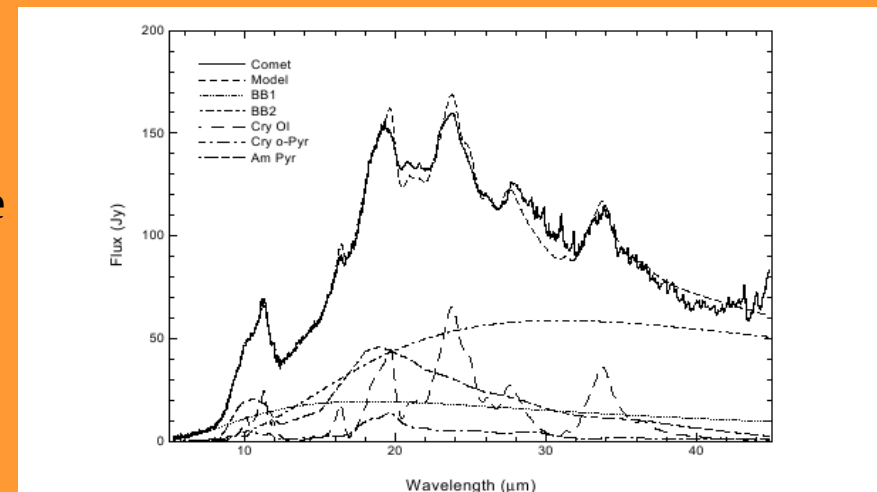
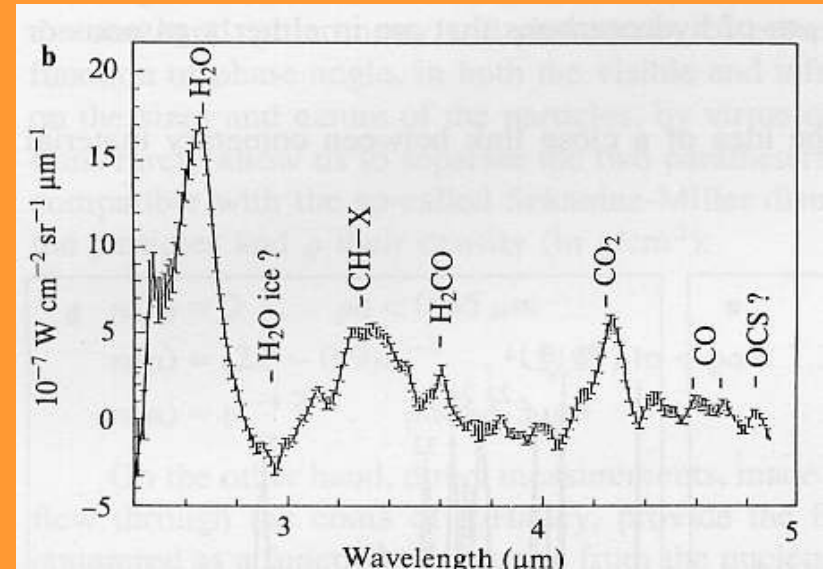


Fig. 2. ISO SWS spectrum of Comet Hale-Bopp at $r = 2.8$ AU, degraded to $\lambda = 500$, compared with a five-component dust model: 280 K blackbody (BB1); 165 K blackbody (BB2); forsterite (Cry OI 22%); orthopyroxene (Cry o-Pyr 8%); and amorphous pyroxene (Am Pyr 70%). From Crovisier et al. (2000).

TABLE I
Chemical Species Identified in Comets

| Identification by radio, microwave, IR, visual, and UV spectra | | | | | | | | | | | | |
|--|--|------------------------------|--|-------------------------------|--|-------------------------------|-------------------------------|-----------------------------|-------------------------------|----|-------------------|----|
| H | C | O | S | CO ₂ | HDO | CHO | DCN | HNC | CO | CS | NH | OH |
| C ₂ | ¹³ C ¹⁸ O | CH | H ₂ C ₂ O ₂ | ¹³ CN | H ¹³ CN | HC ¹⁵ N | OCS | SO ₂ | S ₂ | SO | | |
| C ₃ | NH ₂ | H ₂ O | HCOOH | C ₂ H ₂ | H ₂ S | H ₂ CS | HNCO | CH ₄ | HCO | CN | HC ₃ N | Na |
| NH ₃ | H ₂ CO | HCN | CH ₃ OH | CH ₃ CN | HC ₃ N | NH ₂ CHO | C ₂ H ₆ | | | | | |
| C ⁺ | CO ⁺ | CH ⁺ | CN ⁺ | HCO ⁺ | CO ₂ ⁺ | H ₂ O ⁺ | H ₂ S ⁺ | N ₂ ⁺ | H ₃ O ⁺ | | | |
| Identification by mass spectra | | | | | | | | | | | | |
| Mass | Ions | | Neutrals | | | | | | | | | |
| 1 | H ⁺ | | | | | | | | | | | |
| 12 | C ⁺ | | | | | | | | | | | |
| 13 | CH ⁺ | | | | | | | | | | | |
| 14 | CH ₂ ⁺ | N ⁺ | | | | | | | | | | |
| 15 | CH ₃ ⁺ | NH ⁺ | | | | | | | | | | |
| 16 | O ⁺ | CH ₂ ⁺ | NH ₂ ⁺ | | | | | | | | | |
| 17 | OH ⁺ | NH ₃ ⁺ | CH ₃ ⁺ | | | | | | | | | |
| 18 | H ₂ O ⁺ | NH ₂ ⁺ | H ₂ O | | | | | | | | | |
| 19 | H ₃ O ⁺ | | | | | | | | | | | |
| 23 | Na ⁺ | | | | | | | | | | | |
| 28 | | | CO | N ₂ [?] | C ₂ H ₂ [?] | | | | | | | |
| 30 | | | H ₂ CO | | | | | | | | | |
| 31 | H ₃ CO ⁺ | | | | | | | | | | | |
| 35 | H ₂ S ⁺ | | | | | | | | | | | |
| 36 | C ₂ ⁺ | | | | | | | | | | | |
| 37 | C ₃ H ⁺ | | | | | | | | | | | |
| 39 | C ₂ H ₂ ⁺ | | | | | | | | | | | |
| 44 | | | CO ₂ | | | | | | | | | |

TABLE II
Identified Interstellar Molecules in the Gas Phase

| | | | | | | | |
|---|------------------------------------|------------------------------------|------------------------------------|---|------------------------------------|--------------------------------|--------------------|
| H ₂ | C ₂ | CO | CS | NaCl ^a | HCl | SiO | SiS |
| AlCl ^a | KCl ^a | PN | AlF ^a | SiN ^a | SiH ^b | HF ^b | |
| H ₂ O | SO ₂ | H ₂ S | OCS | HNO | C ₂ ^a | HCN | C ₂ O |
| HNC | SiC ₂ ^a | NH ₂ | N ₂ O | MgNC ^a | MgCN ^a | NaCN ^a | |
| NH ₃ | HC ₂ H | C ₂ O | HNCO | HNCS | C ₃ S | H ₂ CO | H ₂ CS |
| c-C ₃ H | l-C ₃ H | HCCN | H ₂ CN | | | | |
| CH ₄ | SiH ₄ ^a | C ₃ ^a | HC ₃ N | C ₄ Si ^a | OHCHO | H ₂ CNH | CH ₂ CC |
| H ₂ N ₂ CN | CH ₂ CO | C ₂ H ₂ | HCCNC | HNCCC | | | |
| H ₂ CNC | CH ₃ CN | NH ₂ CHO | CH ₂ CHO | H ₂ C ₂ H ₂ ^a | CH ₃ OH | CH ₂ C ₂ | CH ₃ SH |
| HC ₃ N | CH ₂ C ₂ H | CH ₃ CHO | CH ₂ CHCN | H ₂ CNH ₂ | c-CH ₂ OCH ₂ | | |
| CH ₃ C ₂ N | CH ₂ OOCH | CH ₃ COOH | CH ₃ C ₂ N | C ₇ H ^a | C ₂ H ₆ | | |
| HC ₂ N | CH ₂ C ₄ H | CH ₂ CH ₂ CN | CH ₂ CH ₂ OH | CH ₂ OCH ₃ | C ₂ H ^a | | |
| CH ₃ C ₃ N ^b | (CH ₂) ₂ CO | | | | | | |
| HC ₆ N | | | | | | | |
| HC ₁₀ N | | | | | | | |
| (C ₂ H ₂) ₂ O | | | | | | | |
| CH ⁺ | SO ⁺ | CO ⁺ | | | | | |
| HCO ⁺ | HN ₂ ⁺ | HOC ⁺ | HCS ⁺ | H ₂ D ⁺ ^b | H ₂ ⁺ | | |
| HCNH ⁺ | H ₃ O ⁺ | HOCO ⁺ | | | | | |
| CH ₂ NH ⁺ | | | | | | | |
| OH | CH | CN | NO | NS | NH | SO | CP ^a |
| SiC ⁺ | | | | | | | |
| HCO | C ₂ S | C ₃ H | CH ₂ | | | | |
| C ₃ N | | | | | | | |
| C ₂ H | CH ₂ CN | | | | | | |
| C ₃ H | | | | | | | |
| C ₄ H | | | | | | | |

^a Detection only in the envelopes around evolved stars.

^b Claimed but not yet confirmed.

- Dust Tail: dust particles removed from coma by solar radiation pressure
 - Dust sizes: 0.01-100 μm
 - ➔ radiation pressure (strong hyperbolic orbits are possible)

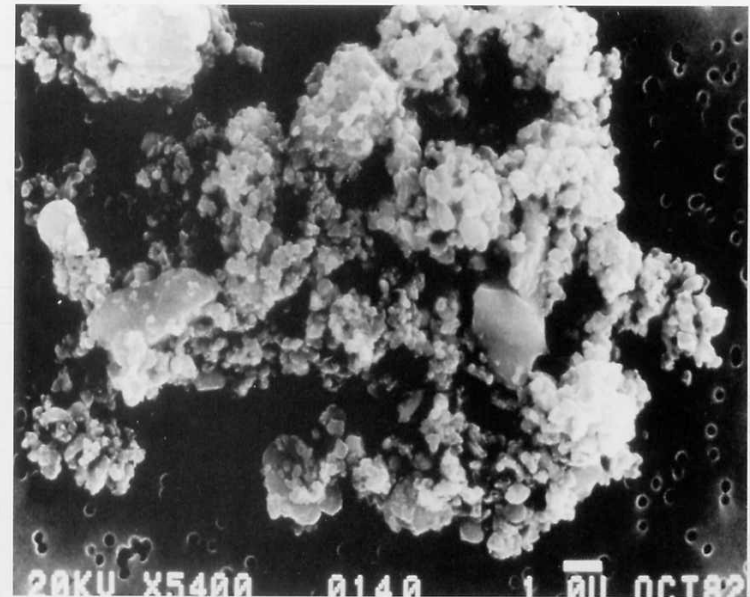
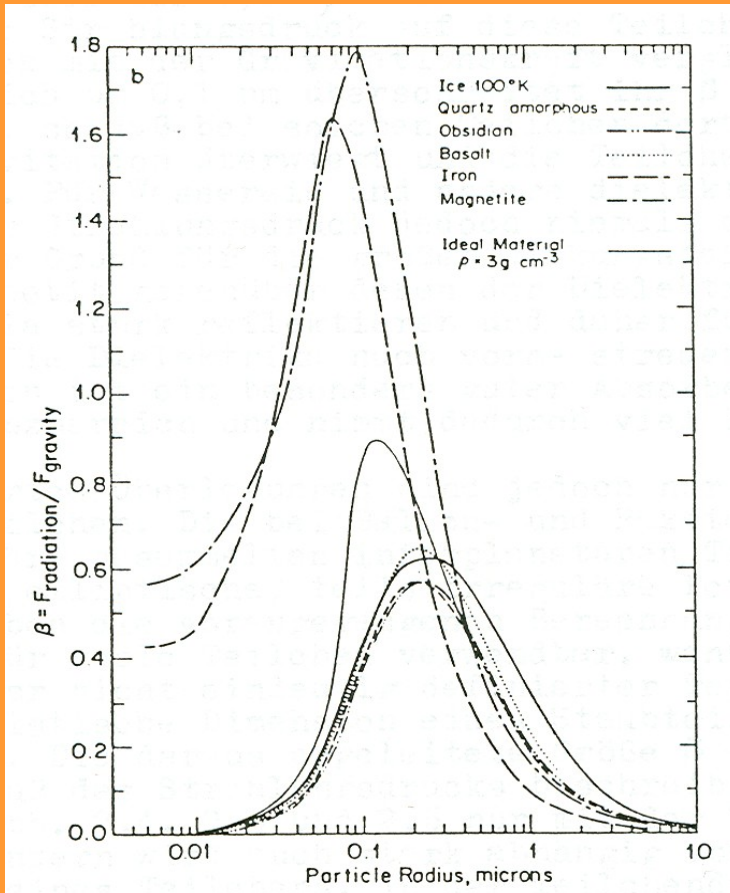


FIGURE 6 A suspected cometary interplanetary dust particle. The IDP is a highly porous, apparently random collection of submicron silicate grains embedded in a carbonaceous matrix. The voids in the IDP may have once been filled with cometary ices. (Courtesy of D. Brownlee, University of Washington.)

Dust particle motion

$$\underline{F}_{\text{total}} = \underline{F}_{\text{grav}} + \underline{F}_{\text{rad}} = ma \underline{e}_r$$

$$\underline{F}_{\text{grav}} = -\gamma m M / r^2 \underline{e}_r$$

$$\underline{F}_{\text{rad}} = LA / 4\pi cr^2 Q \underline{e}_r$$

$$\rightarrow ma \underline{e}_r = -\gamma m M / r^2 \underline{e}_r + LA / 4\pi cr^2 Q \underline{e}_r$$

$$= \underline{F}_{\text{grav}} (1 - \beta)$$

with

$$\beta = LA / 4\pi c Q \gamma m M$$

(radiation pressure coefficient)

$\underline{F}_{\text{grav}}$ = gravity force

$\underline{F}_{\text{rad}}$ = radiation pressure force

a = total acceleration

m = mass of dust particle

M = mass of the Sun

γ = gravity constant

r = distance of the particle from the Sun

L = luminosity of the Sun

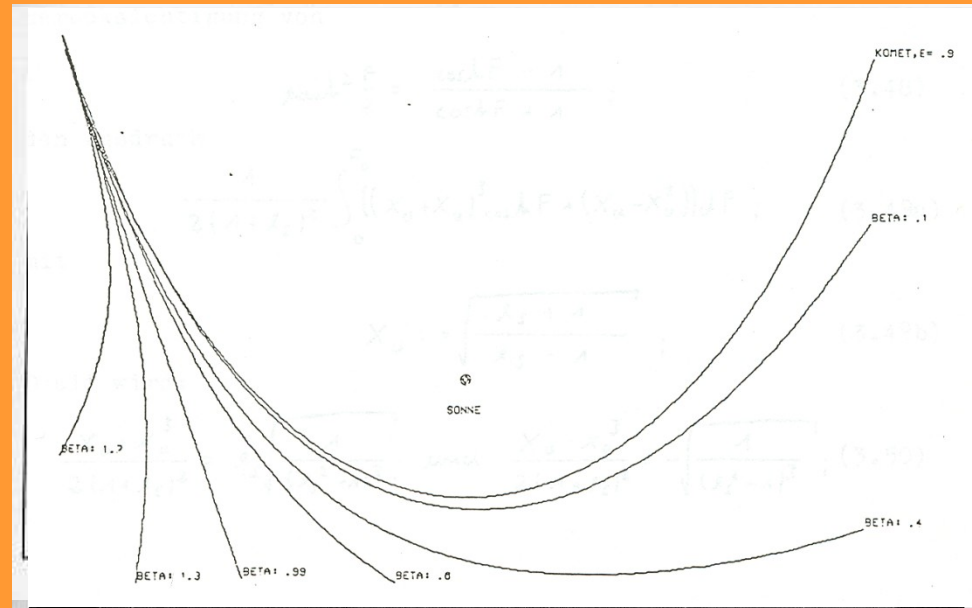
A = cross section of the particle

c = velocity of light

Q = radiation pressure efficiency

\underline{e}_r = unit vector in radial direction to the particle

- equation of motion as for gravity
- reduced (even repulsive) effective force in radial direction (Kepler motion)
- recipe for calculating the dust tail geometry
 - calculate comet orbit
 - calculate dust particle orbit
 - calculate difference
- ➔ synchrones & syndynes



Composition

- Ion Tail: ionized gas removed by magnetic field of solar wind

- Close to solar composition except for volatile elements
- Isotopic composition clearly solar
→ comets are born in solar system

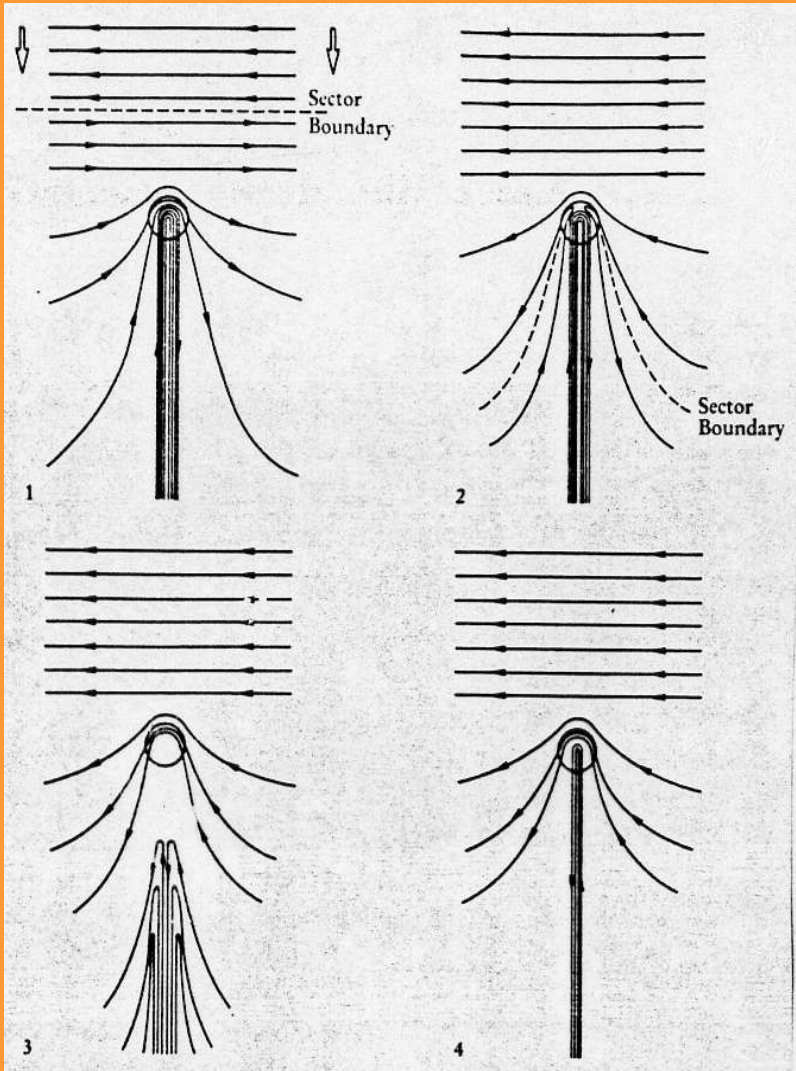


Table 15.3 Elemental Abundances in Comet Halley, CI-Chondrites, and the Solar Photosphere ^a

| Element | Comet P/Halley | | CI-Chondrites | Solar Photosphere |
|---------|----------------|------------|---------------|----------------------|
| | Dust | Dust & Ice | | |
| H | 2025 | 4062 | 520 | 2.63×10 ⁶ |
| C | 814 | 1010 | 74 | 933 |
| N | 42 | 95 | 5.9 | 245 |
| O | 890 | 2040 | 748 | 1950 |
| Na | 10 | 10 | 5.61 | 5.62 |
| Mg | 100 | 100 | 100 | 100 |
| Al | 6.8 | 6.8 | 8.32 | 7.76 |
| Si | 185 | 185 | 97.7 | 93.3 |
| S | 72 | 72 | 43.7 | 42.7 |
| K | 0.2 | 0.2 | 0.363 | 0.347 |
| Ca | 6.3 | 6.3 | 6.31 | 6.03 |
| Ti | 0.4 | 0.4 | 0.234 | 0.288 |
| Cr | 0.9 | 0.9 | 1.32 | 1.23 |
| Mn | 0.5 | 0.5 | 0.912 | 0.646 |
| Fe | 52 | 52 | 83.2 | 85.1 |
| Co | 0.3 | 0.3 | 0.224 | 0.219 |
| Ni | 4.1 | 4.1 | 4.90 | 4.68 |

^a atoms/100 Mg

Note: see also Table 3.5 for solar photospheric abundances and Tables 2.1 and 16.9 for abundances on CI-chondrites

Sources: Jessberger, E. K., & Kissel, J., 1991, in *Comets in the post-Halley era* (Newburn, R., Neugebauer, M., & Rahe, J., eds.), Kluwer Acad. Publ., Dordrecht, The Netherlands, Vol. 2, pp. 1075–1092. Mumma, M. J., Weissman, P. R., & Stern, S. A., in *Protostars & planets III* (Levy, E. H., & Lunine, J. I., eds.) Univ. of Arizona Press, Tucson, 1177–1252.

Table 15.4 Relative Abundances in P/Halley (by Number)

| Molecule | Abundance | Molecule | Abundance | Molecule | Abundance |
|------------------|-----------|--------------------|-----------|-----------------|-----------|
| H ₂ O | 100 | H ₂ CO | 0–5 | N ₂ | ~0.02 |
| CH ₄ | 0–2 | CH ₃ OH | ~1 | NH ₃ | 1–2 |
| CO | 7–8 | OCS | <7 | HCN | ≤0.1 |
| CO ₂ | 3 | CS ₂ | 1 | SO ₂ | <0.002 |

Origin

Isotopic ratios suggest that cometary material is home-made, i.e. typical for the solar system

- Two sources:
 - Short-period comets: Kuiper Belt
 - Oort comets: Jupiter-Neptune region and scattered to outer/inner solar system during early phase of the solar system
- contributed to early bombardment

TABLE V
Isotopic Ratios in Comets and Other Reservoirs

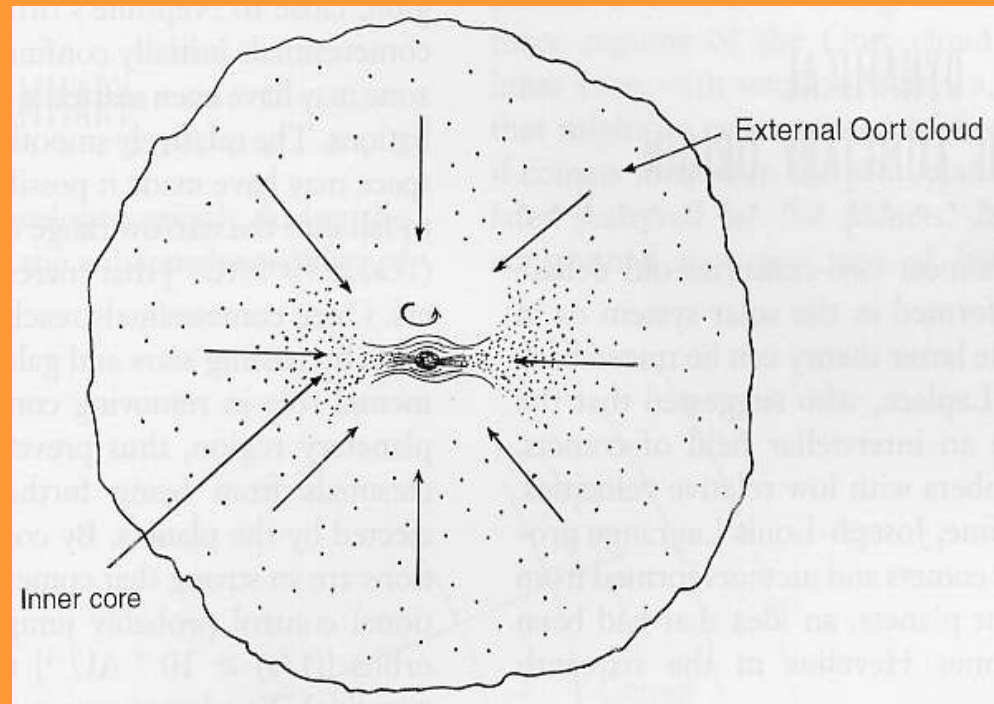
| Species | Solar system | Interstellar matter | Comets |
|---------------------------------|-------------------------|-------------------------|--------------------------------|
| D/H | 1 to 2×10^{-5} | 1.5×10^{-5} | 3.2×10^{-4a} |
| D/H | | 10^{-4} to 10^{-2b} | 1.9 to 3.5×10^{-4c} |
| $^{12}\text{C}/^{13}\text{C}$ | 89 | 43 ± 4^d | 95 ± 12^c |
| $^{12}\text{C}/^{13}\text{C}$ | | 65 ± 20^f | 70 to 130^g |
| $^{12}\text{C}/^{13}\text{C}$ | | 12 to 110^h | 10 to $1,000^h$ |
| $^{14}\text{N}/^{15}\text{N}$ | 272 | $\approx 400^f$ | $>200^e$ |
| $^{16}\text{O}/^{18}\text{O}$ | 498 | $\approx 400^f$ | 493^a |
| $^{24}\text{Mg}/^{25}\text{Mg}$ | 7.8 | | Variable ^h |
| $^{25}\text{Mg}/^{26}\text{Mg}$ | 0.9 | | $<2^h$ |
| $^{32}\text{S}/^{34}\text{S}$ | 22.6 | | 22^h |
| $^{56}\text{Fe}/^{54}\text{Fe}$ | 15.8 | | 15^h |

^a From *in situ* mass spectrometry of Comet Halley coma.

^b Range of observed values in dense ISM clouds.

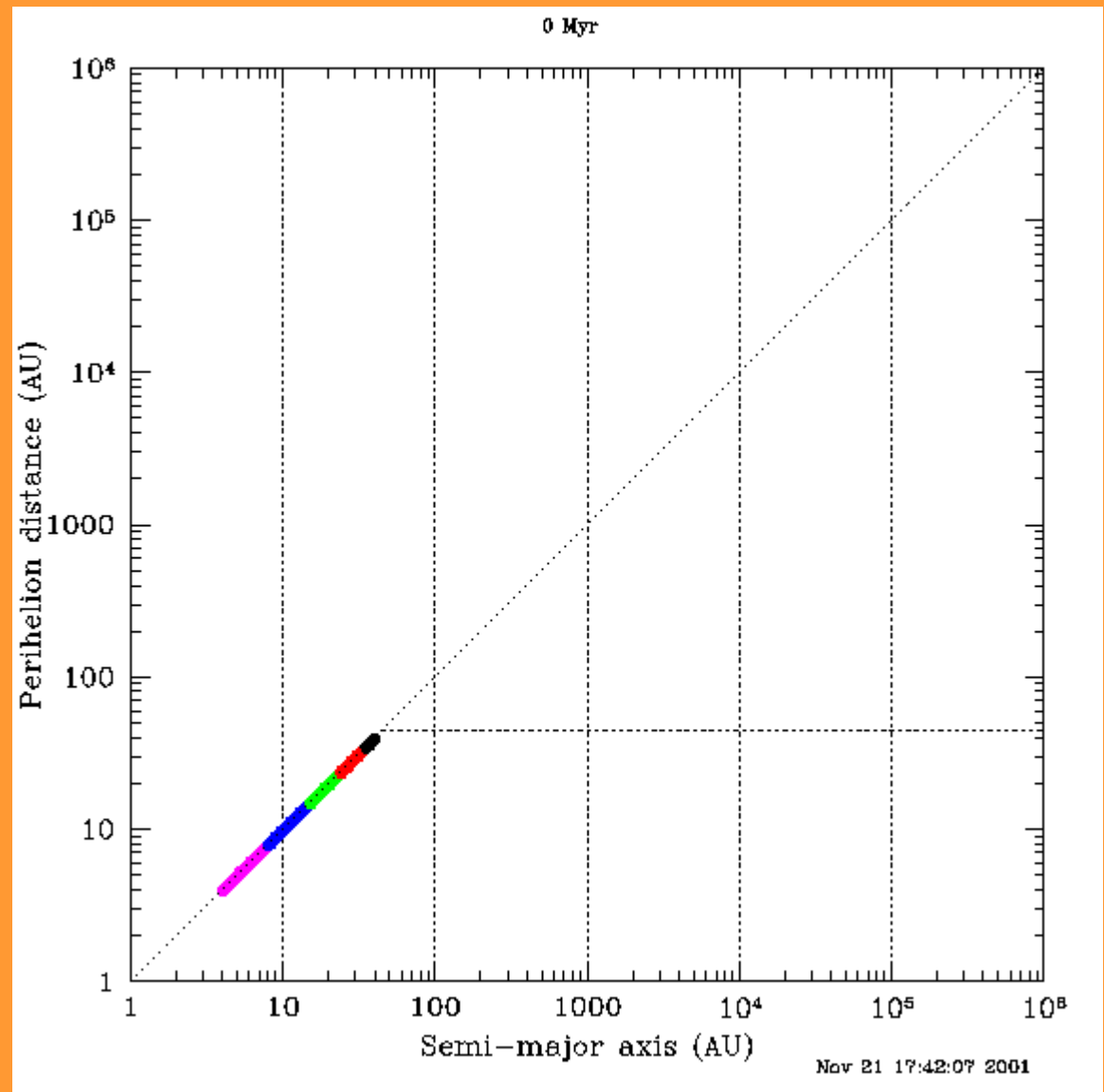
^c From radio wavelength spectra of HDO in Comet Hyakutake.

^d From visual spectra.



Oort Cloud formation – The movie

- **Start:** planetesimals in planetary disk between Jupiter and Neptune
- **Clean-up:** by gravitational scattering of gas giants
- **Thermalization:** through galactic neighbourhood
- **Return of Oort Cloud comet:** through scattering by galactic neighbourhood



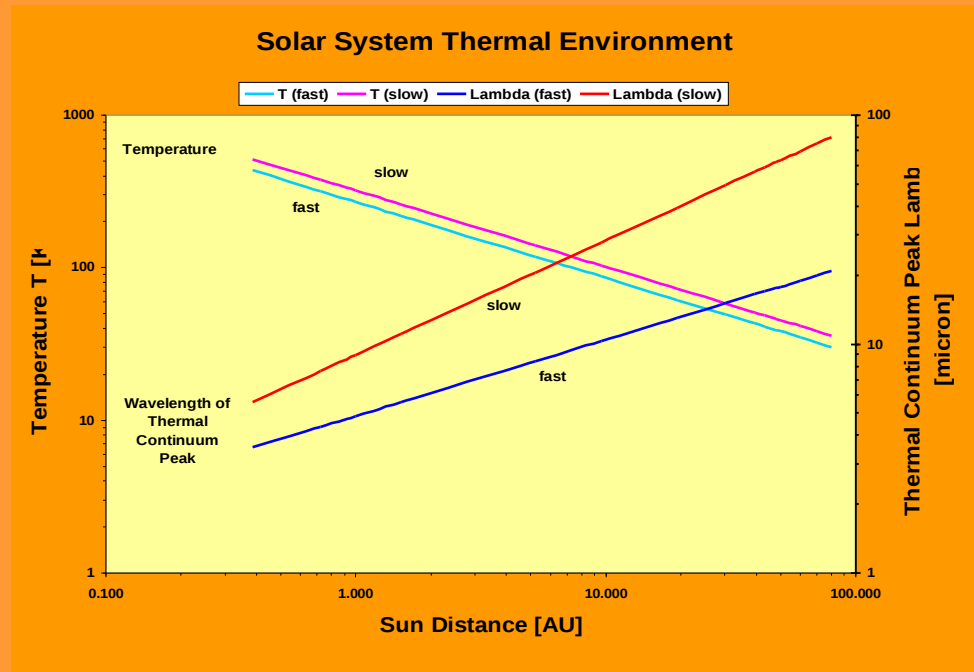
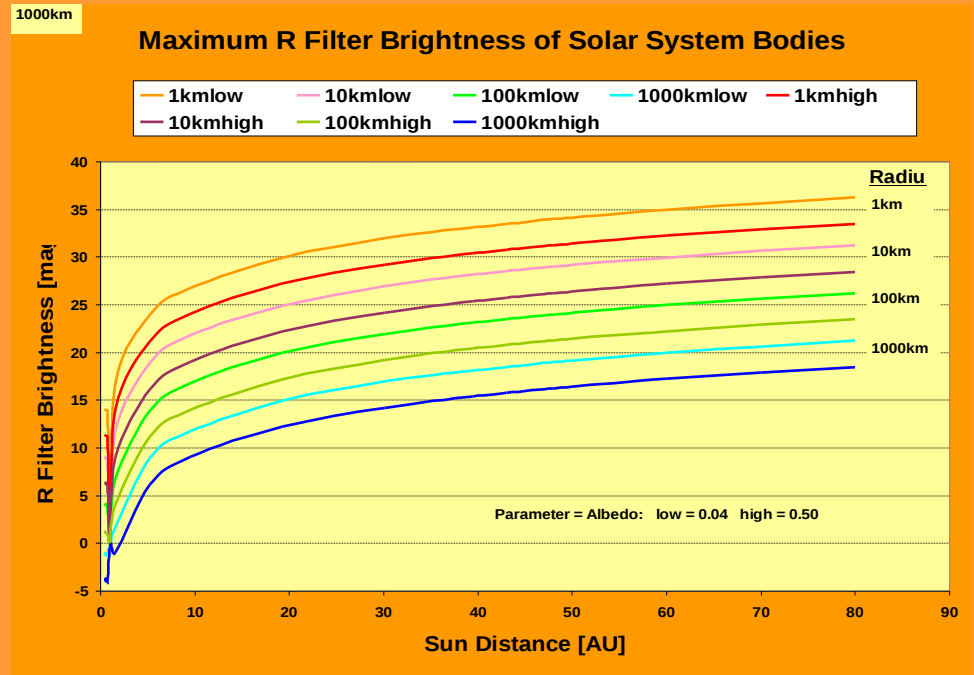
Edgeworth-Kuiper Belt

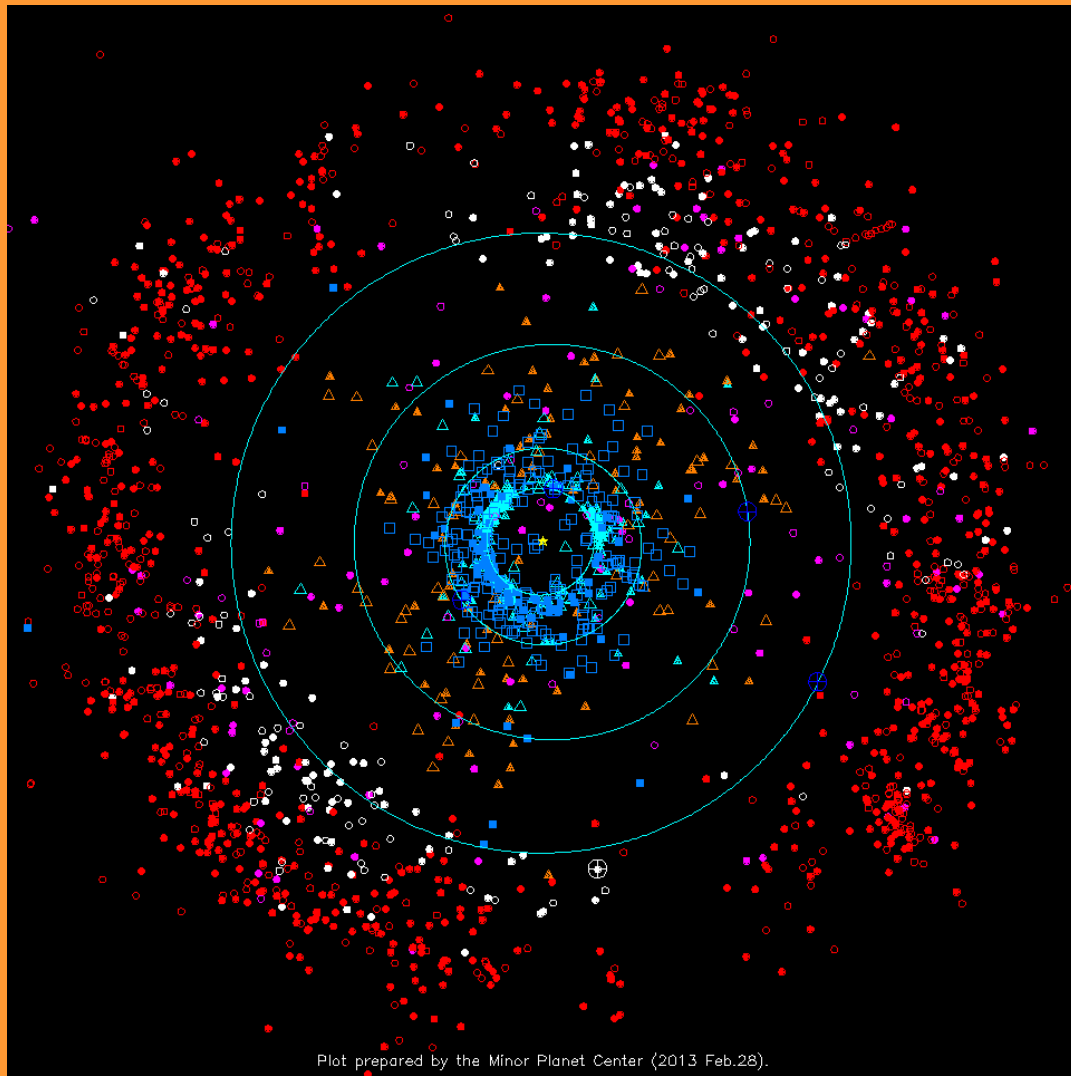
- **Summary**

- Orbits mostly between 35-50 AU
- Large population, with little total mass
- Collision signatures (double objects, size distribution, collision family)
- Icy objects (water, methane) with max radius of order 1000km
- Processed surface: collision, high-energy radiation, activity
- Reservoir for short-period comets

General

- Definition and history:
 - Orbits with semi-major axes larger than Neptune orbit
 - Transneptunian Objects (TNOs = EKBOs)
 - Speculated 1938 (Edgeworth) and 1950 (Kuiper)
 - First object discovered in 1930 (Pluto), more in 1992 (1992 QB1)
 - ~1500 TNOs discovered so far
- Brightness:
 - 20-28mag and fainter
 - slow moving
 - Discovered in wide and deep survey
 - $T \sim 40K \rightarrow$ thermal emission in submm radio range





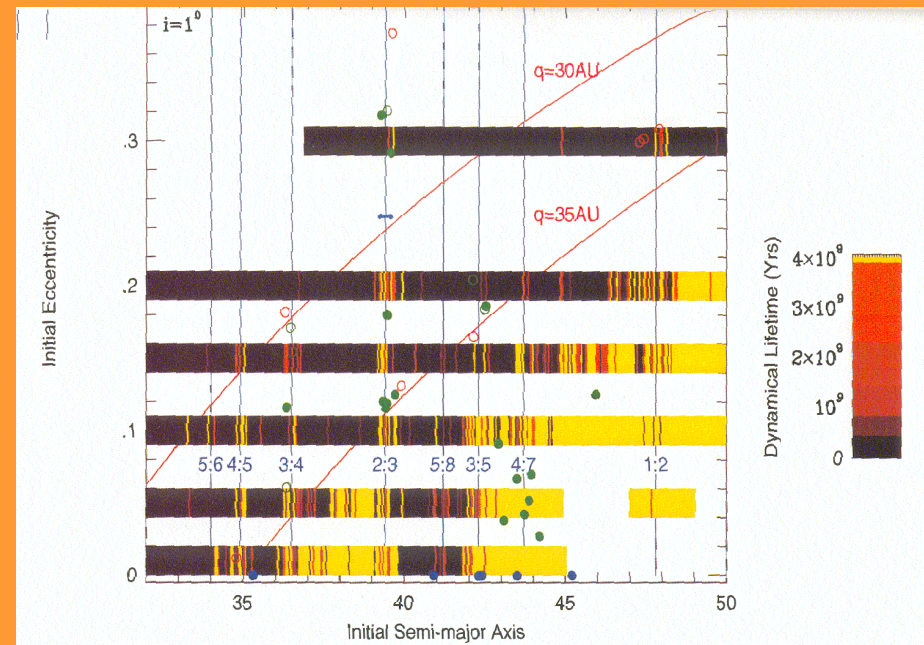
- Cubiwanos
- Plutinos
- ShortP.
- ▲ Comets
- ▲ Centaurs
- Scattered

The Transneptunian Region and its dynamical Population



Dynamical Classification

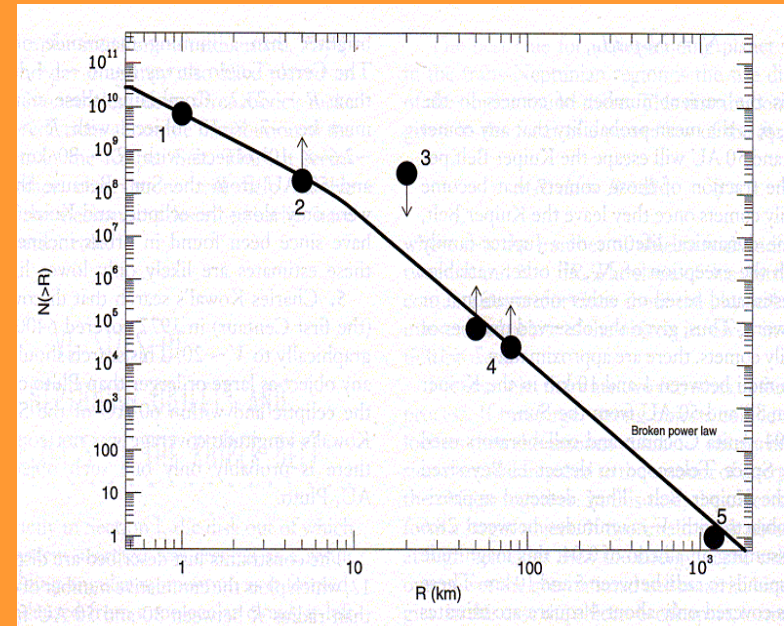
- Plutinos: $a \sim 39$ AU
 $e \sim 0.1 - 0.3$
→ 2:3 resonance with Neptune
- Cubewanos: $a \sim 40 - 46$ AU
(classical disk) $e < 0.1$
→ outside of planet resonance
- Scattered Disk:
 $a > 50$ AU & $q < 35$ AU
- Centaurs:
Jupiter Neptune
→ “eccentric” KB members
no resonance beyond 2:1 ~ 50 AU
- Detached Disk:
 $a > 50$ AU & $q > 50$ AU



- Plutinos, Cubewanos, detached disk objects are in dynamically stable orbits
- Scattered disk will have encounters with planets (Neptune)
- Centaurs are transferred from EKB to inner solar system within $\sim 10^6$ y
→ short-period comets

Population Density and Total Mass

- Population density: see table
 - Size distribution = mixture from formation and evolution
 - Slope change for smaller radii
 - Size distribution gets dominated by collision products
 - more than 10 double TNOs found
 - produced by large impacts
- Total mass: 0.15 Earth masses
(with radius > 100km)

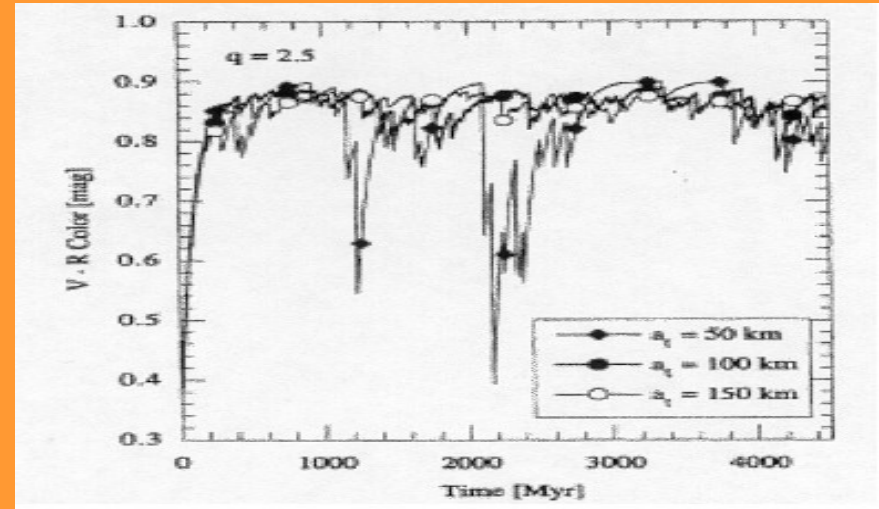
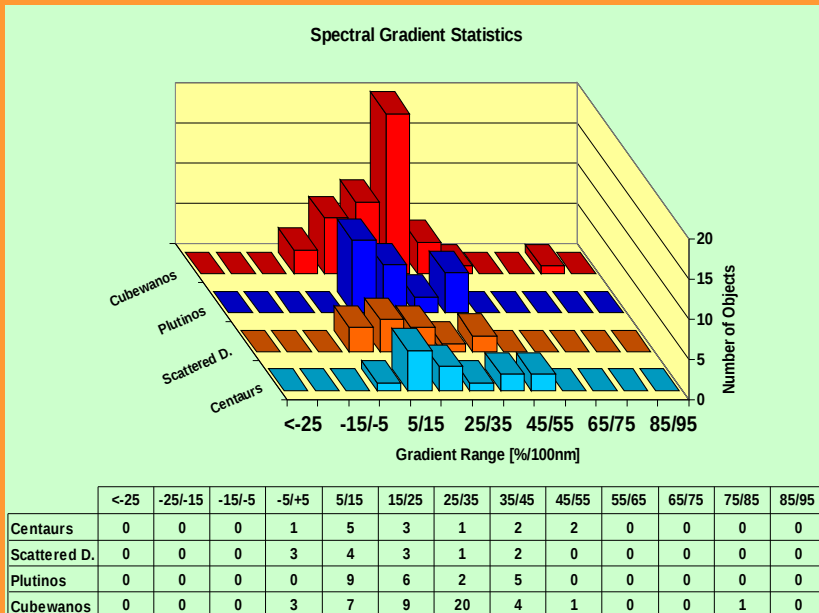


| Limit. R Mag [mag] | Surface Density [deg²] | TNOs In KB < 50 AU | Approx. Radius [km] |
|-----------------------------------|--|--------------------------------------|------------------------------------|
| < 24 | 2.7 | 27000 | 110 |
| < 26 | 33 | 330000 | 45 |
| < 28 | 390 | 3900000 | 20 |

Physical Properties

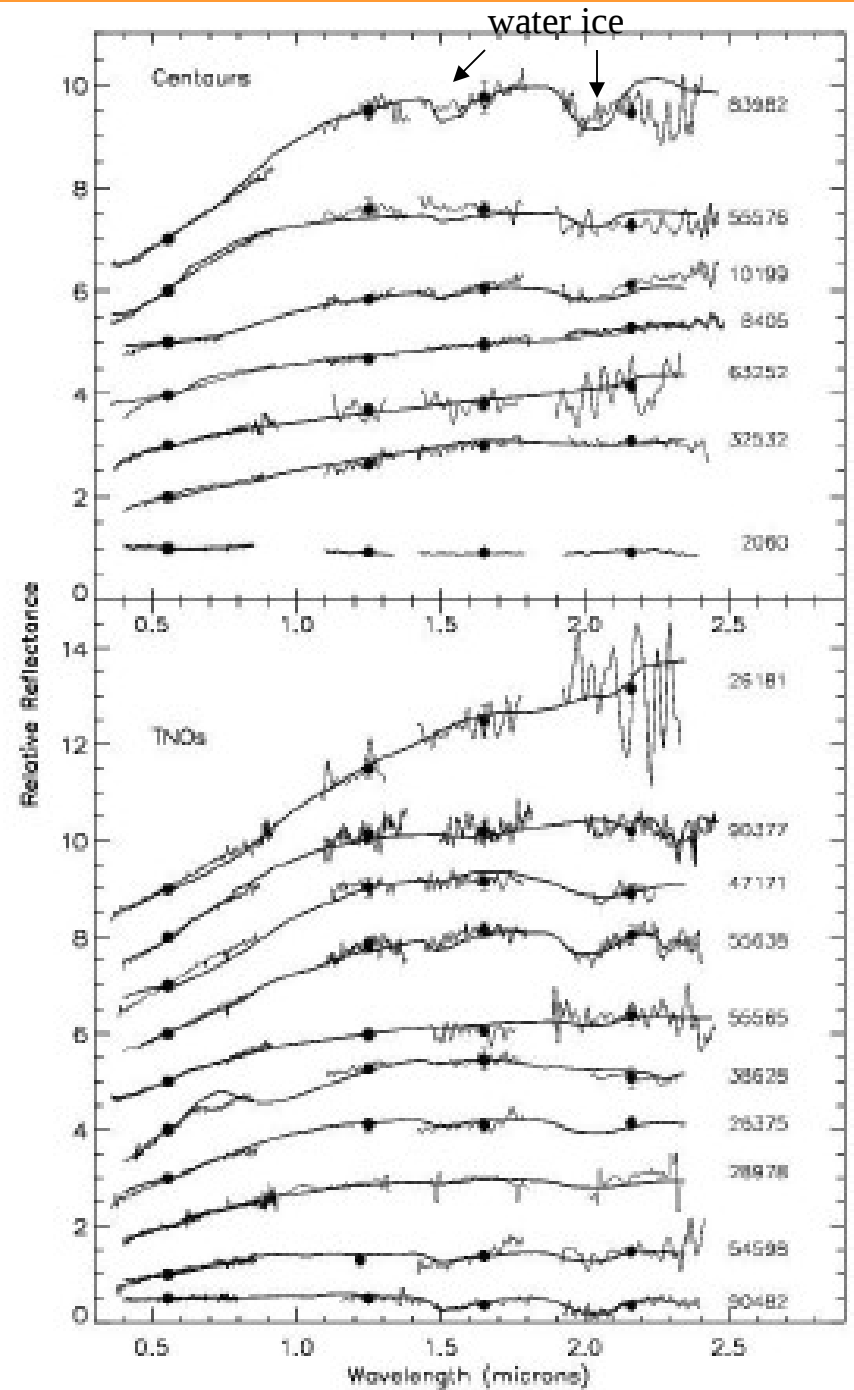
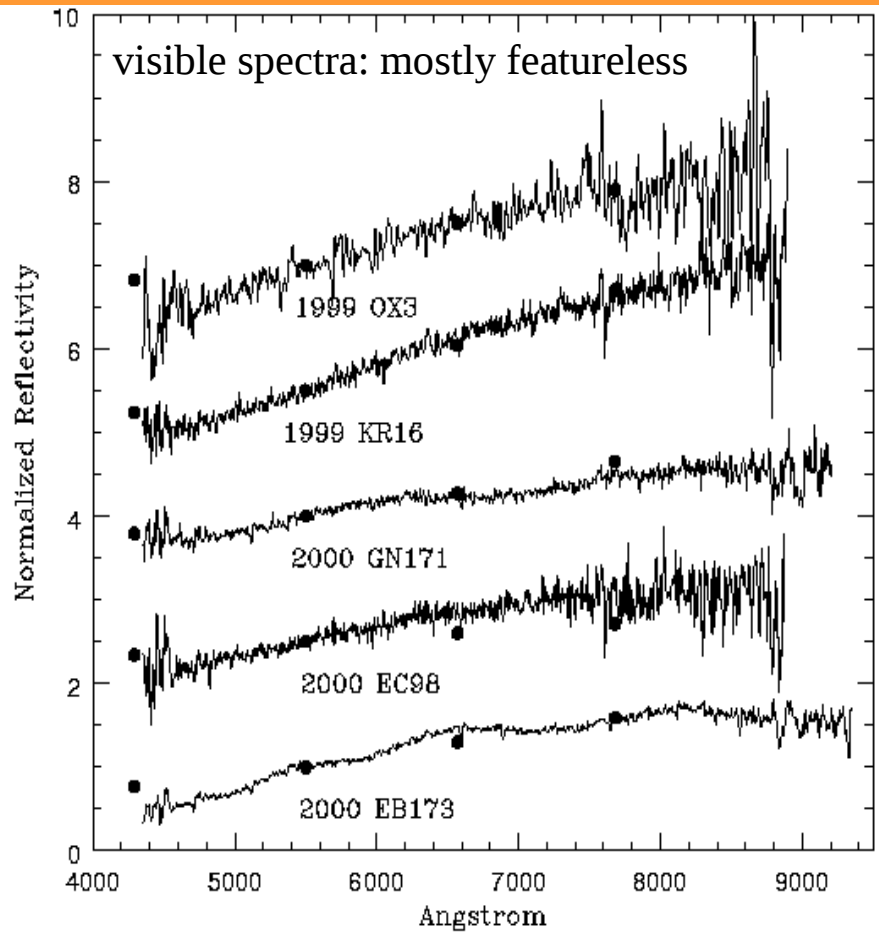
- Size&Shape: 50-1200km radius
Pluto = 2nd largest TNO
large ones spherical, smaller ones asymmetric
- Albedo: dark (5%) – medium (15%)
(except when active: >30%)
- Spectrum: some have strong reddening
→ caused by high-energy radiation
others are neutral compared to Sun
→ due to impact resurfacing or
recondensation of temporary atmosphere

| Object | Radius [km] | Albedo |
|-----------|-------------|----------|
| Pluto | 1150 | 0.5-0.6 |
| Charon | 590 | 0.3-0.35 |
| 1993SC | 160 | 0.02 |
| 1996TL66 | 320 | 0.03 |
| 2000WR106 | 450 | 0.07 |
| Chiron | 180 | 0.15 |
| Pholus | 190 | 0.04 |
| Chariklo | 300 | 0.045 |



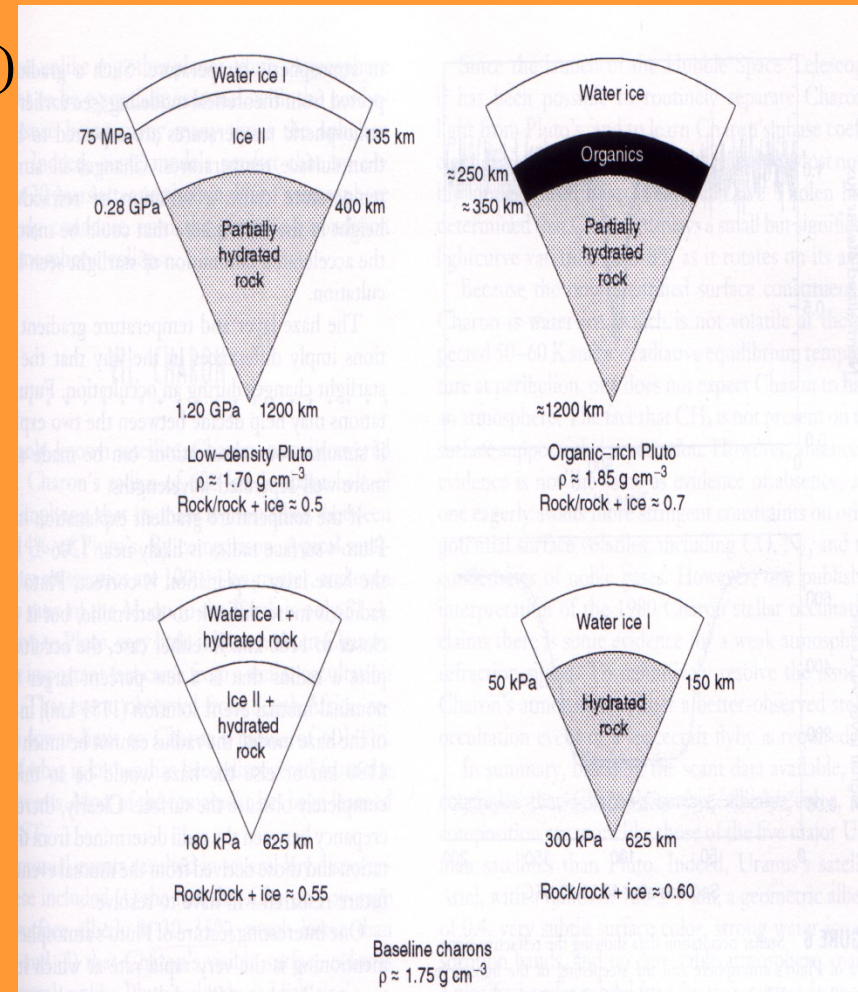
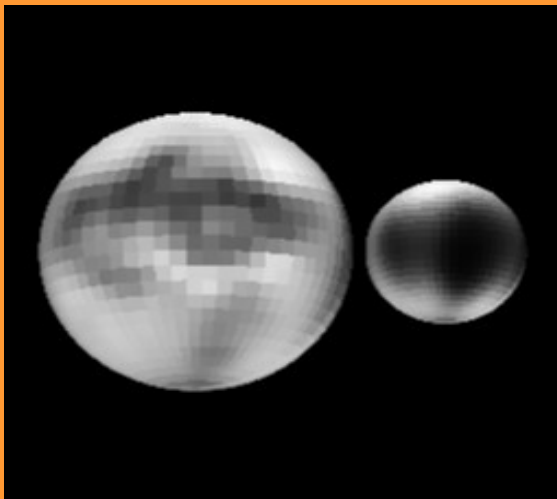
Simulation of reddening changes

- Surface chemistry: some with water/methane ice absorption,
- One case of hydrated silicate dedected → surprise liquid water ?



Pluto & Charon (since 1978)

- Orbit: stable in past, chaotic after $\sim 2 \cdot 10^7$ y
- Size: 1200/600km radius, 2nd largest TNO
- Density: $\sim 1.9 \text{ g/cm}^3$ (high! \rightarrow not only ices)
- Charon synchronous to Pluto orbit (6.4d)
- Albedo: P:0.4-0.6; C:0.3-0.35
- Colours: P = red, C = neutral
- Atmosphere: around perihelion for Pluto
temporary nature \rightarrow resurfacing
- Surface: P: CH_4 , N_2 , CO T $\sim 45\text{-}60\text{K}$
patchy
C: H_2O , little CH_4 more uniform?



(1) Kuiper Belt formation:

- presence of Pluto puts modelling constraint
Try to make Pluto via accretion from 1m-1km
size bodies at 40 AU distance

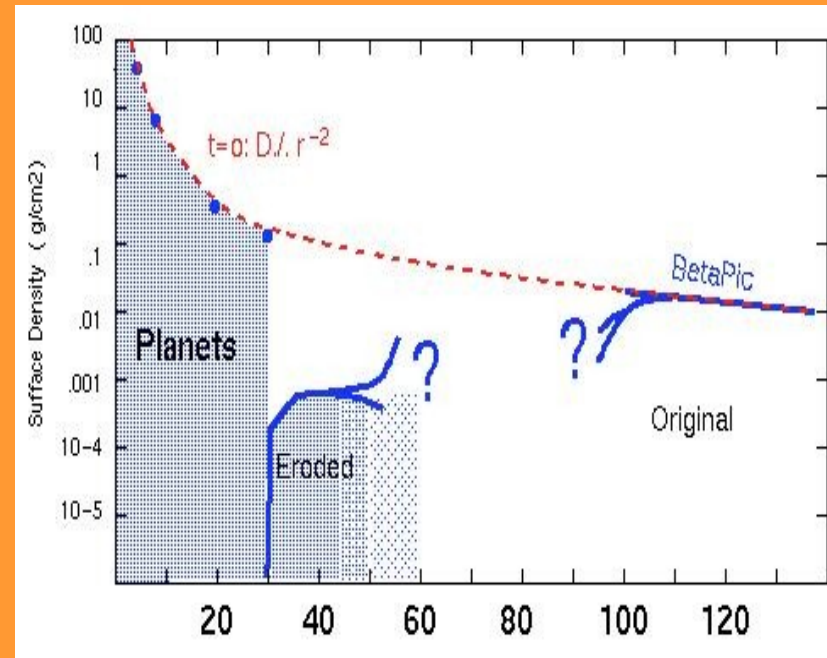
→ more 1000-10000 Earth masses needed
in Kuiper Belt region

→ More than one Pluto is formed
(Eris & Sedna & Triton)

(2) Missing mass problem:

mass surface density of outer planetary system
 $\sim r^{-2}$ in giant planet region
present Kuiper Belt drop by factor 10^2-10^3

(1)+(2) → originally, the Kuiper Belt may
have been massive and may have matched the
extension of the mass surface density function



Interplanetary Dust

- **Summary**
 - Interplanetary dust cloud in inner solar system
 - Sources: cometary dust and collision in asteroid belts
 - Short lifetimes → continuous replenishing

Appearance & Detection

- Zodiacal light: visible close to the horizon as diffuse light before/after sunrise/set
 - dust disk around the Sun, ecliptic oriented
 - Sun illuminated micron-size dust
- Meteors: trails of excited mostly atmospheric molecules in entry channel of mm-cm size dust, 120-60km height
- Other detection techniques: see schematics

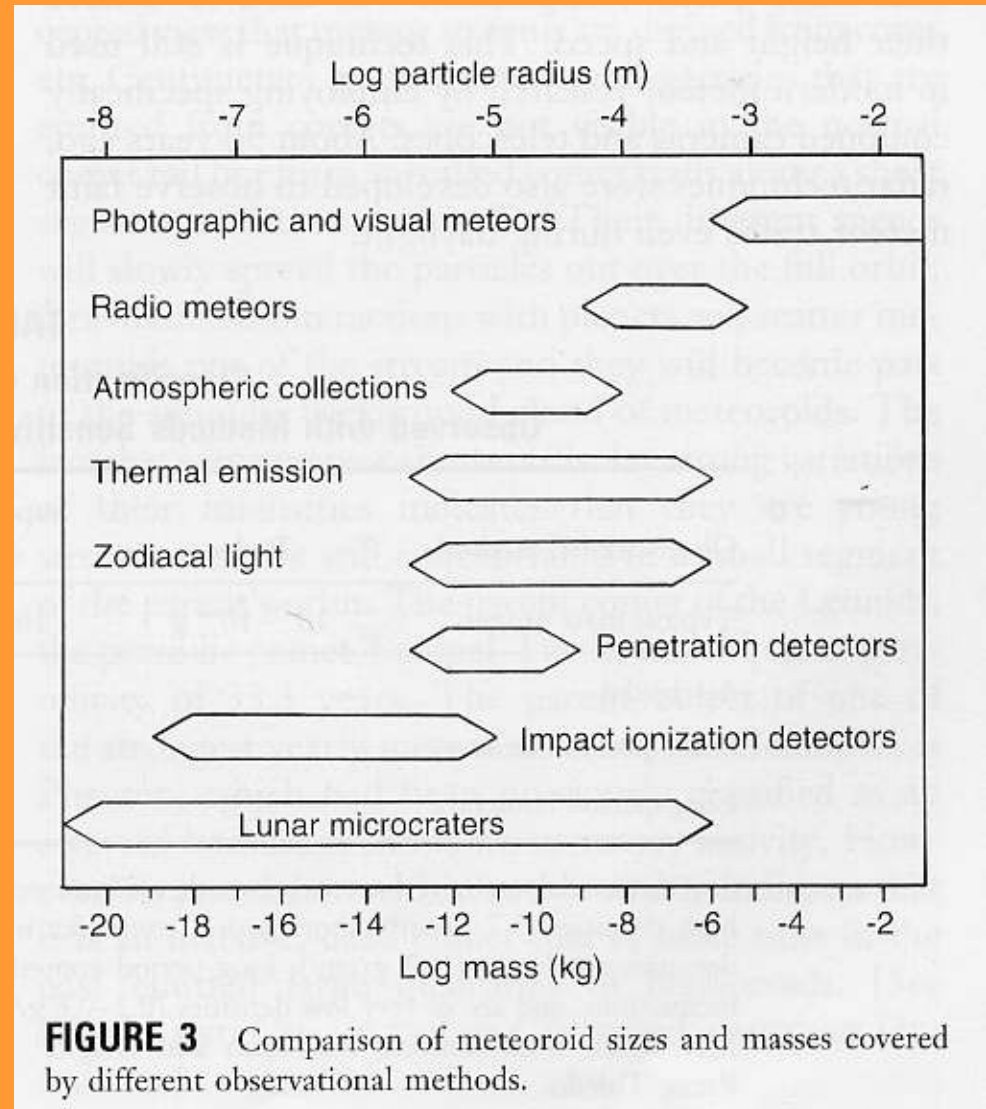


FIGURE 3 Comparison of meteoroid sizes and masses covered by different observational methods.



FIGURE 4 An unusually strong meteor shower (Leonid) was observed on 17 November 1966. The meteor trails seem to radiate from the constellation Leo.

Leonid meteor stream



FIGURE 1 Cone of zodiacal light seen in the west one hour after sunset. The ecliptic plane is delineated by Venus at the top of the cone and the crescent moon just above the horizon. (Courtesy of C. Leinert.)

Zodiacal light

- Meteor streams: enhanced meteor activity with trails converging to the same apparent point in the sky (radiant, meteor streams are named after radiants)

- Orbits of meteors in stream similar to comets
- Trails of dust along cometary orbits
 - ➔ Dust particles from comets
 - ➔ Earth passage through trails causes meteor streams

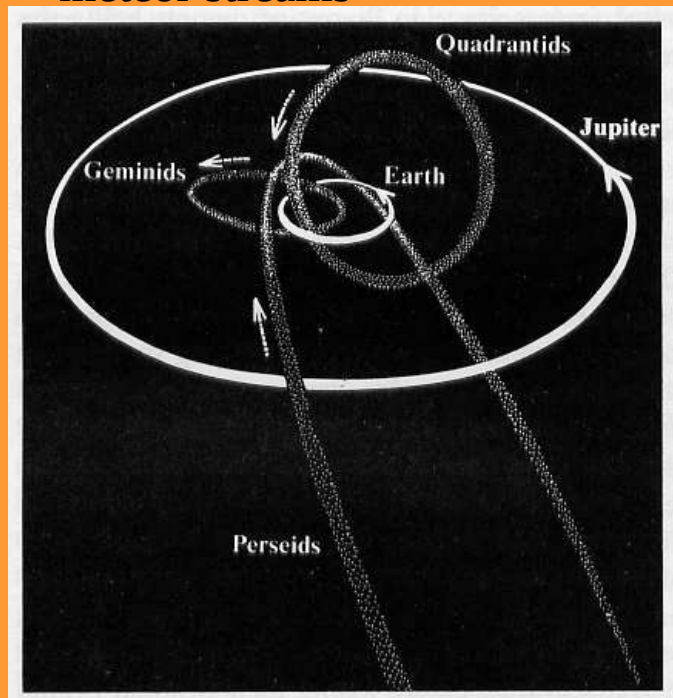
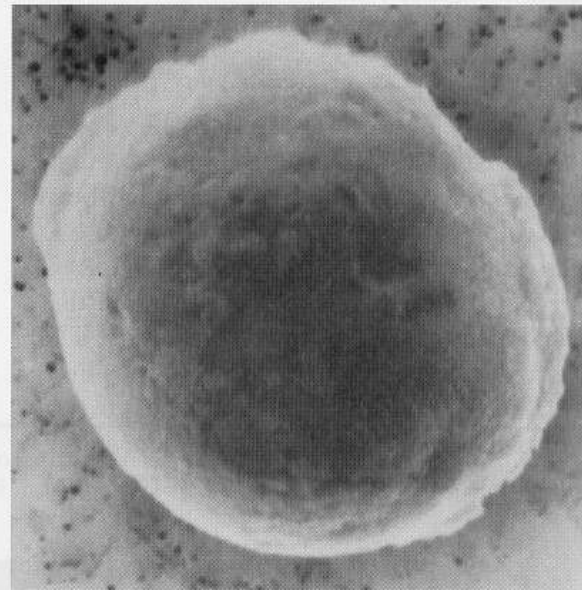
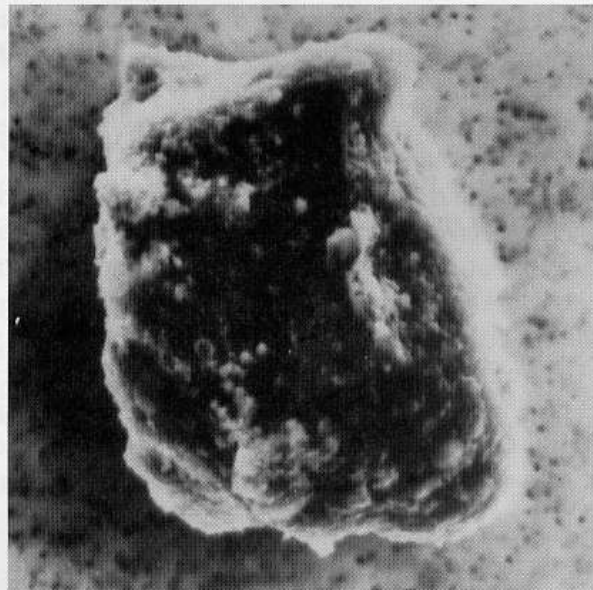
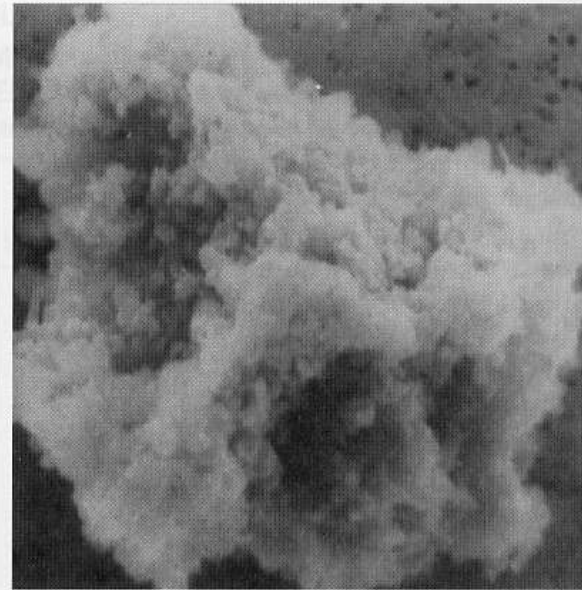
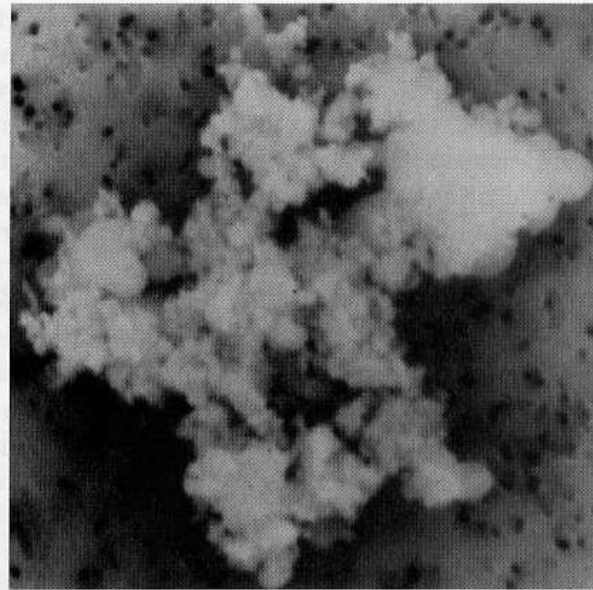


TABLE II
Major Meteor Showers, Date of Shower Maximum, Radiant in Celestial Coordinates (Right Ascension, RA, and Declination, DEC, in Degrees), Geocentric Speed (km/s), Maximum Hourly Rate, and Parent Objects (If Known, Short-Period Comets Are Indicated by P/)^a

| Name | Date | Radiant | | Speed | Rate | Parent object |
|--------------------|---------|---------|-----|-------|-------------|---------------------------|
| | | RA | DEC | | | |
| Quadrantids | Jan. 3 | 230 | +49 | 42 | 140 | |
| April Lyrids | Apr. 22 | 271 | +34 | 48 | 10 | Comet 1861 I Thatcher |
| Eta Aquarids | May 3 | 336 | -2 | 66 | 30 | P/Halley |
| June Lyrids | June 16 | 278 | +35 | 31 | 10 | |
| S. Delta Aquarids | July 29 | 333 | -17 | 41 | 30 | |
| Alpha Capricornids | July 30 | 307 | -10 | 23 | 30 | P/Honda-Mrkos-Pajdusakova |
| S. Iota Aquarids | Aug. 5 | 333 | -15 | 34 | 15 | |
| N. Delta Aquarids | Aug. 12 | 339 | -5 | 42 | 20 | |
| Perseids | Aug. 12 | 46 | +57 | 59 | 400 (1993) | P/Swift-Tuttle |
| N. Iota Aquarids | Aug. 20 | 327 | -6 | 31 | 15 | |
| Aurigids | Sept. 1 | 84 | +42 | 66 | 30 | Comet 1911 II Kiess |
| Giacobinids | Oct. 9 | 262 | +54 | 20 | 10 | P/Giacobini-Zinner |
| Orionids | Oct. 21 | 95 | +16 | 66 | 30 | P/Halley |
| Taurids | Nov. 3 | 51 | +14 | 27 | 10 | P/Encke |
| Taurids | Nov. 13 | 58 | +22 | 29 | 10 | P/Encke |
| Leonids | Nov. 17 | 152 | +22 | 71 | 3000 (1966) | P/Tempel-Tuttle |
| Geminids | Dec. 14 | 112 | +33 | 34 | 70 | Phaeton |
| Ursids | Dec. 22 | 217 | +76 | 33 | 20 | P/Tuttle |

After A. F. Cook (1973). In "Evolutionary and Physical Properties of Meteoroids" (C. L. Hemenway, P. M. Millman, and A. F. Cook, eds.), pp. 183-192. NASA SP-319, National Aeronautics and Space Administration, Washington, D.C.

Airborne collected interplanetary dust particles (IDPs)



Physico-chemical properties

- Composition: IDPs similar to chondrites for lighter stony elements, but enriched in rare earth elements
 - Sizes: power laws with similar exponent
 - Radial distribution: double peak distribution
 - Core population peaks at Sun
 - Distant population peaks in asteroid belt
- ➔ two sources for IPDs:
- Comets (dust release by nucleus)
 - Asteroids (collisions)

TABLE III
Average Elemental Composition (All Major and Selected Minor and Trace Elements) of Several Chondritic IDPs Is Compared with C1 Chondrite Composition*

| Element | C1 | IDP | Variation | T_c |
|---------|-----------|-----|-----------|-------|
| Mg | 1,071,000 | 0.9 | 0.6–1.1 | 1067 |
| Si | 1,000,000 | 1.2 | 0.8–1.7 | 1311 |
| Fe | 900,000 | 1 | 1 | 1336 |
| S | 515,000 | 0.8 | 0.6–1.1 | 648 |
| Al | 84,900 | 1.4 | 0.8–2.3 | 1650 |
| Ca | 61,100 | 0.4 | 0.3–0.6 | 1518 |
| Ni | 49,300 | 1.3 | 1.0–1.7 | 1354 |
| Cr | 13,500 | 1.1 | 0.9–1.4 | 1277 |
| Mn | 9,550 | 1.1 | 0.8–1.6 | 1190 |
| Cl | 5,240 | 3.6 | 2.8–4.6 | 863 |
| K | 3,770 | 2.2 | 2.0–2.5 | 1000 |
| Ti | 2,400 | 1.5 | 1.3–1.7 | 1549 |
| Co | 2,250 | 1.9 | 1.2–2.9 | 1351 |
| Zn | 1,260 | 1.4 | 1.1–1.8 | 660 |
| Cu | 522 | 2.8 | 1.9–4.2 | 1037 |
| Ge | 119 | 2.3 | 1.6–3.4 | 825 |
| Se | 62 | 2.2 | 1.6–3.0 | 684 |
| Ga | 38 | 2.9 | 2.1–3.9 | 918 |
| Br | 12 | 34 | 23–50 | 690 |

* The IDP abundances are normalized to iron (Fe) and to C1. C1 abundance is normalized to Si = 1,000,000 condensation temperatures T_c (°C). From E. K. Jessberger et al. (1992). *Earth Planet. Sci. Lett.* **112**, 91–99.

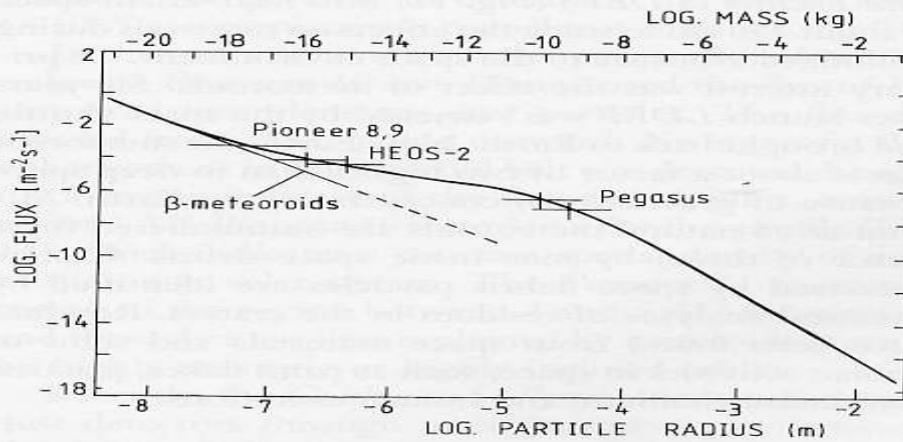


FIGURE 10 Cumulative flux of interplanetary meteoroids on a spinning flat plate at 1 AU from the Sun. The solid line has been derived from lunar microcrater statistics and it is compared with satellite and spaceprobe measurements.

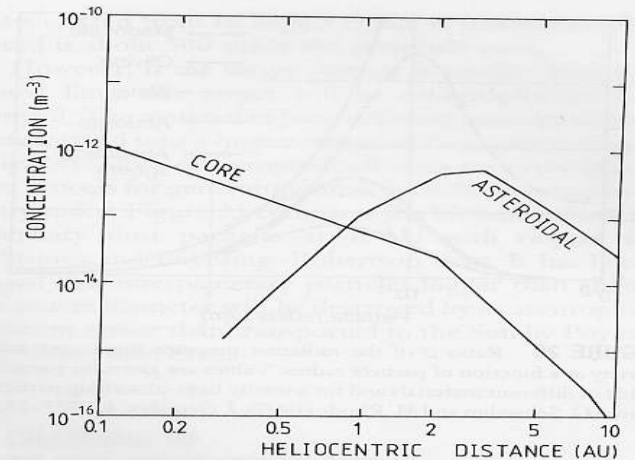


FIGURE 19 Radial dependence of meteoroid concentrations for two main populations in interplanetary space according to Divine (1993). The values given refer to particles with masses $> 10^{-4}$ g. The zodiacal core population comprises particles of all sizes, whereas the asteroidal population comprises only big ($> 10^{-6}$ g) particles.

- Lifetime of dust: short lifetime ~ 1000 - 100000 y
 - Removal effects
 - Poynting-Robertson effect
(IPDs either blown out of the solar system or spiraling into the Sun)
 - Destruction effects
 - Collisions
 - Electrostatic disruption
 - Heating & evaporation
 - Continuous supply necessary!

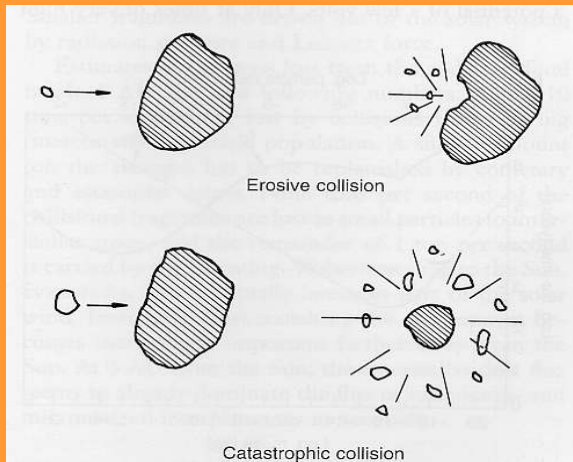


FIGURE 23 Schematics of meteoroid collisions in space. If the projectile is very small compared to the target particle, only a crater is formed in the bigger one. If the projectile exceeds a certain size limit the bigger particle is also shattered into many fragments. The transition from one type to the other is abrupt.

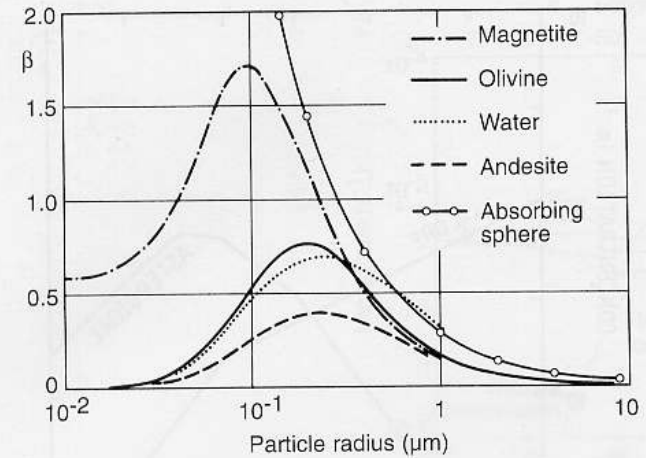


FIGURE 20 Ratio β of the radiation pressure force over solar gravity as a function of particle radius. Values are given for particles made of different materials and for a totally light-absorbing particle. [From G. Schwehm and M. Rhode (1997). *J. Geophys.* **42**, 727–735.]

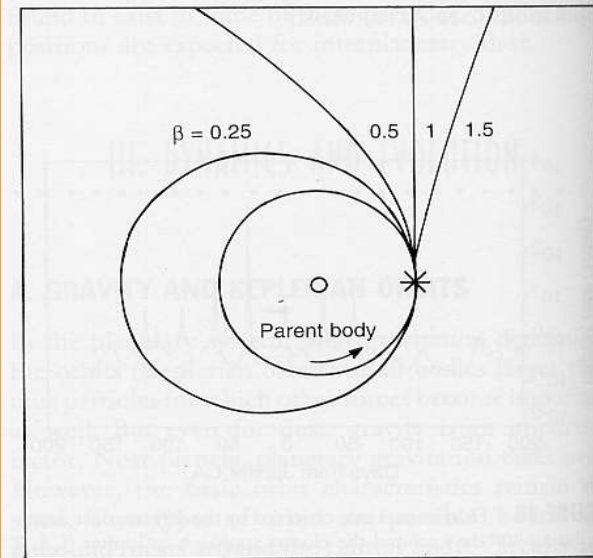


FIGURE 21 Orbits of beta-meteoroids that were generated from a parent body at the position indicated by the asterisk. β values of differently sized fragments are indicated; big β values refer to small particles.

Mass flow of IDPs

Lifetime of IDPs

- radiation pressure
- collision

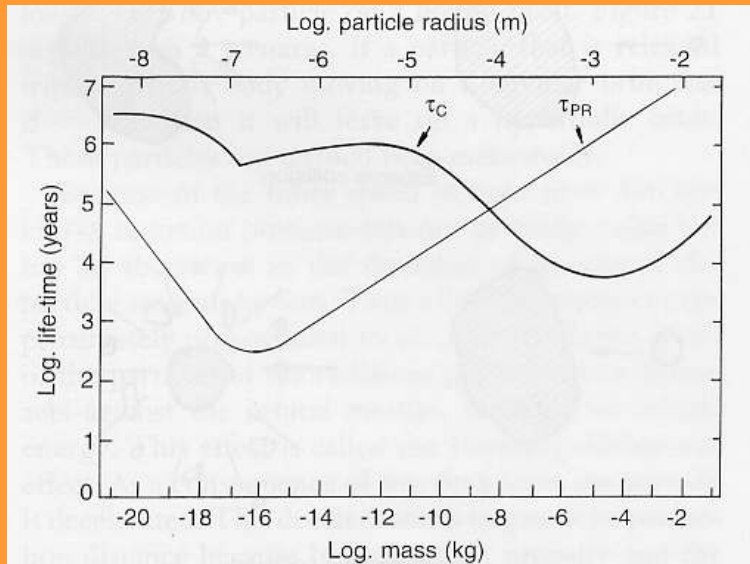


FIGURE 25 Life-times of meteoroids in interplanetary space with respect to destruction by collisions τ_C and transport to the Sun by the Poynting–Robertson effect τ_{PR} as a function of particle mass. The shorter the lifetime, the more effective is the process of removing particles out of the zodiacal cloud.

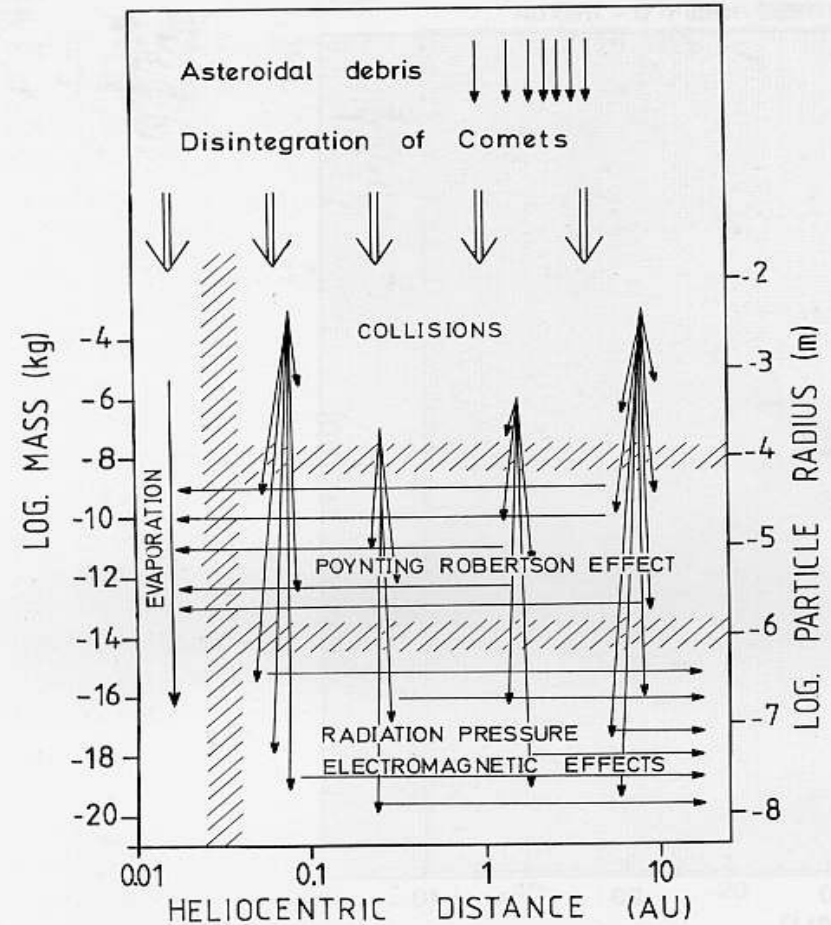


FIGURE 28 Mass flow of meteoritic matter through the solar system. Most of the interplanetary dust is produced by collisions of larger meteoroids, which represent a reservoir continually being replenished by disintegration of comets or asteroids. Most of it is blown out of the solar system as submicron-sized grains. The remainder is lost by evaporation after being driven close to the Sun by the Poynting–Robertson effect. In addition to the flow of interplanetary matter shown, there is a flow of interstellar grains through the planetary system.

Formation & Evolution of the Solar/Planetary System

- *Summary*

- Planetary system formed during/shortly after formation of the Sun
- Collapse of interstellar gas/dust cloud
- Disk formation by gas friction
- Cold disk to grow m size bodies and planetesimals
- Runaway grow of planets
- Clean-up by collision down-grinding, scattering, impacts (early & late heavy bombardment) and radiation pressure
- Atmosphere evolving from magma gas release and impacts
- Proto-planetary disk was full of organics including L/D aminoacids
- Sun will expand as red giant star to orbit of Mars

Observational Indications

- Primitive asteroids, comets, TNOs: primordial = remnants from formation period of planetary system (planetesimal state and before)
- For the Formation and its environment:
 - Environment: star forming regions
 - Dense interstellar clouds
 - Formation temperature: relatively cold
 - Organics in meteorites ($T < 300\text{K}$)
 - Not from cooled Sun material: deuterium is lost in nuclear reactions within 10^6 y
 $D/H(\text{giant planets}) \gg D/H(\text{sun})$
 - Isotopic ratios Sun to Meteorites/Comets identical (for heavier elements)
 - Mixing of H and He in Jupiter/Saturn as in Sun
 - Ingredients: stellar formation regions
 - Interstellar gas with most abundant elements H, He
 - Interstellar gas that can form volatile ices (H_2O , CO, CO_2 , NH_3 , CH_4 etc.)
 - Interstellar dust, strongly shocked or enriched in supernova produced elements
(diamonds=shocked C, ^{26}Mg from ^{26}Al in chondrites higher than in current neighbourhood)
 - Mass: > 1.02 solar mass

- For the Formation time:
 - Meteorites → $4.56 \cdot 10^9$ a
 - not necessarily in present stellar neighbourhood, but probably in star cluster (Galactic rotation and differential motion of stars, proper motion of the Sun)
- For formation time scales:
 - Meteorites, i.e. cm → m size bodies $\pm 10 \cdot 10^6$ y around formation time
 - Oldest impact craters (on moon) $\sim 4.3 \cdot 10^9$ y
 - planet (moon!) formation widely 'finished' within $100 \cdot 10^6$ y from chondrite formation
- For the typical size and geometry (some times during formation process):
 - Kuiper Belt extension ~ 50 AU at one time (maybe even smaller: Nice model and Neptune migration)
 - Ecliptic-orientation of planets and the belts and analogy to circumstellar disks and proplydes in star formation regions
 - flat disk-shape geometry
 - Mass concentrated in Sun, angular momentum in planets
- Objects produced:

| | |
|--|----------------------|
| – Sun (star) | 1 solar mass |
| – Terrestrial planets | 10^{-5} solar mass |
| – Gas giants | 10^{-3} solar mass |
| – Icy planetesimals and fragile comets | 10^{-3} solar mass |

all appeared quasi-simultaneously

Formation Scenario

- Step 1 - Protostellar collapse:
 - Jeans criterion for collapse of gas clouds: self-gravitation energy > thermal energy in cloud
self-gravity $\sim GM^2/R \sim GM\rho R^2$
(M,R = mass/radius of cloud, G = grav. Const)
thermal energy $\sim Mv_s^2 \sim k^2MT^2$ (v_s/T = speed of sound/temperature in cloud)

$$R = (\pi v_s^2 / G\rho)^{1/2} \quad (\text{Jeans criterion})$$

→ from star forming regions:

$$R \sim 0.1 \text{ pc } (3 \cdot 10^{15} \text{ m}), T \sim 10\text{K}$$

collapse time scale: $t \sim R/v_s \sim 10^6 \text{ y}$

min. mass involved for protosolar nebula ~ 1.02
solar mass (Sun+planets)



- Step 2 – Disk formation:

- Radial collapse & conservation of angular momentum

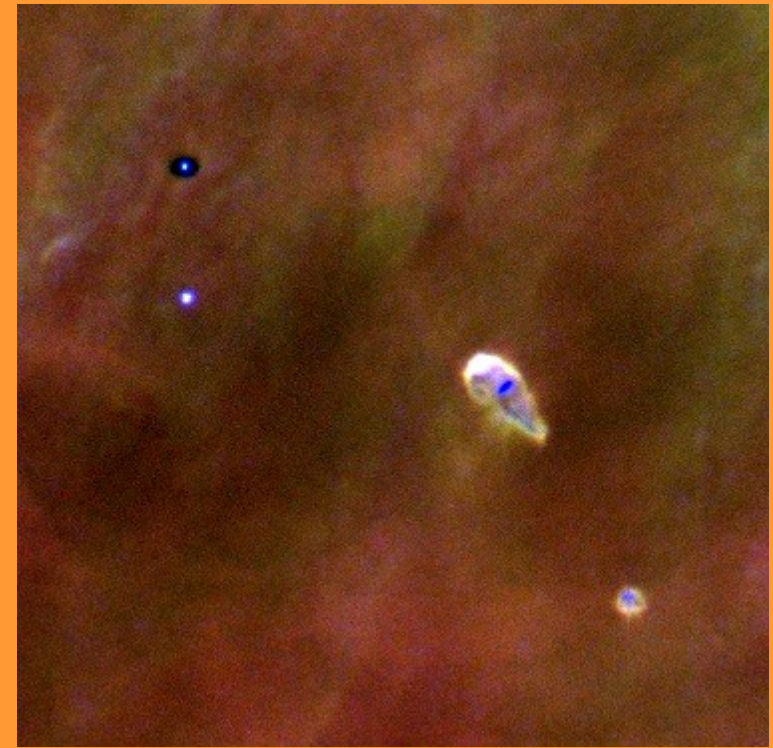
- flat disk is formed

- Collapse along rotation axis of cloud continues, inside disk has to overcome centrifugal forces

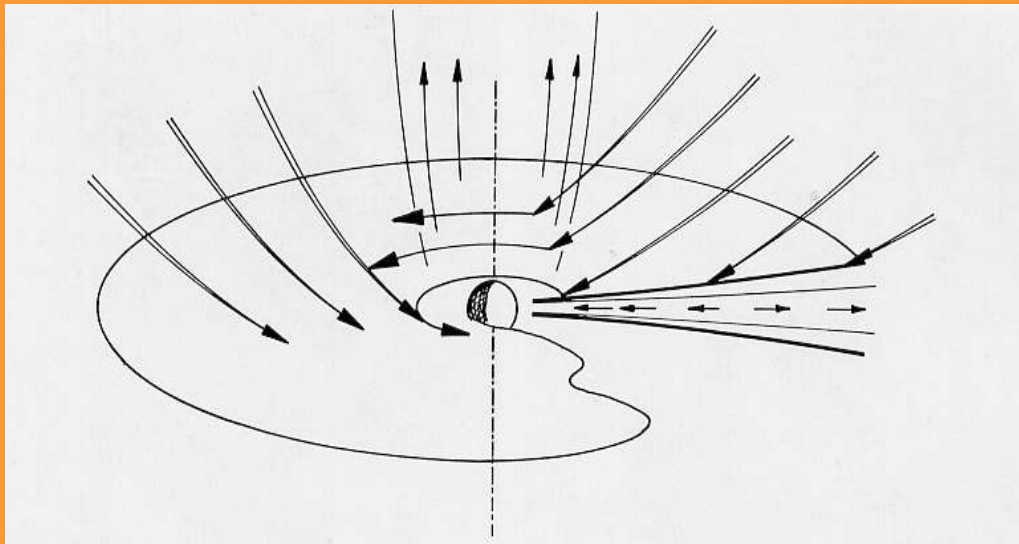
- Angular momentum in disk is transformed into thermal energy via friction

- Heating, towards center stronger, i.e. more efficient friction, better angular momentum transfer

- Proto-sun forms in disk center



- Time scale: $2 \cdot 10^7$ y
- Most of mass in Sun
- Disk thickness $\sim 1/10$ diameter
- Inner disk (~ 1 AU) is hot >1500 K
dust vaporizes, lighter molecules dissociates (not heavier ones)
mass ~ 0.03 solar masses
- Outer disk (>2 AU) remains cool
dust intact, more molecular gas



Step 3 – Growth of cm/m size grains (meteorites):

- Inner disk: rapid cooling through IR radiation
 → stony molecules crystallize rapidly to μm grains

Outer disk: gas freezes on dust grains

- dust grains start to agglomerate

$$dm/dt \sim a^2 v \rho_{\text{dust}} \quad (a/\rho_{\text{dust}} = \text{radius/density of dust})$$

$v \sim$ speed of dust settling towards disk plane

Important: works only for relative velocities of dust < 10 cm/s

- **dust aggregates only in dynamically cold disk**

dynamically cold = dust grains have similar orbits (e,i), otherwise destruction by collision

- dust sticking is supported by formation of inter-grain matrix through condensation and surface reactions of gas molecules

- larger grains grow in very thin (out-of-plane) disk

Time scale: $< 10^3$ orbits $\sim 10^3 - 10^5$ y

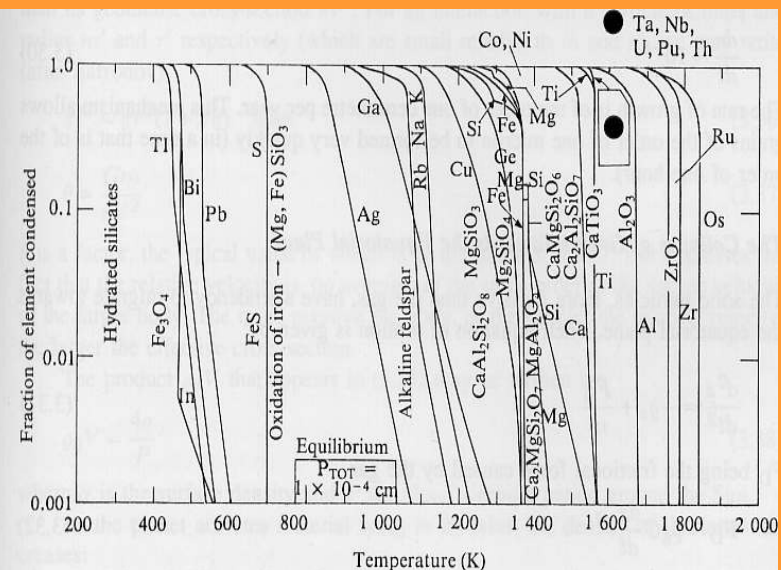


Fig. 3.1. The condensation sequence for a gas with solar composition. [After L. Grossman J.W. Larimer: Review of Geophysics and Space Physics 12, 71 (1974)]

Step 4 – Growth of planetesimals:

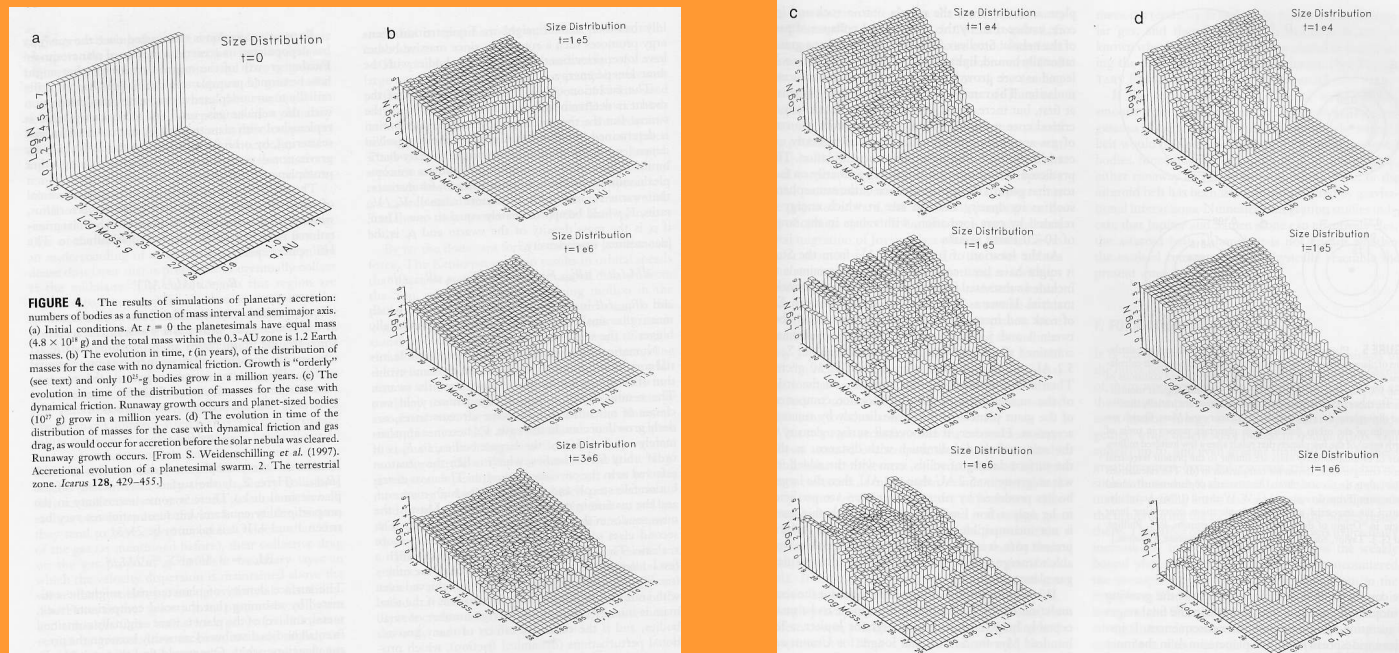
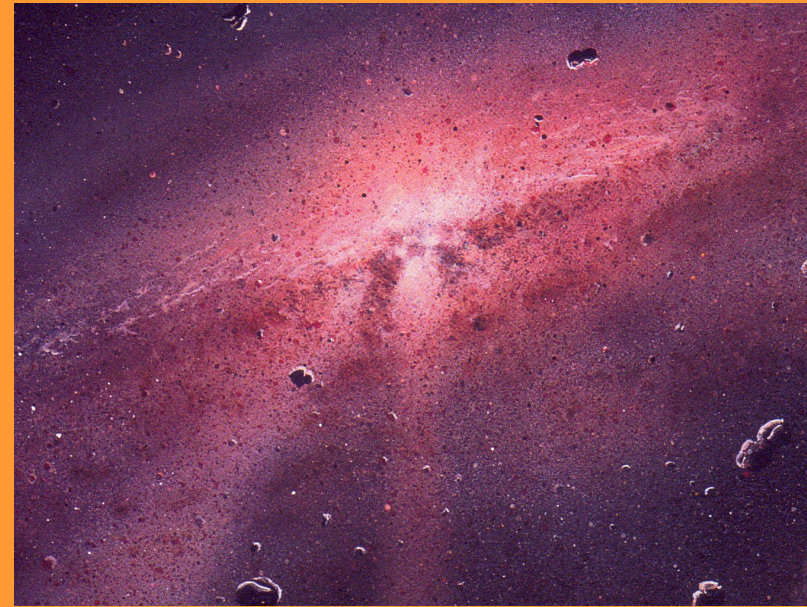
- continuous gentle collisions of m size bodies grow planetesimals (~1km size) sticking by self-gravity

Time scale: similar to step 3

→ cold disk gets slightly ,excited‘ due grav. interaction of planetesimals

Step 5 – Runaway accretion of planets:

planetesimals continue to collide and grow simulations → 10^6 - 10^7 y few planet size bodies form, random behaviour for distances of planets



- Step 6 – Disk clean-up:

- Proto-planets in environment of planetesimals, meteorites, dust and gas

all planets: perturbation on orbits in neighbouring disk environment

→ cold disk gets excited

→ collisions more energetic, i.e. impacts and scattering of planetesimals occur

→ planetesimal collisions causes down-grinding of objects to dust grain size

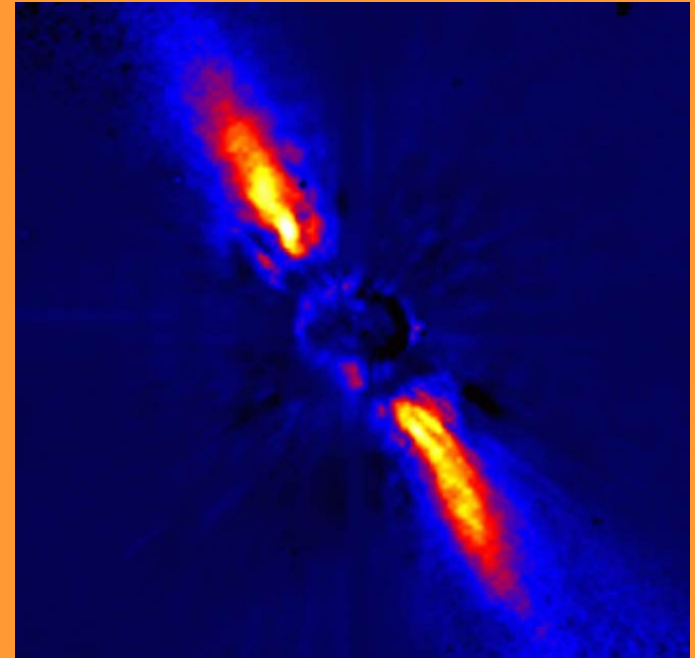
→ dust removed by radiation pressure

→ proto-planets grow further, disk loses mass towards Sun and outer solar system (interstellar space)

terrestrial planets: H_2 , He disk gas too hot and planet mass too small to allow accretion by condensation, only heavier molecule (H_2O , CO_2 , CH_4 , NH_3) can be accreted.

giant planets: Earth size protoplanet is capable of accreting H_2 , He gas since in colder environment

Time scale: 10^7 - 10^8 y



Debris disk around β Pictoris

- Some notes to step 6:

- Mass transfer/removal:
 - clean-up of sphere of gravitational influence around orbit of planets
- Mass transfer through scattering is enormous
 - Kuiper-Belt: several 1000 Earth masses closer to the Sun most likely even more inbound/outbound scattering occurs
 - period of early & late heavy bombardment
- Transfer of angular momentum:
 - scattering transfers angular momentum to planets
 - planets can migrate away from original orbit
 - Mercury: collection of heavier material at larger distances
 - Excited Cubewano population in Kuiper Belt:
 - objects with $a > 42$ AU have wider (a,e) and (a,i) distributions than expected from a simple collision environment
 - Excitation from swiping of Neptune resonance during outward migration of the planet
 - late heavy bombardment caused by excitement of Kuiper Belt due to 1:2 resonance crossing of Jupiter&Saturn

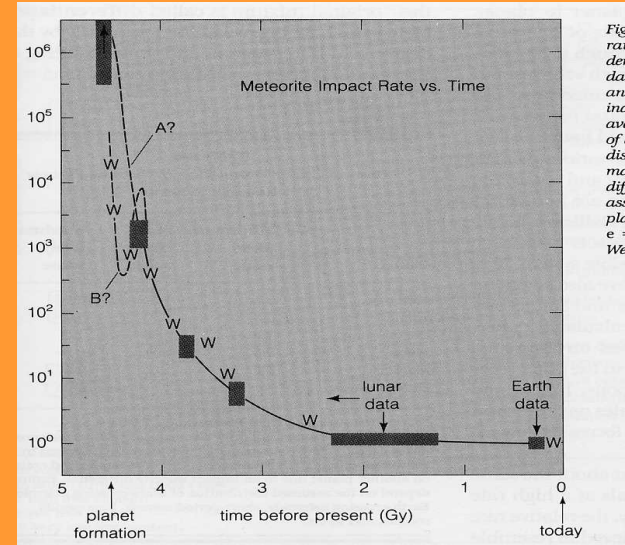
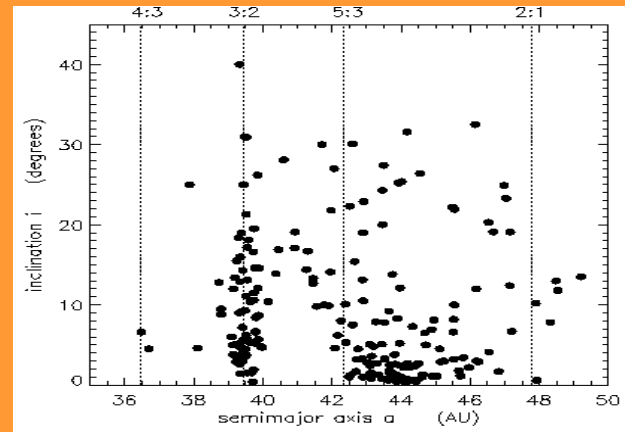
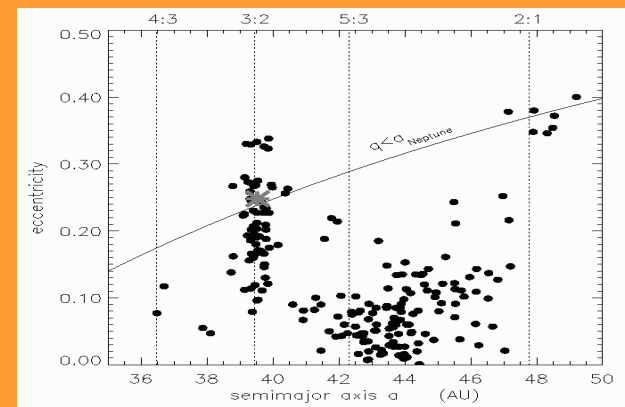


Fig 1
rate
data
an
inc
av
of
dis
ma
dif
ass
ple
e
we



– Oort cloud formation:

during period of disk clean-up scattering from region of gas giants towards outer solar system

→ ‚thermalization‘ of scattered comets by neighbouring stars and galactic molecular clouds

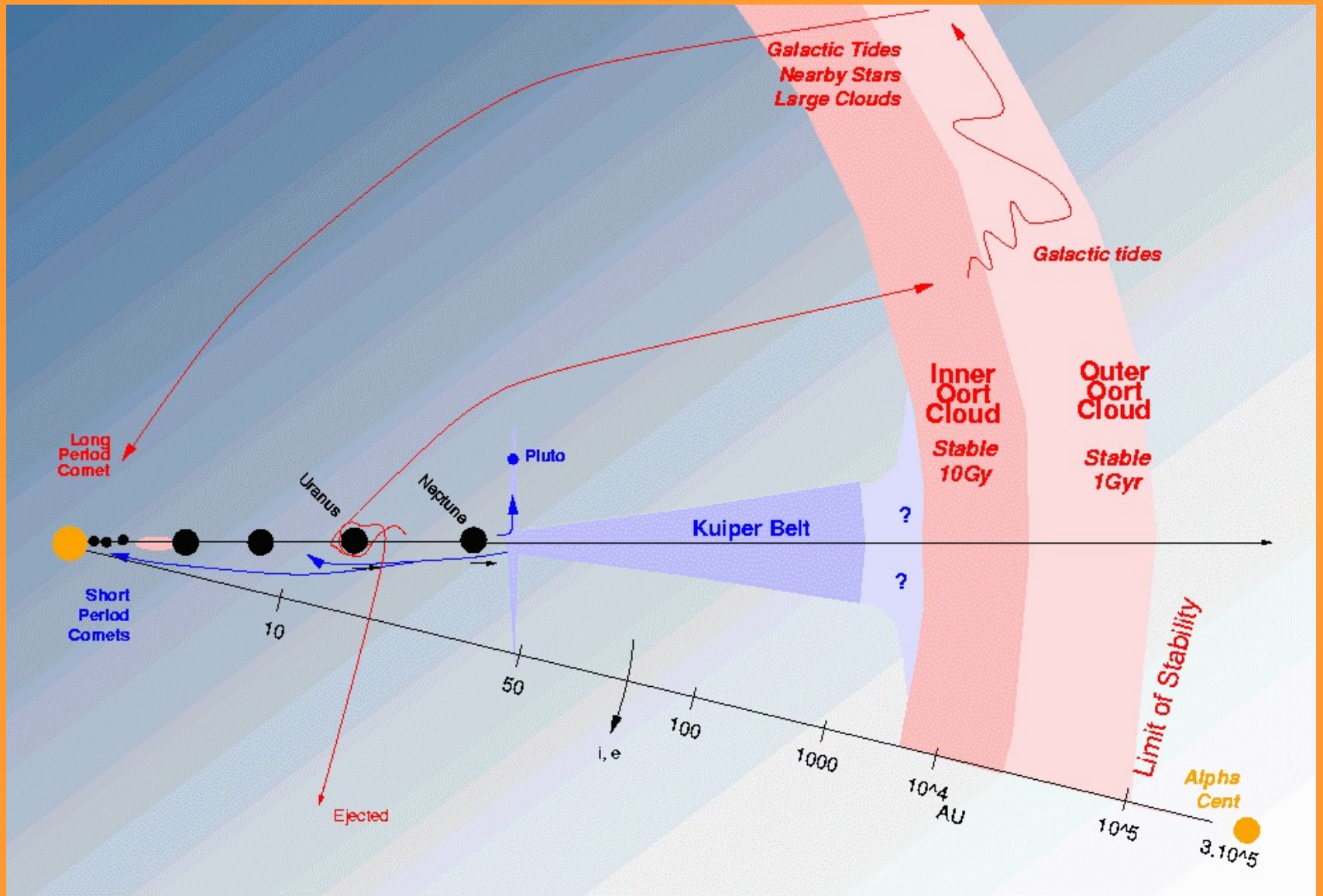
→ distribution in spherical cloud at the edge of the solar system

Arguments: ‚temperature-tracer ices‘ present/absent in Oort cloud comets

→ matches expected temperature range for formation in giant planet regions, Kuiper Belt too cold

• End of the spectacular:

~ $4 \cdot 10^9$ y from now



Planet Evolution

(first 10^9 y)

- Heat-up by gravitational accretion: planets get hot during accretion due to 'absorption' of impact / gravitational energy
 - planet gets liquid, volatile molecules disappear to space or get destroyed in magma
 - different density of metal and silicate materials causes differentiation
 - iron-core formation, silicate at surface
- Terrestrial planets: cooling of silicate forms crust of terrestrial planets, vulcanism releases dissolved magma gases, heavy bombardment delivers further volatile gases
 - original atmosphere (reducing character) forms
- Giant planets: hot core is surrounded by dense H_2/He atmosphere, i.e. efficient cooling of core, gets colder and solid again in parallel differentiation of gas atmosphere (H_2 fluid, He droplets)

Planet Evolution

(Scenarios for next 10^{10} y)

- Some chaotic dynamics: planets may start migrating, colliding & scattering again
- Sun becomes red giant: photosphere growing to Mars orbit
 - terrestrial planet will be gone
 - gas giants will start evaporating their atmospheres

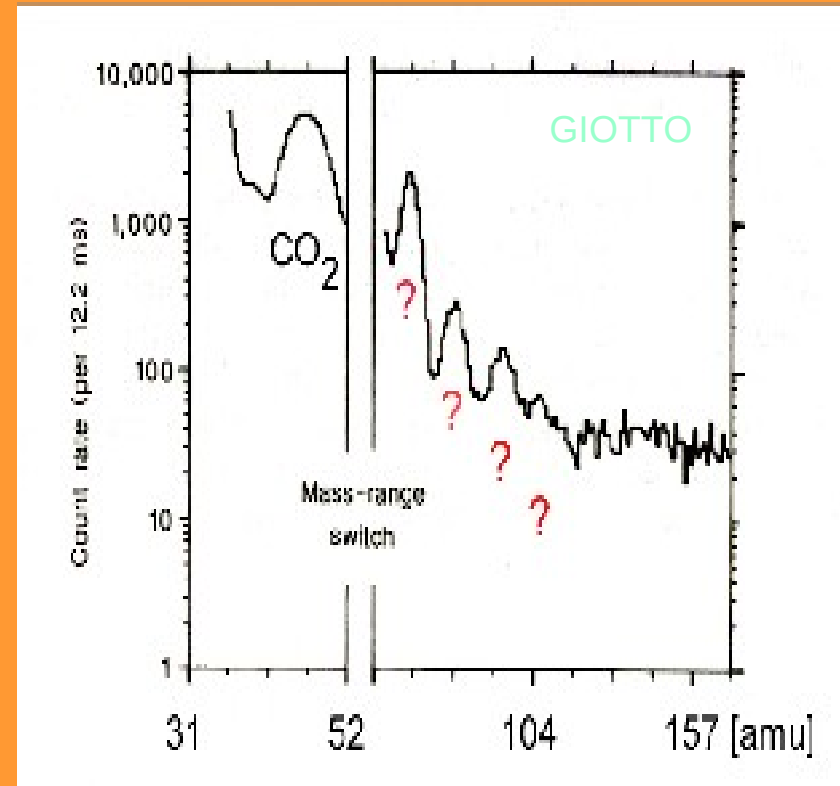
Bioastronomy in the Solar System

- Life on Earth (difficult to detect from space)
- Comets contain water ice (in part source of terrestrial water?; imported during late heavy bombardment)
- Existence of liquid water (oceans) is possible in large KBOs (like Pluto)

→ KBO collision fragments = comets:

hence comets may contain relics from liquid phase

- Coma gas contains organic molecules (organic polymers?)



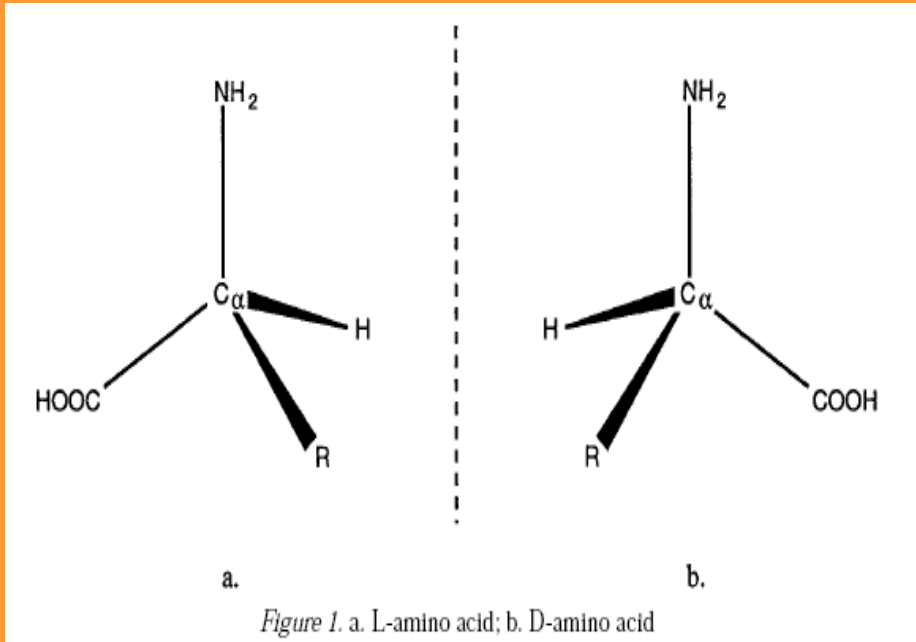
Bioastronomy in the Solar System

- Dust contains lots of CHON particles (GIOTTO at Halley)
- CI chondrites are suspected to contain primordial material from the formation period of the Sun
- CI chondrites are suspected to originate from comets
- Aminoacids exist in interplanetary space, i.e. found in some CI chondrites
- Murchinson CI contains aminoacids in non-racemic mixture (more L type)



→ Comets might be seen as carrier and bringer of pre-biotic material to Earth

Aminoacids: L and D Types



– Aminoacids: important pre-requisites for life formation on Earth

– Aminoacids come in two enantiomers: L and D type

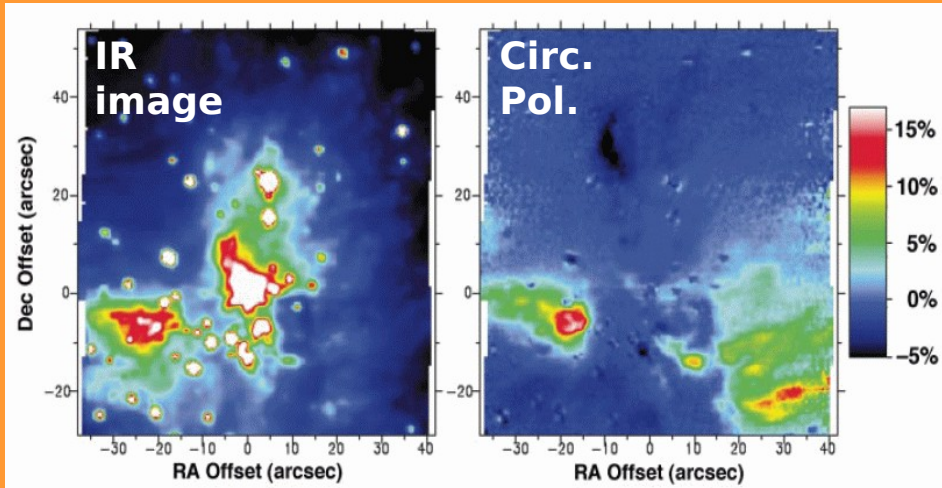
– Terrestrial life built on L type aminoacids

→ Can this be produced in space?

– L and D aminoacids show different optical activity: left and right-handed polarization

→ Can this be used to detect them?

Polarized Light & Homochirality



– High (17% level) circular polarization measured in Orion dust clouds (Bailey et al. 1998)

– Photolysis of L/D molecules is affected by circ. pol. light

➔ more efficient process than any other terrestrial fractionation effect for chiral molecules

- Homochirality of aminoacids through circ. pol. UV radiation from dust reflected star light

➔ most, but not all natural aminoacids on Earth are to be considered biogenic (Cref & Jorissen 2000)

